Matej Barbič

Isolation and identification of the constituents from *Ruscus aculeatus* L. and their *in vitro* activity

Regensburg 2010

Isolation and identification of the constituents from *Ruscus aculeatus* L. and their *in vitro* activity

Von der Fakultät für Chemie und Pharmazie
der Universität Regensburg
genehmigte

Dissertation

zur Erlangung des akademischen Grades
Doctor Rerum Naturalium
(Dr. rer. nat.)

vorgelegt von
Matej Barbič
aus Ivančna Gorica, Slowenien

2010

Dekan:	Prof. Dr. Sigurd Elz
Erster Gutachter:	Prof. Dr. Jörg Heilmann
Zweiter Gutachter:	Prof. Dr. İhsan Çaliş
Tag der Promotion:	12.01.2011

Following thesis was prepared under supervision of Prof. Dr. Jörg Heilmann at the Department of Pharmaceutical Biology, University of Regensburg. *In vitro* measurements of macromolecular permeability were performed by Mrs Elisabeth Willer at the Department of Pharmaceutical Biology (Prof. Dr. Angelika Vollmar), Ludwig-Maximilians University of Munich. Determination of the absolute stereochemistry of sugars by capillary electrophoresis was conducted by Mr Martin Rothenhöfer at the Department of Pharmaceutical and Medicinal Chemistry (Prof. Dr. Armin Buschauer), University of Regensburg.

Acknowledgements

It is a great pleasure to thank all the people who made this thesis possible.

It is hard to overstate my gratitude to my Ph.D. supervisor, Prof. Dr. Jörg Heilmann. I would like to express my deep and sincere appreciation for giving me the opportunity to work on my thesis in such great research environment. Prof. Heilmann showed me the way to become a better scientist and always listened, when advice was needed. With his enthusiasm, cheerful character and excellent teaching ability, he always showed me new insights of the problem and gave me inspiration to find a clear and simple solution.

I am also deeply grateful to my second supervisor, Dr. Guido Jürgenliemk, who coordinated and guided me through my research work. I have to thank him for pushing me hard and supporting me with his always fresh and glowing ideas, but also for being a good friend and a shoulder to lean on. On this occasion, I have to thank his lovely wife Uta, for tolerating some of the 'boys nights' at their home and for fruitful discussions about newest pharmaceutical products on the market.

I owe my most sincere gratitude to Prof. Dr. İhsan Çaliş of the Faculty of Pharmacy, Near East University, Turkish Republic of Northern Cyprus. Prof. Çaliş showed me the first steps in the analytics and inspired me to work on the natural products. He was always willing to help with his experience and supported me with tips and analytical tricks throughout my research.

My sincere thanks are due to Prof. Dr. Samo Kreft of the Faculty of Pharmacy, University of Ljubljana, Slovenia, who helped me start my research at the University of Regensburg by tutoring my diploma thesis. With his unique and amazing way to inspire people, Prof. Kreft was the reason for me to participate in Erasmus exchange program, which opened the door for me at the University of Regensburg in the first place.

I would like to thank all my current and ex-colleagues for providing a stimulating and fun environment. Special thanks go to Mrs Gabi Brunner, for being a great lab mate and for performing the cell counting cytotoxicity assays.
Furthermore, I must thank colleagues and friends, whose support and colleagueship meant a lot, especially: Dr. Tobias Brem, Dr. Stefan Jenning, Dr. Susann Haase, Dr. Birgit Kraus, Anne Freischmidt, Susanne Knuth, Katharina Zenger, Rosmarie Scherübl, Magdalena Motyl, Dr. Sarah Sutor, Anne Grashuber, Irena Brunskole, Sebastian Schmidt, Daniel Bücherl, Marcel Flemming, Thomas Reintjes and my fitness partner Matthias Henke.
I would also like to thank our trainees Sara Samiei and Matthias Hautmann for supporting me during the fractionation and isolation process. Help of following students must also be acknowledged: Amelie Bindl, Stephanie Nolde, Sarah Barthold and Eva Tavčar.

I also warmly thank Allan Patrick Macabeo for always being a good colleague and encouraging me during some long evenings in the lab.

Special thanks go to the Department of Pharmaceutical Biology, Ludwig-Maximilians University of Munich and Prof. Dr. Angelika Vollmar for our fruitful cooperation. I would like to thank Mrs Elisabeth Willer for testing my isolates in the permeability assay and Dr. Robert Fürst for interresting discussions about the results.

The Department of Pharmaceutical and Medicinal Chemistry, University of Regensburg and Prof. Dr. Armin Buschauer are acknowledged for offering us cooperation concerning capillary electrophoresis. I am indebted to Mr Martin Rothenhöfer for performing the analysis of the absolute stereochemistry of the sugars from compounds isolated during this work. I am sincerely grateful for his patience and long hours spent on the CE analysis of my samples. I would also like to thank him and Prof. Dr. Günther Bernhardt for fruitful discussions about capillary electrophoresis.

Thanks are given to Dr. Edwin Ades, Mr. Fransisco J. Candal of CDC (USA) and Dr. Thomas Lawley of Emory University (USA) for providing us with the HMEC-1 cells.

I am also grateful to the NMR department at the University of Regensburg for the measurements of the diverse NMR experiment. Special thanks go to Dr. Thomas Burgemeister and Mr Fritz Kastner for the help on interpretation of the spectra.

For the measurements of all MS experiments, I wish to thank the MS department of the NWF IV (University of Regensburg). I warmly thank Mr Josef Kiermaier, for his patience and excellent discussions about MS analysis.

I thank Deutscher Akademischer Austausch Dienst (DAAD) for the financial support and for the trust in me and my research.

To my beloved wife...
My beautiful wife Mira has always offered me the support that I needed to complete this thesis during the last couple of years. In good times and in bad, she stood by my side and gave me the reason to continue. Mira, you showed me what it means to love and to be loved, I am a better person with you on my side. I thank you for your faithful patience and all the wonderful moments shared together, I thank you for being who you are.

...and family
I would also like to thank my mother-in-law, Bonka and brother-in-law, Plamen, for the time spent together and all the support from your side.

Alja, I also thank you for being such a nice sister, who always believed in me and loved me the way I am.

I thank my aunt Helena for supplying me with energy and motivation during my whole schooling.

Last, but not least, my grandmother Milena, my aunt Tejka, and especially my parents, Mirja and Rajko, receive my deepest gratitude and love for their dedication and trust in me. You showed me the importance of education and helped me find the right way on every step of my life. In my eyes, you have always been the ones to turn to and made me proud to have a family like you. For your love and endless support, I am dedicating this thesis to you.
I would also like to dedicate this work to Mira's father Janko, who deceased in the late spring of 2008.

Matej Barbič
Regensburg, 02 March 2011

Abbreviations

^{13}C	Carbon isotope measured in NMR
^{1}H	Proton isotope measured in NMR
ACN	Acetonitrile
approx.	approximately
CAM	Cell Adhesion Molecules
CC	Column Chromatography
CE	Capillary Electrophoresis
COSY	Correlation Spectroscopy
CV	Crystal Violet
CVD	Chronic Vascular Disease
CVI	Chronic Venous Insufficiency
DCM	Dichloromethane
ECGM	Endothelial Cell Growth Medium
EDTA	Ethylenediaminetetraacetic acid
EHP	Endothelial Hyperpermeability
EtOAc	Ethyl acetate
EtOH	Ethanol
FCS	Fetal Calf Serum
FR	Fraction
HMBC	Heteronuclear Multiple Bond Correlation
HMEC	Human Microvascular Endothelial Cells
HPLC	High Performance Liquid Chromatography
HSQC	Heteronuclear Single Quantum Coherence
ICAM-1	Inter-Cellular Adhesion Molecule 1
MeOH	Methanol
MeOD	Deuterated methanol
med.	medium
min	minutes
MPLC	Medium Pressure Liquid Chromatography
MS	Mass spectrometry
MTT	3-[4,5-Dimethylthiazol-2-yl]-2,5-diphenyltetrazoliumbromid
n-BuOH	1-butanol
NMR	Nuclear Magnetic Resonance
p.	page number
Pyr d_5	Deuterated pyridine
ROESY	Rotating frame Overhause Effect Spectroscopy
rpm	revolutions per minute
SD	standard deviation
SDS	sodium dodecyl sulfate
SE	standard error
sol.	solution
TLC	Thin Layer Chromatography
VCAM-1	Vascular Cell Adhesion Molecule 1
VLC	Vacuum Liquid Chromatography

Table of contents

1 Introduction

1.1 *Ruscus aculeatus* L.

Ruscus aculeatus L., also known as Butcher’s Broom, Kneeholy, Jew's Myrtle or Sweet Broom, belongs to the family Ruscaceae (Ziegler *et al.*: Strasburger - Lehrbuch der Botanik für Hochschulen), but is sometimes classified also in the families of Liliaceae, Asparagaceae or Convallariaceae. *R. aculeatus* is a low evergreen plant and can also be described as a shrub due to its appearance. Green flat sprouts, ending with a spine, are also known as phylloclades and must not be confused with leaves. They are the main photosynthetic organs of the plant. Butcher's Broom is a dioecious plant and has therefore unisexual flowers (**Fig. 1.1** and **1.2**, p. 2). They both appear in spring and are placed in the middle of the phylloclades. It has been found that *R. aculeatus* has a relatively long flowering season, lasting for approx. seven months. Female flowers develop fleshy fruits with 1-4 large seeds and can be observed as red berries on the top of the phylloclades (**Fig. 1.3,** p. 3). Beside seed distribution, Butcher's Broom also spreads vegetatively. It has been noted that several species recovered after fires. The plant occurs in Mediterranean space and is frequently found in woods and bushes. Natural habitats of Butcher's Broom can be found in the South- and West-Central Europe, Asia Minor, Northern Africa and Caucasus (Martinez-Palle & Aronne 1999, Frohne 2002, Wichtl 2002, Ziegler *et al.* 2002, Schönfelder 2004, Hänsel & Sticher 2007).

Fig. 1.1: *Ruscus aculeatus*, phylloclades with female flowers*

Fig. 1.2: *Ruscus aculeatus*, phylloclade with male flower*

* - source: http://www2.arnes.si/~bzwitt/flora/ruscus_aculeatus.html

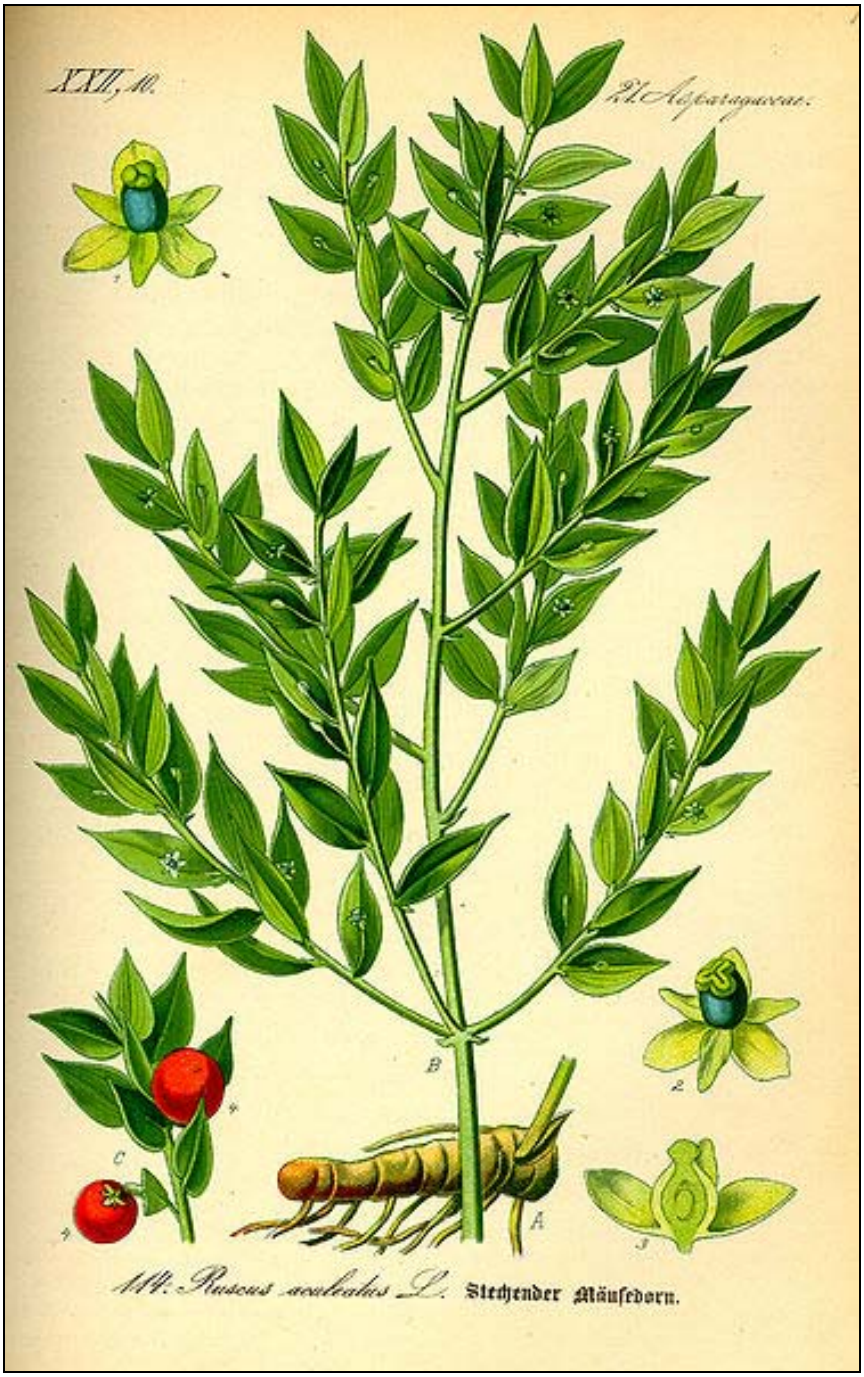

Fig. 1.3: *Ruscus aculeatus* L., 1, 2, 3 - Rusci flos, 4 - Rusci fructus, A - Rusci rhizoma, B - Rusci herba*

* - source:
http://commons.wikimedia.org/wiki/File:Illustration_Ruscus_aculeatus0.jpg

1.2 Constituents of *Ruscus aculeatus*

The steroidal saponins as main ingredients of Butcher's Broom can be divided into two major groups: spirostanols (ruscogenin- and neoruscogenin-type) and furostanols (ruscoside-type, **Fig. 1.4,** p. 5). Major differences between saponins of the same type lie in the structure of the sugar part at C-1, where several acetylated, sulphated and other derivatives have been reported so far (Mimaki *et al.* 1998 a/b/c, 1999, 2003, 2008). The OH-goup at C-3 is normally not glycosidated. Furostanol-type saponins are stable only with a glucose attached to the terminal C-26 atom of the aglycone, which prevents the generation of a full ketal between C-22 and C-26. When the glucose is detached, furostanols automatically turn into energy favourable spirostanols. Mimaki *et al.* (1998 a and b) isolated both, C-22 hydroxylated and methoxylated furostanol derivatives. So far, it is not clear whether one of the both derivatives is an isolation artefact.
Other constituents have also been isolated, including steroid sapogenines, sterols, flavonoids, coumarines, alkaloids (spartein), benzofurans (euparon), thyramine and glycolic acid (El Sohly *et al.* 1975). Although the aerial parts and the rhizomes contain saponins, the concentration of these compounds is much higher in the rhizomes, the part of the plant traditionally used for treatment of several deseases.

European Pharmacopoeia describes rhizomes from Butcher's Broom (Rusci rhizoma), including analysis of its identity and purity as well as quantification of the saponins. Percentage of all saponins requires minimally 1% calculated for ruscogenins (neoruscogenin and ruscogenin, European Pharmacopoeia 5.3).

Medical use of Butcher's Broom was first mentioned back in the Antique Greece, when the rhizomes were administrated for the treatment of inflammations and also used as a diuretic laxative as the treatment for hemorrhoids and urinary disorders.
The most studied therapeutic indications of *R. aculeatus* nowadays are: venous insufficiency, edema, premenstrual syndrome and hemorrhoids. In clinical studies, patients were normally treated with 72 to 75 mg of Butcher's Broom extract (methanol 60%, daily application for 12 weeks, Escop, Vanscheidt *et al.* 2002, Mackay 2001).

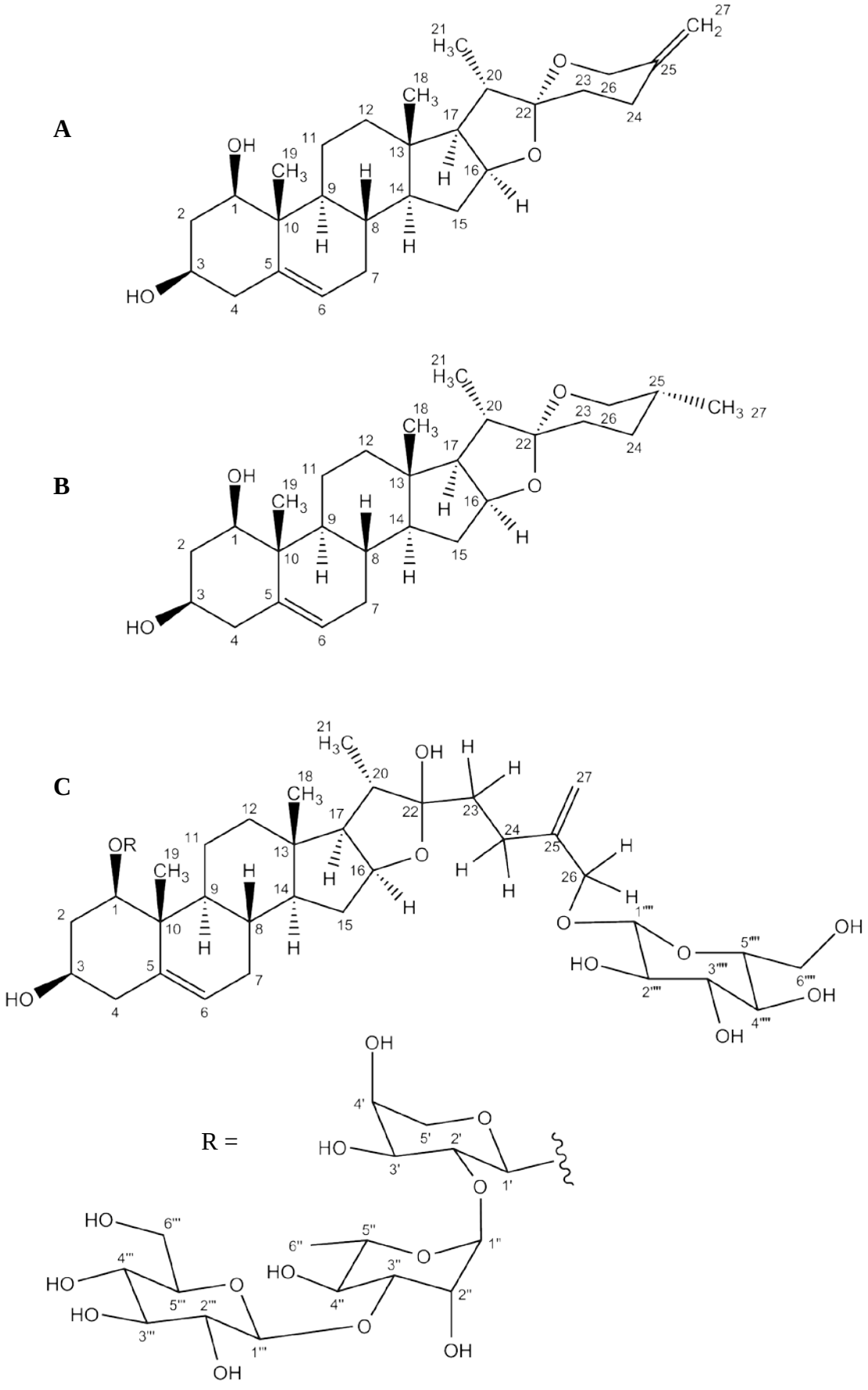

Fig. 1.4: Basic spirostanols: **A** – neuruscogenin (aglycone), **B** – ruscogenin (aglycone), Basic furostanol: **C** – ruscoside

1.3 Pharmacological properties of extracts and compounds from *Ruscus aculeatus*

1.3.1 *In vitro* experiments

1.3.1.1 Vasoconstriction

It has been shown that Butcher's Broom extracts (methanol) induce dose-dependent contractions (0.001-1 mg/ml) of the rings from saphenous vein removed from female rabbits and ensure valvular closure when the veins are exposed to the inversed blood flow (Lauressergues *et al.* 1984, Harker *et al.* 1988). Further studies including experiments on human veins have been performed to show the effects of the extracts on vein contraction. After inducing the contraction, maximal vein tonus induced by Butcher's Broom extracts (concentration range 0.001-1 mg/mL) was reduced or completely eliminated by blocking α- and β-adrenergic receptors with prazosin, rauwolscine or propranolol. This suggests sympathomimetic effects of the extracts (Marcelon *et al.* 1983 and 1988, Rubany *et al.* 1984, Miller *et al.* 2000).

1.3.1.2 Permeability

Veins isolated from pig ear were damaged by ethacrynic acid. Pre-incubation with Butcher's Broom extracts reduced permeability of water and proteins (Hönig *et al.* 1989).

Other effects, such as vasoprotection, effect on lymphatic vessels and elastase activity, as one of the possible anti-inflammatory mechanisms according to Benedek *et al.* 2007, have also been reported (Escop, Facino *et al.* 1995). Huang *et al.* 2008 showed anti-inflammatory effects of ruscogenin *in vitro* (ICAM-1 expression, NF-κB activation, 0.01-1 µM).

1.3.2 *In vivo* experiments

1.3.2.1 Vasoconstriction

Methanolic extracts from Butcher's Broom have been tested for influence on extracorporal circulation of anaesthetized dogs. Results showed that treatment with the extract caused a reversible increase of the venous pressure (Escop).

Assays on hamster cheek pouch have also been performed. When applied topically, a temperature dependent vasoconstrictive effect was found (0.01-0.05 mg/mL). At higher temperatures constriction was higher than at lower. Intravenous administration also showed increase in venular constriction. Oral application (150 g/kg body weight) of a solution of Butcher's Broom extract (methanol) for 28 days gave a 30% increase of constriction of the venules (Bouskela *et al.* 1991).

1.3.2.2 Permeability

Topical (0.002-2 mg/ml/min) and intravenous (5 mg/kg body weight) application of Butcher's Broom extracts to male hamster showed decreased permeability in hamster cheek pouch stimulated by permeability-inducing substances such as histamine or bradykinin (Bouskela *et al.* 1994).

1.3.3 Clinical studies

Several double-blind, placebo-controlled studies have been performed on humans suffering from chronic venous disease, such as chronic venous insufficiency and hemorrhoids. Studies have shown that *R. aculeatus* extracts remarkably improve the symptoms of such venous diseases (Escop).

Double blind and placebo controlled studies indicated an improvement of the typical symptoms caused by CVI. These manifestations, such as increased ankle diameter, tensions in the legs, cramps and edema clearly improved after administration of extracts (72-75 mg, methanol 60%, daily application for 12 weeks) from *R. aculeatus*. It was shown that the treatment with Butcher's Broom also reduces the venous diameter and causes significant reduction of leg volumes and circumference of the legs and ankles. Other symptoms, such as tiredness and heaviness of the legs, have also improved after 12 weeks of treatment with extracts from Rusci rhizoma. A final decision, suggesting that extracts from *R. aculeatus* are a safe and effective treatment for cases of chronic venous insufficiency, has been concluded (Vanscheidt *et al.* 2002).

According to the studies on patients with CVI, it is obvious that extracts from Butcher's Broom significantly diminish development of the disease. Therefore a therapy with products from *R. aculeatus* has to be taken into consideration as a treatment. Other studies showed that treatment of CVI is a domain of natural products and plant extracts (Beltramino *et al.* 2000, Methlie & Schjøtt 2009, Monsieur & Van Snick 2006).

1.3.4 Pharmacokinetics

In animals, radio-labelled extracts from Butcher's Broom were administrated orally to determine the presence of compounds in blood. Radioactivity was measured in different periods of time for 24 hours. Constituents from the extract were eliminated in the feces, renally and biliary (Escop).

In humans, *R. aculeatus* extracts were applied orally and concentration of spirostanol saponins in blood was measured using HPLC. It has been proven that spirostanol saponins enter blood after an oral administration of 1 g of Butcher's Broom extract. The study showed t_{max} for deglucoruscin between 90-120 min and C_{max} of 2.5 µg/mL (Rauwald *et al.* 1991).

1.4 Chronic Venous Insufficiency (CVI) - pathophysiology and treatment

Venous pathology can be described as condition when pressure in veins is increased and the return of blood to the heart is disturbed. There are several known mechanisms, which are believed to be responsible for such conditions. Two main reasons for blood reflux are valvular incompetence and venous obstruction. These factors lead to a state called venous hypertension, which can be accompanied by edema and eventually lead to primary CVI. Changes in the venous pressure also contribute to the microcirculatory hemodynamic disturbances which result, when not treated, in dermal changes like hyperpigmentation, tissue fibrosis and in later stages ulcerations (**Fig. 1.5**, p. 9, Eberhardt *et al.* 2005).

There are several non- and invasive methods which are used in diagnosis of CVI and can help to determine the early stage of desease. The most common and conservative treatment of CVI involves measures to reduce symptoms and help prevent the development of secondary complications and the progression of the desease. If the measures such as elevating legs and the use of compressive stockings fail to provide an apropriate response, further treatment based on anatomic and pathophysilogical features is considered. These involve combination of several surgical procedures and special excercise programs based on individuals (Eberhardt *et al.* 2005).

For better understanding of the pathophysiology of chronic vascular deseases (CVDs) such as CVI, several experiments on the vascular system of patients with CVI have been performed. It has been proven that valves and veins removed from patients with CVI show various signs of inflammation. Infiltration of monocytes and macrophages in the valves and venous wall has been spotted together with enhanced expression of intercellular adhesion molecule-1 (ICAM-

1). Furthermore, in patients suffering from CVI, circulating leukocytes also showed higher levels of activation. All these facts suggest that inflammation may be a cause and not only a consequence of CVI (Bergan 2007, Bergan *et al.* 2008).

Advances in the understanding of pathophysiology have shown how molecular mechanisms of the inflammation cascade are involved in these findings. It has been shown that leukocytes accumulate in the lower extremities, when veins are exposed to hypertension. The reason for that are most probably increased leukocyte adhesion on the endothelium and migration through the endothelium of small vessels. A release of plasminogen activator has also been proven, which indicates leukocyte activation. All the inflammatory hallmarks, like leukocyte activation, adhesion and migration suggest that inflammatory plays a key role in the pathogenesis of CVI (Bergan 2007).

Fig. 1.5: Manifestations of CVI: A - Uncomplicated varicose veins. B - Hyperpigmentation, dermatitis, and severe edema. C - Active and healed venous ulcerations. * - source: see Eberhardt 2005

1.5 Inflammation and role of the endothelium activation

The main role of the endothelium is its function as a barrier. It is particularly important for regulation of the passage of several molecules and fluids between blood and tissue. Especially proteins and other high-weight molecules are restricted to enter the tissue. Transmigration of cells is also one of the main parameters that is regulated by the endothelium (Aird 2008, Pries *et al.* 2000, Pasyk & Jakobczak 2004).
Loss of this function is normally followed by tissue inflammation and plays hereby a major role in inflammation-induced diseases. Molecules such as thrombin, bradykinin and histamine have a great influence on endothelium and cause disruption of the barrier by disturbing the organization of endothelial junctions (Hansson 2009, Sprague & Khalil 2009).

Constant activation of endothelium, caused by chronic inflammation, is an important parameter in development of CVDs and could also be responsible for the progression of CVI. Two most important hallmarks of the endothelial activation are expression of endothelial cell adhesion molecules (CAMs), such as ICAM-1 and VCAM-1, and endothelial hyperpermeability (EHP). Inflitration of leukocytes into the tissue during initiation of the inflammatory response contributes to the progression of the CVD. The increase in EHP is normally followed by edema formation and tissue damage (Weis 2008).
Expression of adhesion molecules on the surface of the endothelial cells is crucial for transmigration of leukocytes into tissue surrounding the blood vessels. Furthermore, the increased expression promotes inflammatory process and hereby leads to progression of CVDs. CVD itself leads to further endothelium activation via higher CAM expression and EHP, which closes this vicious circle. If not treated, CVDs in the long-term lead to complications, which most certainly lower quality of life. Untreated CVI patients suffer from skin changes, varicose veins and in worst case scenario tissue necrosis and ulcerations (**Fig. 1.5**, p. 9).

1.6 Aim of the study

Several studies have proven that extracts produced from *R. aculeatus* are effective in the treatment of CVI (see CVI and treatment, p. 8). It has been shown that steroidal saponins from Butcher's Broom can reach bloodstream when applied oraly as an extract (Rauwald *et al.* 1991). This fact and the high amount of steroidal saponins in the plant, suggest that the positive effect on the CVI is due to the saponins. On the other hand there are no reports indicating which compounds contribute to the overall efficacy of Butcher´s Broom preparations.

Aim of the present work was to isolate saponins and phenolic compounds from Rusci rhizoma and to elucidate their structure. If possible, new compounds from the underground part of Butcher's Broom should be found.

It should be investigated, whether furostanol C-22 hydroxylated and methoxylated derivatives are both genuine natural products of the plant or if one of them is only an isolation artefact.

The isolated compounds should be tested *in vitro* to determine their:
1. influence on the TNF-α induced expression of ICAM-1
2. influence on the thrombin induced hyperpermeability of endothelial cells.

If possible, a structure-activity-relationship should be described.

These results would broaden the knowledge about the genuine ingredients of Rusci rhizoma and their possible contribution to the efficacy of the plant in the treatment of chronic venous diseases, such as CVI.

2 Materials and Methods

2.1 Materials for chromatography, spectroscopy and spectrometry

2.1.1 Plant material

Rhizomes from Butcher's Broom (Rusci rhizoma, dry, 1 kg) were acquired from Caelo (Caesar & Loretz GmbH, Batch Nr.: 40088474)

2.1.2 Solvents and chemicals used for chromatography

- 1-Butanol, for analysis, Sigma-Aldrich
- Acetic acid (100%), anhydrous, for analysis, Merck
- Acetonitrile, gradient grade for liquid chromatography, Merck
- Anisaldehyde (98%), Aldrich
- Dichloromethane, for analysis, Acros Organics
- Ethanol (99%), absolute, for analysis, Baker
- Methanol, for analysis, Merck
- Methanol, gradient grade for liquid chromatography, Merck
- Methanol, Uvasol®, Merck
- Sulfuric acid (95-97%), for analysis, Merck
- Water, deionised
- Water, drinking

2.1.3 Spray reagents

- Anisaldehyde reagent:
  - Anisaldehyde 0.5 mL
  - MeOH 85 mL
  - Acetic acid (95%) 10 mL
  - Sulfuric acid (conc.) 5 mL

- 20% Sulfuric acid (conc., in MeOH)

- Naturstoffreagenz A:
  - 2 g diphenylboryloxyethylamine
  - 200 mL MeOH

  +

  - 10 g polyethyleneglycol 400
  - 200 mL MeOH

2.1.4 Stationary phases for CC, VLC or Flash

- Silica gel 60 (0.063-0.200 mm) for column chromatography, Merck
- Silica gel 60 (0.040-0.063 mm) for column chromatography, Merck
- LiChroprep RP-18 (0.025-0.040 mm) for column chromatography, Merck
- Sephadex LH-20®, Sigma-Aldrich

2.1.5 Columns used in chromatography

- Normal glass columns with stopcock for CC
- VLC glass columns without stopcock modified for application of vacuum
- Plastic pre-packed columns for flash, Silica 60 (0.015-0.040 mm), 30 g, Merck Chimie SAS (all flash columns)
- Plastic pre-packed columns for flash, Silica 60 (0.015-0.040 mm), 90 g
- Plastic pre-packed columns for flash, RP-18 (0.015-0.040 mm) 30 g
- Plastic columns for flash for self-packing, 30 g
- Plastic columns for flash for self-packing, 90 g
- HPLC semi-preparative column, RP-18 (7 µm), 2 cm x 25 cm, Knauer
- HPLC analytical column, RP-18 (5 µm), 0.46 x 25 cm, Purospher® STAR, Merck
- LC-MS HPLC column, Gemini NX 3U C18, 10 cm x 0.2 cm, Phenomenex

2.1.6 Other materials

- TLC Silica gel 60 F_{256} aluminium sheets, Merck
- TLC Silica gel 60 RP-18 F_{256}s, Merck
- TLC chambers 10x10 cm, Camag (small chambers)

- TLC chambers 20x20 cm, Camag (big chambers)
- TLC spotting capillaries, 5 µl, Brand
- Folin-Ciocalteu reagent, Fluka

2.1.7 NMR materials

- Pyridine-d_5 (99.5%), Deutero
- Methanol-d_4 (99.8%), Deutero
- NMR tubes 507-HP, Norell

2.1.8 CE Materials

- D-Glucose, Sigma-Aldrich
- L-Glucose, Roth
- D-Arabinose, Sigma-Aldrich
- L-Arabinose, Sigma-Aldrich
- D-Galactose, Merck
- L-Galactose, Sigma-Aldrich
- L-Rhamnose, Sigma-Aldrich
- Sodium cyanoborohydride, Sigma-Aldrich
- S-(-)-1-Phenylethyamin, Sigma-Aldrich
- Sodium borate, Sigma-Aldrich

2.2 Cell culture materials

2.2.1 Cells and media

- HMEC-1 cells
- Endothelial Cell Growth Medium with Supplement and Antibiotics, Provitro
- Medium 199, PAN GmbH
- Buffer PBS Dulbecco, w/o Mg^{2+}, Ca^{2+}, Biochrom AG
- Collagen G, Biochrom AG
- Fetal Calf Serum (FCS), Biochrom AG
- Trypsin/EDTA in (10x) PBS, w/o Mg^{2+}, Ca^{2+}, Biochrom AG
- ICAM-1, FITC labelled antibodies, Biozol
- TNF-α, Sigma Aldrich
- MTT, Sigma Aldrich
- Crystal violet (CV), Merck
- Trypan blue, Sigma-Aldrich
- FITC-labelled dextran, Sigma Aldrich
- SDS, Merck

2.2.2 Ready-to-use media

		Storage	Amount
Cells:	HMEC-1	-196 °C	
Growth med.:	ECGM	4 °C	500 mL
	Supplement	-20 °C	23.5 mL
	Antibiotics	-20 °C	3.5 mL
	FCS (inactivated)	-20 °C	50 mL
Stop med.:	Medium 199	4 °C	500 mL
	FCS (inactivated)	-20 °C	50 mL
Coating sol.:	PBS	4 °C	500 mL
	Collagen G (Biochrom, 4 mg/mL)	4 °C	1.25 mL
Trypsin/EDTA:	Trypsin/EDTA in PBS	-20 °C	100 mL

2.2.3 Other

- Cell cultivation bottles, 75 cm^2, TPP
- 96-well plates, TPP
- 24-well plates, TPP
- Disposable pipettes, Sarstedt
- 12-well Transwell® plate inserts, Corning

2.3 List of equipment

2.3.1 General

Analytical scales	Sartorius
Ultrasonic bath	Sonorex, Bandelin
Rotary vacuum evaporator	Laborota 4003, Heidolph
Freeze Dryer	Ilvac Pia 100, Pietkowski
UV lamp, 254/366 nm	Camag

2.3.2 Spectroscopy and other

UV spectroscopy	Cary 50 Scan, Varian
Optical rotation	Unipol L1000, Schmidt & Haensch
NMR spectrometers	Avance 300, Bruker
	Avance 600, Bruker
	Avance III 600 kryo, Bruker
MS spectrometers	EI-MS: Finnigan MAT 95
	ESI, LC-MS: ThermoQuest Finnigan TSQ 7000
HPLC preparative	Pro Star 210 (pump system with detector), Model 410 autosampler
	Model 701 fraction collector, Varian

HPLC analytical	L-2130 pump system, L-2455 detector, L2350 column oven, VWR Hitachi
Flash	Armen Instrument
Capillary electrophoresis	Biofocus 3000, Bio Rad
TLC scanner	Reprostar 3, Camag
Speed extractor	E-916, Büchi

2.3.3 Cell culture equipment

Centrifuge	Megafuge 1.0 R, Heraeus Sepatech
Laminar air flow	Clan Laf, Claus Damm
Incubator	New Brunswick Scientific
Plate reader	SpectraFluor plus,Tecan
Vortex	Bender & Hobein AG
Pipettes	Eppendorf
Neubauer cell counting chamber	Brand

2.4 Methods used in chromatography, spectroscopy and spectrometry

2.4.1 Column Chromatography (CC)

Normal glass columns with stopcock were used to perform chromatography. Stationary phases (p. 13) were applied as a suspension in the starting solvent mixture used for the elution, using a ratio of solvent/silica = 2 mL/1 g). After sedimentation of the stationary phase, the rest of the solvent was emerged from the column. As the level of the solvent reached the stationary phase, the flow was stopped to prevent drying of the material.
Samples (extracts, fractions) dissolved in starting solvent mixture were applied to the column. The amount of stationary phase was determined by the weight of the sample. A ratio of 1 g sample per 150 g silica was used under condition that the minimum column length (~ 20 cm) was reached. The height of the sample applied to the column was not higher than ~ 2 mm (1% of the minimum column length). The speed of elution was determined by the type of stopcock, varying between 2 and 3 mL/min.
The fractionation started after the first 80% of the column volume was eluted.
Methods used were:

CC 1

Column: Normal glass column with stopcock, Ø = 3 cm, Silica 60 (~ 45 g)
Fractions: ~ 9 mL
Solvent system:

- 100 mL DCM:MeOH = 90:10
- 200 mL DCM:MeOH = 85:15
- 600 mL DCM:MeOH = 80:20

CC 2

Column: Normal glass column with stopcock, Ø = 3 cm, Silica 60 (~ 75 g)
Fractions: ~ 9 mL
Solvent system:

- 600 mL DCM:MeOH = 80:20
- 1100 mL DCM:MeOH = 75:25
- 200 mL DCM:MeOH = 70:30

CC 3

Column: Normal glass column with stopcock, Ø = 3 cm, Silica 60 (~ 75 g)

Fractions: ~ 9 mL

Solvent system:

- 1300 mL DCM:MeOH = 80:20
- 900 mL DCM:MeOH = 75:25
- 300 mL DCM:MeOH = 70:30

CC 4

Column: Normal glass column with stopcock, Ø = 2 cm, Silica 60 (~ 50 g)

Fractions: ~ 9 mL

Solvent system:

- 500 mL DCM:MeOH = 90:10
- 500 mL DCM:MeOH = 80:20
- 500 mL DCM:MeOH = 70:30

CC 5

Column: Normal glass column with stopcock, Ø = 1.8 cm, RP-18 (~ 20 g)

Fractions: ~ 9 mL

Solvent system:

- 200 mL MeOH:H_2O = 20:80

CC 6

Column: Normal glass column with stopcock, Ø = 2.1 cm, RP-18 (~ 40 g)

Fractions: ~ 9 mL

Solvent system:

- 400 mL MeOH:H_2O = 50:50

2.4.2 Vacuum Liquid Chromatography (VLC)

Normal glass columns without stopcock were modified such that vacuum (water pump) could have been applied to the chromatographic system. Columns were packed with dry materials (silica gel, RP-18 silica). Before the samples were applied, the columns were washed with the starting solvent mixture under vacuum.

Sample (extracts, fractions) was pre-adsorbed on a small amount of silica and applied dry to the column. Sea sand was used to prevent the damage on the sample layer during solvent addition.

Method used:

VLC 1

Column: Glass column for VLC, Ø = 6 cm, Silica 60 (~ 140 g)

Collection scheme:

Fraction	Solvent system DCM:MeOH
FR 1	400 mL 100:0 + 400 mL 95:5
FR 2	2 x 200 mL 90:10
FR 3	5 x 200 mL 90:10
FR 4	3 x 200 mL 90:10
FR 5	4 x 100 mL 90:10
FR 6	5 x 100 mL 90:10
FR 7	5 x 200 mL 90:10
FR 8	9 x 200 mL 90:10 + 200 mL 85:15
FR 9	6 x 200 mL 85:15
FR 10	3 x 200 mL 85:15
FR 11	200 mL 85:15 + 2 x 200 mL 80:20
FR 12	200 mL 80:20 + 200 mL 70:30
FR 13	600 mL 60:40

2.4.3 Flash Chromatography

A computer aided Armen Instrument machine equipped with two-pump system, UV/VIS detector and a fraction collector was used for preparative analysis and purification of samples. Special pre- or self-packed plastic columns (p. 13) were applied for the separation, normally using a 30 g column as pre-column and a bigger 90 g column as main column. Sample was applied dry and pre-adsorbed on the silica after the system had been purged by initial solvent system. These chromatographic systems allow flows up to 40 mL/min and a maximum pressure of 7 bar. Maximum pressure is limited by plastic columns which can not endure pressures higher than 7 bar. Fractions were collected using a fraction collector.
Methods used:

Flash 1

Column: 30 g pre-column and 90 g main column; pre-packed Silica 60 (0.015-0.040 mm)
Fraction collector: 20 mL/test tube
Start of collection: 20 min after start of the method
Method:

Time [min]	Flow [mL/min]	DCM:MeOH
0-3	20	100:0
3-15	20	100:0 → 90:10
15-23	20	90:10 → 85:15
23-60	20	85:15 → 65:35
60-90	20	70:30 → 60:40
90-140	20	60:40 → 50:50

Flash 2

Column: 30 g pre-column and 90 g main column; self-packed Silica 60 (0.040-0.063 mm)
Fraction collector: 20 mL/test tube
Start of collection: 5 min after start of the method

Method:

Time [min]	Flow [mL/min]	DCM:MeOH
0-2	20	100:0 → 90:10
2-4	20	90:10
5-20	20	80:20
20-60	20	80:20 → 60:40
60-90	20	60:40 → 50:50
90-120	20	50:50 → 40:60

Flash 3

Column: 30 g pre-column; self-packed LiChroprep RP-18 (0.025-0.040 mm)

Fraction collector: 20 mL/test tube

Start of collection: 1 min after start of the method

Method:

Time [min]	Flow [mL/min]	MeOH:H_2O
0-30	10	60:40

Flash 4

Column: 2x 30 g pre-column; self-packed Silica 60 (0.040-0.063 mm)

Fraction collector: 10 mL/glass

Start of collection: 1 min after start of the method

Method:

Time [min]	Flow [mL/min]	DCM:MeOH:H_2O
0-15	20	95:5:0.5
16-30	20	90:10:1
31-60	20	85:15:1.5
60-65	20	85:15:1.5

Flash 5

Column: 30 g pre-column; pre-packed Silica 60 (0.015-0.040 mm)

Fraction collector: 20 mL/test tube

Start of collection: 1 min after start of the method

Method:

Time [min]	Flow [mL/min]	DCM:MeOH:H_2O
0-15	20	90:10:1
16-30	20	85:15:1.5
31-50	20	80:20:2

Flash 6

Column: 30 g pre-column; self-packed LiChroprep RP-18 (0.025-0.040 mm)

Fraction collector: 20 mL/test tube

Start of collection: 1 min after start of the method

Method:

Time [min]	Flow [mL/min]	MeOH:H_2O
0-15	20	80:20
16-35	20	90:10
36-65	20	100:0

Flash 7

Column: 2x 30 g pre-column; self-packed LiChroprep RP-18 (0.025-0.040 mm)

Fraction collector: 15 mL/glass

Start of collection: 1 min after start of the method

Method:

Time [min]	Flow [mL/min]	MeOH:H_2O
0-10	15	20:80
10.5-25	15	30:70
25.5-40	15	40:60
40.5-50	15	50:50
50-110	15	60:40

Flash 8

Column: 30 g pre-column and 90 g main column; self-packed Silica 60 (0.040-0.063 mm)

Fraction collector: 20 mL/test tube

Start of collection: 10 min after start of the method

Method:

Time [min]	**Flow [mL/min]**	**DCM:MeOH:H_2O**
0-20	20	90:10:1
21-30	20	85:15:1.5
31-50	20	80:20:2
51-60	20	75:25:2.5
61-75	20	70:30:3
76-100	20	60:40:4

Flash 9

Column: 30 g pre-column; self-packed LiChroprep RP-18 (0.025-0.040 mm)

Fraction collector: 20 mL/test tube

Start of collection: 1 min after start of the method

Method:

Time [min]	**Flow [mL/min]**	**MeOH:H_2O**
0-5	20	40:60
5.5-10	20	50:50
10.5-20	20	60:40
20.5-30	20	70:30
30.5-45	20	80:20
45.5-50	20	100:0

Flash 10

Column: 30 g pre-column; pre-packed Silica 60 (0.040-0.063 mm)

Fraction collector: 20 mL/test tube

Start of collection: 2 min after start of the method

Method:

Time [min]	Flow [mL/min]	DCM:MeOH:H_2O
0-5	20	90:10:1
5-15	20	90:10:1 → 85:15:1.5
15-20	20	85:15:1.5
20.5-25	20	83:17:1.7
25.5-50	20	80:20:2

Flash 11

Column: 30 g pre-column; pre-packed Silica 60 (0.040-0.063 mm)

Fraction collector: 20 mL/test tube (10-25 min)
10 mL/glass (25-45 min)
20 mL/test tube (40-50 min)

Start of collection: 10 min after start of the method

Method:

Time [min]	Flow [mL/min]	DCM:MeOH:H_2O
0-5	20	90:10:1
5-20	20	90:10:1 → 85:15:1.5
20.5-25	20	85:15:1.5
25.5-50	20	80:20:2

2.4.4 Semi-preparative High Performance Liquid Chromatography

Semi-preparative Varian HPLC machine was used for the final purification of some samples. Samples were injected manually by a syringe. Pure compounds were collected manually by monitoring the chromatogram (190-400 nm).

Column used: RP-18 (p. 13), at room temperature
Injection volume: 600-800 μL
Solvents used: MeOH, ACN, H_2O (p. 13)
Methods used:

HPLC 1

Time [min]	Flow [mL/min]	H_2O:MeOH
0-5	10	60:40
6-10	10	50:50
11-40	10	40:60
41-45	10	60:40

HPLC 2

Time [min]	Flow [mL/min]	H_2O:MeOH
0-5	10	50:50
6-16	10	40:60
17-20	10	30:70
21-24	10	0:100

HPLC 3

Time [min]	Flow [mL/min]	H_2O:MeOH
0-5	10	60:40
6-10	10	50:50
11-28	10	40:60
29-35	10	10:90

HPLC 4

Time [min]	Flow [mL/min]	H_2O:MeOH
0-5	10	50:50
6-20	10	40:60
21-25	10	10:90

HPLC 5

Time [min]	Flow [mL/min]	H_2O:MeOH
0-5	10	70:30
6-10	10	65:35
11-15	10	60:40
16-20	10	50:50
21-25	10	40:60

HPLC 6

Time [min]	Flow [mL/min]	H_2O:MeOH
0-3	10	20:80
4-8	10	15:85
9-18	10	10:90
19-20	10	0:100

HPLC 7

Time [min]	Flow [mL/min]	H_2O:ACN
0-3	10	45:55
3.5-7	10	40:60
7.5-11	10	35:65
11.5-18	10	30:70

HPLC 8

Time [min]	Flow [mL/min]	H_2O:MeOH
0-4	10	70:30
5-9	10	65:35
10-14	10	60:40
15-19	10	55:45

HPLC 9

Time [min]	Flow [mL/min]	H_2O:MeOH
0-4	10	70:30
4.5-9	10	65:35
9.5-14	10	60:40
14.5-19	10	50:50
19.5-21	10	40:60
21.5-24	10	90:10

HPLC 10

Time [min]	Flow [mL/min]	H_2O:MeOH
0-3	10	50:50
3.5-6	10	45:55
6.5-9	10	40:60
9.5-12.5	10	35:65
13-16	10	20:80
16.5-19	10	10:90

2.4.5 Analytical High Performance Liquid Chromatography

VWR Hitachi analytical machine equipped with autosampler, two-pump system, UV/VIS DAD detector, oven and a fraction collector was used for the quantification (p. 31) of the extracts according to Ph. Eur. (European Pharmacopoeia 5.3).
Method used:

Quanti

Time [min]	Flow [mL/min]	H_2O:ACN
0-25	1.2	40:60
27-37	1.2	0:100
39-42	1.2	40:60

2.4.6 Thin Layer Chromatography (TLC)

TLC was used for the optimization of solvent systems used in CC, VLC, Flash and HPLC as well as for determination of fractions after running a column. In order to optimize the solvent system, spots (compounds) should show good separation on the TLC plate. For fractionation monitoring, solvent system should be used, separating all compounds and distributing it in the chromatogram between $0.2 < Rf < 0.8$. For optimization of starting solvent system for CC, VLC, Flash and HPLC, compounds with the highest Rf values should lie between Rf = 0.2-0.3. Standard TLC solvent mixture was DCM:MeOH:H_2O = 70:30:3.

Samples were applied to the plate (1 cm from the edge for small chambers and 1.5 cm for big chambers) using 5 µL spotting capillaries (either into spot or line). After developing, the TLC plates were dried with a hair dryer and treated with an appropriate spray reagent.
For visualization of the TLCs, a Camag UV lamp and a Camag TLC scanner (software: WinCATS) were used.

2.4.7 Liquid-Liquid Extraction

Solvent extraction and partitioning was used as a work-up method during the process of isolation and purification of the extract. The crude extract and fractions were initially dissolved with organic solvent and placed in the separatory funnel. The remaining residue was stirred with water and added to the organic solvent. The funnel was closed and shaken gently by inverting it several times. Excess internal pressure was released by opening the stopcock. After repeating the procedure for at least three times, the separatory funnel was set aside to allow the separation of both phases. Compounds were separated based on their relative solubility in two immiscible solvents.

2.4.8 NMR spectroscopy

Samples were dissolved in 600 µL of deuterated solvent and transferred to special NMR tubes. (p. 14) If necessary, samples were filtered using Pasteur pipettes and glass wool. Tubes were applied to the NMR instruments to obtain one- and two-dimensional spectra (^{1}H, ^{13}C, HSQC, HMBC, COSY and ROESY). Measurement parameters are given for single compounds in section Results & Discussion (referenced against undeuterated solvent).
Software: Bruker Top Spin 2.1

2.4.9 MS spectrometry

A very small amount of the testing sample was applied into a small glass tube and given for the analysis.
ES-MS: 70 eV, mass range: 34-800
ESI-MS: Voltage: 3 kV, capillary T: 250 °C, mass range: 10-2500

2.4.10 UV and optical rotation

Samples were dissolved in MeOH Uvasol® (0.1 mg /100 mL) to measure the optical rotations. Compounds for the measurements of UV-absorption maxima (λ_{max}) were also dissolved in MeOH Uvasol® (0.1 mg /mL).

2.4.11 Absolute stereochemisty of sugars via capillary electrophoresis (CE)

Derivatization procedure and CE method was perfomed according to (Noe & Freissmuth 1995) with some modifications.

Samples (1 mg) were dissolved in 0.5 mL 23% aqueous TFA and sealed in a 1 mL glass tube. After 60 min reaction at 120 °C, the TFA solution was transferred into a pear-shaped flask using 2 mL of water. TFA was treated with additional water (3 times) and completely removed by evaporation on a rotary vacuum evaporator. The remaining hydrolysis product and all D- and L- sugar references (1 mg per sample) were derivatized with 60 µL of 0.1 M S-(-)-1-phenylethylamin to afford the corresponding Schiff base, which was immediately reduced to the corresponding diastereoisomers using 22.5 µL of 0.46 M aqueous sodium cyanoborohydride solution.

10 µL of every derivatized sugar reference solution were mixed to obtain a standard solution of all sugar diastereoisomers. To determine the signals of single sugars in the electropherogram, a standard diastereoisomer solution was spiked with single diastereisomers. In order to determine the sugars in compounds isolated from *R. aculeatus*, the standard diastereoisomer solution was spiked with single derivatized compounds. Compounds **8** and **9** were used for the derivatization and determination of the absolute stereochemistry.

The prepared solutions were applied to CE.

CE system used:

Capillary:	70/75 cm, 50 µm, Quarz
Buffer:	50 mM $Na_2B_4O_7$ in 23% aqueous ACN, pH 10.3
Injection:	3 psi sec
Voltage:	30 kV
Detection:	200 nm
Temperature:	27 °C

2.4.12 Quantification

2.4.12.1 Saponins

Quantification of the saponins from *R. aculeatus* was performed according to the Ph. Eur. (European Pharmacopoeia 5.3) using method *Quanti* (p. 28).

2.4.12.2 Phenolics

Quantification of the phenolic compounds in rhizome from Butcher's Broom was performed according to the quantification of phenolic compounds in Tormentillae rhizoma (Ph. Eur. 5.3 using specific absorption of 1100, proposed by Glasl 1983).

2.4.13 Isolation of compounds from *Ruscus aculeatus*

2.4.13.1 Extraction

Underground parts from Butcher's Broom (dry Rusci rhizoma, 1 kg) were pulverised and mixed with sea sand in ratio of 2:1 (rhizome:sea sand). The prepared extraction material was filled into glass columns and macerated for 48 h in DCM (500 mL per column), followed by two percolations with DCM (2 x 300 mL per column). After extraction, the DCM extracts were collected in one round bottom flask. After drying the material, the same procedure was repeated with MeOH to get the main extract (250 g).
MeOH extract and all further fractions were developed on Silica 60 TLC plates (p. 13) to check the variety of compounds using chromatographic solvent system DCM:MeOH:H_2O. Depending on the polarity of the fraction, different mixtures were used. A standard TLC solvent mixture was DCM:MeOH:H_2O = 70:30:3. After development of the plates, anisaldehyde spray reagent (p. 12) was used to visualize the compounds. As an alternative spray reagent a standard 20% methanolic sulfuric acid solution was used. For better visualization of phenolic compounds the Naturstoffreagenz A was used. All chromatograms were also analyzed under UV light (254 nm and 366 nm).

2.4.13.2 Fractionation

In order to separate very polar compounds from saponins, a liquid-liquid extraction (p. 29) was performed with the MeOH extract. Water was used as the hydrophilic phase and n-BuOH as the lipophilic phase. To prevent generation of an emulsion, n-BuOH was first saturated with water using separatory funnel. After extracting with n-BuOH (5x), the n-BuOH and the water phase were obtained. The separation was monitored via TLC (**Fig. 3.1**, p. 46).

2.4.13.3 Sephadex fractionation I

As the next step of fractionation CC chromatography using Sephadex LH-20® (Materials, p. 13) was performed. Glass column (4 x 100 cm) was filled with Sephadex (4 x 55 cm) suspended in MeOH. The n-BuOH fraction (3 g) dissolved in 8 mL of MeOH was applied to the column and fractions (approx. 9 mL at 3 mL/min) were collected after approx. 130 mL had been eluted. The chromatography was repeated 5 times to obtain 5 x 160 fractions, which were combined to 15 fractions according to the TLC (**Fig. 2.1**, p. 33).

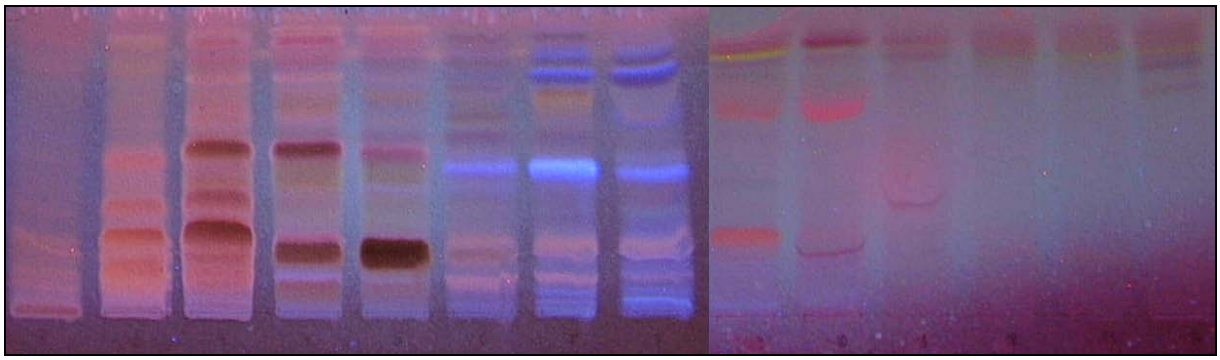

1 2 3 4 5 6 7 8 9 10 11 12 13 14

Fig. 2.1: TLC plates of the FR 1-14 from first fractionation with Sephadex (see Sephadex fractionation I) DCM:MeOH:H_2O = 70:30:3, anisaldehyde reagent, 366 nm

2.4.13.4 Sephadex fractionation II

The n-BuOH (3 g) fraction was dissolved in 8 mL MeOH and applied to the Sephadex LH-20® column (see Sephadex fractionation I) and fractions (approx. 9 mL at 3 mL/min) were collected after 130 mL had been eluted separately. TLC showed that around fraction 30 most of the saponins already eluted from the column, whereas most of the phenolics started to elute. The rest of the fractions were collected into a round bottom flask. At the end of this fractionation, the first fraction, poor on phenolics (PPF) and the second one, rich on phenolics (PRF), were obtained. The procedure was repeated 10 times to get combined fractions of PPF and PRF.

2.4.13.5 Fractionation of PPF

Fraction containing most of the saponins from the extract (PPF) was chromatographed using flash chromatography. Fraction PPF (2 g) was pre-adsorbed on Silica 60 and applied dry to the column. After running *Flash 1* (Flash methods, p. 21), 120 fractions were collected and combined into 8 fractions according to similarity in the TLC. Eventually, columns were washed with MeOH to produce fraction 9. FR 1 (test tube: 1-28), FR 2 (29-31), FR 3 (32-38), FR 4 (39-41), FR 5 (42-46), FR 6 (47-54), FR 7 (55-64), FR 8 (65-120), FR 9 (MeOH).
The procedure was repeated 10 times. (**Fig. 2.2**, p. 34)

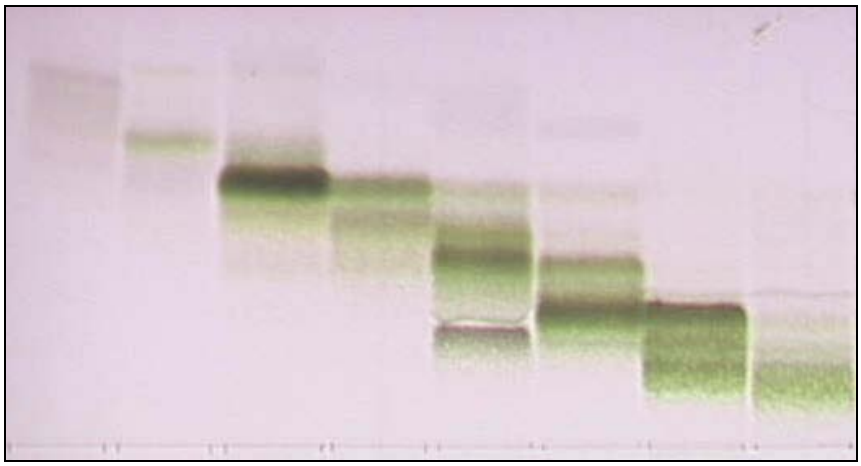

1 2 3 4 5 6 7 8

Fig. 2.2: TLC plate of the FR 1-8 from first flash chromatography of PPF. (see fractionation of PPF) DCM:MeOH:H_2O = 70:30:3, anisaldehyde reagent, VIS

2.4.13.6 Fractionation of PRF

Fraction rich on polyphenols (PRF) was chromatographed using flash chromatography. Fraction PRF (2.2 g) was pre-adsorbed on LiChroprep RP-18 (0.025-0.040 mm) silica and applied dry to the column. After running method *Flash 2* (Flash methods, p. 21), 120 fractions were collected and combined into 10 fractions according to the TLC (**Fig. 2.3** and **2.4**, p. 35).

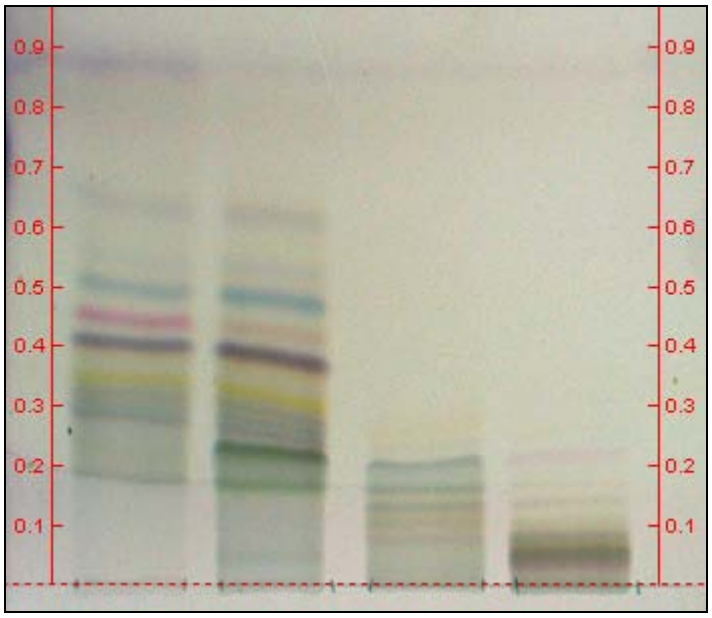

Fig. 2.3: TLC plate of the FR 1-4 from flash chromatography of PRF (see fractionation of PRF). DCM:MeOH:H_2O = 90:10:1, anisaldehyde reagent, VIS

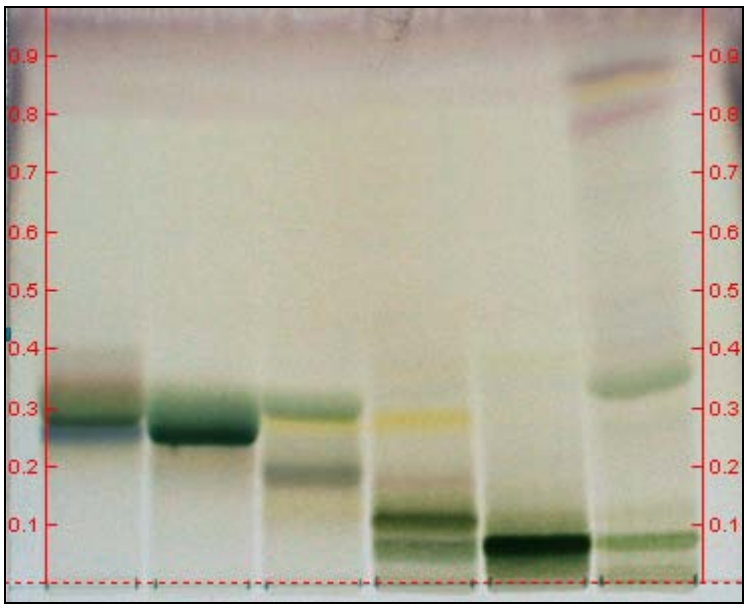

Fig. 2.4: TLC plate of the FR 5-10 from flash chromatography of PRF (see fractionation of PRF). DCM:MeOH:H_2O = 80:20:2, anisaldehyde reagent, VIS

2.4.13.7 Isolation procedure

After the first sephadex fractionation (Sephadex fractionation I, p. 33), all fractions were freeze dried and weighed. Fraction 3 (~ 4.6 g) was chromatographed on Silica 60 using a *VLC 1* method (VLC methods, p. 20) to get 13 fractions (FR I-XIII). Further fractionation of FR VII (~ 242 mg) using *CC 1* (CC methods, p. 18) yielded **1** (test tubes: 12-47, 25.7 mg). Fraction X (1 g) was separated twice using *CC 2* and *CC 3*. Fractionation using *CC 2* (~ 500 mg of FR X) gave **2** (test tube: 30-55, 227.5 mg). Fractionation using *CC 3* (~ 500 mg of FR X) gave **4** (test tubes: 1-8, 3.7 mg).

Fraction 7 (~ 281 mg) from Sephadex fractionation I (Sephadex fractionation I, p. 33) was chromatographed using *CC 4* where fraction from test tubes: 78-130 (~ 36 mg) was further fractionated using *CC 5* to get **10** (test tubes: 7-17, 1.0 mg).

PPF (2 g) was chromatographed using method *Flash 1* to get 120 fractions. They were combined similar to **Fig. 2.2**, p. 34 to get 9 fractions where FR 7 (~ 227 mg) was further fractionated via *CC 6*. Fraction containing test tubes: 10-80 (~ 46 mg) was purified using *HPLC 1* to yield **3** (10 min, 10.6 mg).

FR 2 from PPF fractionation (~ 514 mg, Fractionation of PPF, p. 34) was submitted to flash using *Flash 5* to get 50 fractions, where FR 21-23 were further chromatographed using *Flash 6* to get 25 fractions. FR 9-25 was submitted to semi-preparative HPLC for final purification. *HPLC 6* was used to obtain D1 (13 min), D2 (14 min) and D3 (16 min). Fraction D3 was re-crystallized in ACN to get **6** (13.4 mg). Fraction D2 was purified twice via *HPLC 7* to afford D2-2 (14.5 min), which was identified as **7** (1.8 mg).

FR 5 from PPF fractionation (~ 4.3 g, Fractionation of PRF, p. 34) was submitted to flash chromatography using *Flash 8* to get almost pure **8** and was finally purified using *Flash 9* and *Flash 10* to get 50 fractions. FR 35-38 was identified as **8** (87.4 mg). FR 30-32 was purified using *Flash 11* to get **9** (11.1 mg).

FR 6 (~ 87 mg) from PRF fractionation (Fractionation of PRF, p. 34) was purified using *Flash 3* to get 16 fractions. Further fractionation of FR 11-16 (~ 45 mg) via *HPLC 2* yielded **5** (18 min).

FR 1 (~ 83 mg) from PRF fractionation (Fractionation of PRF, p. 34) was chromatographed using *Flash 4* to get 100 fractions. FR 7-24 was submitted to semi-preparative HPLC using *HPLC 3* to get A1 (4.5 min), A2 (9 min), A3 (10 min), A4 (15 min), A5 (22 min) and A6 (24 min). Due to low weight, the only relevant fraction was

A6, which was purified using *HPLC 4* to get **11** (19 min, 0.3 mg). FR 25-40 was purified using *HPLC 3* to get B1 (14.5 min), B2 (18.5 min) and B3 (24 min). B3 was also identified as **11** (0.2 mg).

FR 2 (~ 450 mg) from PRF fractionation (Fractionation of PRF, p. 34) was fractionated using *Flash 7* to get 100 fractions. FR 14-23 was purified twice using *HPLC 5* to get **12** (6 min, 7.3 mg). FR 48-54 was purified using *HPLC 8* and *HPLC 9* to get **13** (23 min, 0.4 mg), which was identified as a mixture of diastereoisomers and was therefore not described in the Results & Discussion section. FR 71-78 was purified using *HPLC 10* to yield **14** (15 min, 1.2 mg).

2.4.14 Origin of C-22 hydroxy- and methoxylated compounds

2.4.14.1 Inert extraction from Butcher's Broom rhizome via speed extractor

Plant material (rhizome) was first de-fatted with DCM and EtOAc followed by the extraction with n-BuOH. For control, a parallel extract was produced with water followed by liquid-liquid extraction with n-BuOH. Together, four different samples were produced.

For extraction, Büchi Speed extractor E-916 was used. A mixture of sea sand and powdered rhizomes (10:1) was prepared. Special 20 mL steel cartridges were filled with 10 g of the mixture and placed into the extractor. Automated extraction was performed according to the pre-set method.

Speed extractor method used:

Temperature: 85^0C
Pressure: 100 bar
Rinsing with solvent: 2 min
Rinsing with gas: 3 min
Number of cycles: 4

2.4.14.2 LC-MS analysis of the extracts

HPLC-MS coupled experiments (ESI-MS) on the extracts from speed extractor were performed by following methods:

Column: RP-18 (p. 13)
Methods:

MS 1

Time [min]	Flow [mL/min]	H_2O*:ACN*
0-20	0.3	97:3 → 2:98
20-25	0.3	2:98
25-26	0.3	2:98 → 97:3
26-30	0.3	97:3

* - including 1% acetic acid

MS 2

Time [min]	Flow [mL/min]	H_2O*:ACN*
0-20	0.3	97:3 → 2:98
20-25	0.3	2:98
25-26	0.3	2:98 → 97:3
26-30	0.3	97:3

* - including 0.1% formic acid

MS 3

Time [min]	Flow [mL/min]	H_2O*:ACN*
0-30	0.4	90:10 → 60:40
30-35	0.4	60:40 → 2:98
35-40	0.4	2:98
40-41	0.4	2:98 → 90:10
41-45	0.4	90:10

* - including 0.1% formic acid

2.4.14.3 Time dependent NMR meausurements on C-22 hydroxylated coumpound in MeOD

Compound **3** (p. 57) was dissolved in MeOD and incubated in NMR tube. Possible changes during the incubation time were measured on a Bruker Avance III 600 Kryo spectrometer. Proton spectrum was measured every day in the first week. After 3 weeks, 3 months and 6 months further ^{1}H-spectra were recorded. After 6 months, deuterated methanol was removed and **3** was dissolved in pyridine-d_5 to perform a complete 1 and 2D spectrum analysis. After removing the pyridine, investigated sample was incubated in water for three days. After drying the sample, 1 and 2D NMR analysis in pyridine-d_5 followed.

2.5 Cell culture assays and cultivation

2.5.1 FCS inactivation

FCS (500 mL bottle) was partially thawed at room temperature and totally thawed at 37 °C. Water bath was set to 56 °C. After the temperature in a reference bottle reached 56°C, FCS was inactivated for 30 min. So prepared FCS was partitioned into 50 mL falcons and stored at -20°C after cooling down.

2.5.2 Coating

All bottles and plates used for cell cultivation were coated with Collagen G solution for 30 min before the cells were applied. Volumes used were 10 mL for bottles, 100 µL/well for 96-well plates and 500 µL/well for 24-well plates. Collagen G is used for better adhesion of the cells on the bottom of the cultivation bottles and wells.

2.5.3 Cell splitting and cultivation

After removing exhausted growth medium from the bottle, cells were carefully washed twice with PBS buffer solution. Cells were dissolved by trypsin/EDTA solution for 3 min in incubator at 37 °C and 5% CO_2. The detachment of cells was checked by microscopy. To stop the trypsinization process, stop medium was added. After light shaking, re-suspended cells were transferred into a falcon and applied to centrifuge for 5 min at 1000 rpm. Supernatant was removed and the cells were re-suspended in fresh growth medium to get the basic cell suspension. Depending on the splitting ratio, a small amount of this suspension was diluted in growth medium to 25 mL and applied into the pre-coated bottle. Labelled bottles were incubated at 37 °C and 5% CO_2.

2.5.4 ICAM-1 expression inhibition assay and flow cytometry

ICAM-1 expression (ICAM-1 assay) was measured according to Dirsch *et al.* 2004 with some modifications. Confluent grown HMEC-1 cells were pre-incubated with test samples (dissolved in medium), parthenolide (10 µM in medium; positive control) and only with medium (negative control) in 24-well plates (n = 2 for each value). 20 min later TNF-α (10

ng/mL) was added into the wells, except for the negative control, to stimulate ICAM-1 expression. After 24 h cells were removed from the plates, fixed with formalin and washed with PBS. FITC-labelled mouse antibodies against ICAM-1 were added in order to detect the adhesion molecules. For quantification, the amount of fluorescence was measured by flow cytometer - FACS analysis (Becton/Dickinson FACSCalibur with argon laser, FL1 detector, excitation: 495 nm, emission: 519 nm, voltage: 500 V, flow: 60 µl/min, gated cells: 5000).
Flow cytometry allows sorting, counting and analysing of several parameters of single cells suspended in a fluid. Cells or parts of the cells are first dyed with a fluorescence dye or marked with fluorescence-emitting antibodies, which can then be detected in the cytometer.

2.5.5 Macromolecular permeability assay

Permeability assay was performed by E. Willer and Dr. Robert Fürst at the LMU in Munich. HMECs were seeded on 12-well Transwell® plate inserts (n = 3; collagen G pre-coated, pore size 0.4 µm, polyester membrane) and incubated for 48 h. FITC-dextran (40 kDa; 1 mg/mL) was added to the upper compartment at t = 0 min. Cells were stimulated with thrombin (3 U/mL, t = 0 min) after preincubation with compounds. At t = 0, 5, 10, 15 and 30 min, samples were taken from the lower compartment. The increase in fluorescence of the samples was measured with a SpectraFluor plus plate reader at 560 nm where the mean fluorescence of with thrombin stimulated cells at t = 30 min was set as 100% and that of non-stimulated cells as 0%. The rest of the data (with compounds stimulated cells) were expressed as the percent of fluorescence of the 100% control. The higher the value the higher is also the permeability.

2.5.6 Viability assay

The MTT viability assay (n = 3) was performed according to Mosmann 1983 with modifications. Confluent grown HMEC-1 cells were incubated with test samples in 96-well plates (in growth medium; n = 6). Pure growth medium was used as the negative control (n = 6). After 24 h the substances and the supernatant were removed and 10 µL MTT (5 mg/mL) in 90 µL medium were added for 3 h. This solution was exchanged for 10% sodium dodecyl sulfate (100 µL) and 24 h later the absorbance was measured with a SpectraFluor plus plate reader at 560 nm.

2.5.7 IC_{50} value of compound 6 in viability assay

Confluent grown HMEC-1 cells were incubated with compound **6** at following concentrations: 50 µM, 40 µM, 35 µM, 30 µM, 25 µM, 20 µM 15 µM and 10 µM in 96-well plates (in growth medium; pure growth medium for negative control; n = 6 for each value). Further procedure was equal to the normal MTT assay. IC_{50} was determined by using a logarithmic dose-dependent curve, displayed in Microsoft Excel.

2.5.8 Influence of ruscin and deglucoruscin on the HMEC-1 cell density

2.5.8.1 Cell staining using CV

Confluent grown HMEC-1 cells were incubated with **1** (deglucoruscin) and **8** (ruscin), using 50 µM solutions in 96-well plates (n = 3; in growth medium; pure growth medium for negative control; n = 6 for each value). After 24 h, the substances and the supernatant were removed and the cells were stained with an ethanolic solution of crystal violet (CV, 0.5% in 20% MeOH) for 15 min and washed with water. For quantification, the CV was dissolved with 100 µL of a 0.1 M ethanolic sodium citrate solution and the absorbance was measured with a SpectraFluor plus plate reader (Tecan) at 560 nm.

2.5.8.2 Cell counting assay using Trypan blue (24 well)

Confluent grown HMEC-1 cells were incubated with **1** and **8** using 50 µM solutions in 24-well plates (n = 3; in growth medium; pure growth medium for negative control; n = 3 for each value). After 24 h, the substances and the supernatant were removed and the cells were dissolved by 500 µL trypsin/EDTA (Cell splitting, p. 41). Stop medium (500 µL) was added. Resuspended cells were transferred to falcon and applied to centrifuge for 5 min at 1000 rpm. The supernatant was removed and the cells were resuspended in 1000 µL fresh growth medium to get the base cell suspension. Cell suspension (50 µL) was mixed with trypan blue solution and the cells were counted using a Neubauer cell counting chamber.

2.5.8.3 Cell counting assay using Trypan blue (6 well)

Confluent grown HMEC-1 cells were incubated with **1** and **8** using 50 µM solutions in 6-well plates (n = 3; 2000 µL growth medium; pure growth medium for negative control; n = 3 for each value). After 24 h the substances and the supernatant were removed and the cells were

dissolved by 1000 µL trypsin/EDTA (Cell splitting, p. 41). Stop medium (1000 µL) was added and cells were resuspended in fresh growth medium to get 5000 µL of the base cell suspension. Cell suspension (50 µL) was mixed with trypan blue solution (50 µL) and the cells were counted using a Neubauer cell counting chamber.

2.6 Statistical analysis

Experiments were performed three times (n = 3) and data were expressed as mean value ± SD or SE, as indicated in the figures. Grubbs' test was performed to expunge the outliers. Significances towards control values were calculated using Student's t-test (*** $p < 0.001$, ** $p < 0.01$, * $p < 0.05$).

3 Results and Discussion

3.1 Isolation and identification of compounds from *Ruscus aculeatus*

3.1.1 Fractionation and isolation

Since Rusci rhizoma is the most common part of Butcher's Broom that has been worked on in the past and used for treatment of chronical venous diseases, rhizomes from *R. aculeatus* (Materials & Methods, p. 12) were chosen as starting material for extraction and further purification. Most common solvent for extraction from Rusci rhizoma is MeOH, therefore initial extract was produced with MeOH after de-fatting the rhizomes with DCM (Extraction, p. 32). Extract was characterized by TLC on normal phase silica using solvent system DCM:MeOH:H_2O = 70:30:3 as the mobile phase. The same system was used for other TLC experiments performed during this research, since it gave the best overview of the compound spectrum. To derivatize the compounds on TLC plates, anisaldehyde and sulfuric acid spray reagents were used. Saponins sprayed with anisaldehyde reagent gave dark green, whereas the same compounds sprayed with sulphuric acid gave brown spots. Under UV (366 nm), saponins were fluorescent red with both anisaldehyde and sulphuric acid. Anisaldehyde was set to be standard spray reagent in this work, as several compounds were able to be visualized under UV after derivatization.

As expected for rhizomes, the MeOH extract contained several sugars, from mono- to oligosaccharides. These compounds can disturb further fractionation and are also very inconvenient to work with. In order to remove a great part of the saccharides, the MeOH extract was partitioned between n-BuOH and water. Most of the very polar compounds were successfully removed from the methanolic extract (**Fig. 3.1**, p. 46).

According to the TLC and literature, it was clear that butanolic extract contained several different saponins. In order to develop a reproducible method for saponin isolation a different approach has been chosen. Instead of standard fractionation based on silica column chromatography, a method with Sephadex LH-20® was used. Sephadex is a dextran gel cross-linked with epichlorhydrin and is most frequently used for size exclusion chromatography in biochemical procedure. Bigger molecules normally travel through the gel faster as the smaller ones. In case of secondary metabolites separation occurs partially also due to the different polarity of the compounds and for phenolics due to adsorption effects leading a decelerated

elution of aromatic compounds in comparison to non-aromatic ones. Starting sephadex fractionation with MeOH (Sephadex fractionation I, p. 33) gave first impressions about the separation. Information about other compounds than saponins was also gathered. Most of the compounds eluting from the column later than the saponins showed different UV/VIS coloration. Derivatization with NSR showed the presence of several phenolic compounds which were under UV at 366 nm detected as yellow, orange and blue spots. This suggested that the extract contained flavonoid and caffeic acid derivatives. It was possible to develop a method (Sephadex fractionation II, p. 33) where only two major fractions were collected: a fraction poor on phenolics (PPF) and a fraction rich on phenolics (PRF, **Fig. 3.1**, p. 46).

Sephadex fractionation I gave some interesting saponin and phenolic fractions. Due to high amount of fractions, only some of them were further chromatographed. Low weight phenolic fractions with a very diverse compound spectrum were even more problematic.

Most common fractionation and purification method of the fractions from the first sephadex fractionation was column chromatography (CC, Materials & Methods, p. 18) using a combination of normal phase silica and reverse phase RP-18 material. For very raw fractions a vacuum liquid chromatography (VLC, Materials & Methods, p. 20) was performed.

Further fractionation steps were performed by Flash (Materials & Methods p. 21) due to a better and more reproducible separation quality as well as massive time and solvent reduction compared to CC. Using enough starting material, final purification would also be possible.

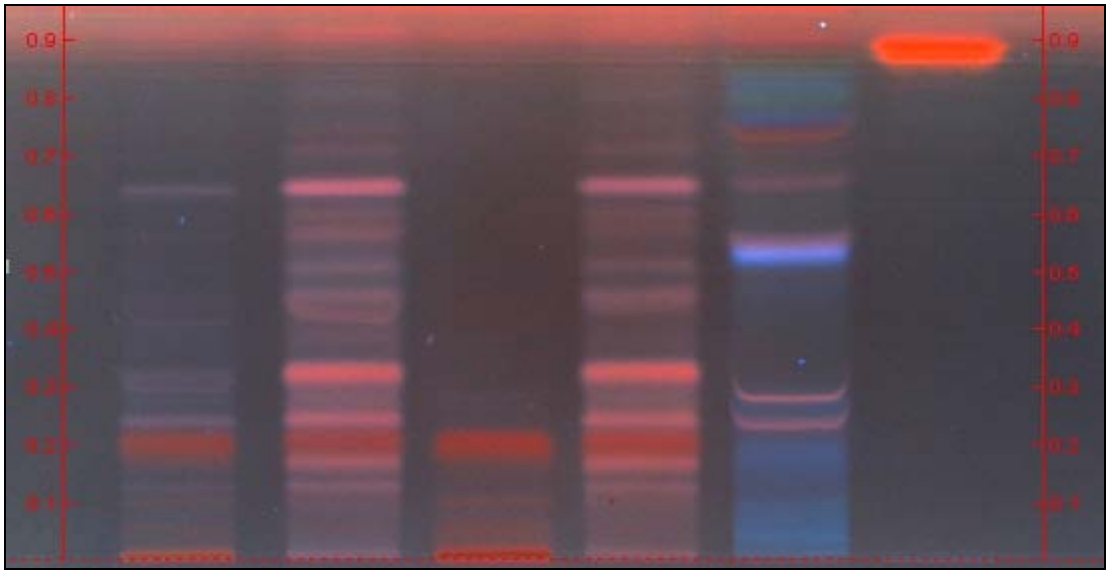

1 2 3 4 5 6

Fig. 3.1: TLC Plate of the MeOH extract (1), n-BuOH phase (2), water phase (3), PPF (4), PRF (5) and ruscogenins (6). Silica 60, DCM:MeOH:H_2O = 70:30:3, anisaldehyde reagent, 366 nm

Most of the final purifications were performed using a semi-preparative HPLC (Materials & Methods p. 26). Smaller fractions, such as minor saponin mixtures and low weight phenolic fractions were purified with the same chromatographic system. Main problem of the saponin isolation is the lacking chromophore resulting in a detection wavelength at around 200 nm. Therefore final purifications of the saponins had to be confirmed by TLC and derivatized with anisaldehyde reagent.

Another analytical problem was the structural similarity of different saponins resulting in a difficult seperation. On the other hand, the small amount of phenolic compounds also made them difficult to isolate. Advantageous in case of phenolic compounds is their existing chromophore. All isolation pathways leading to pure compounds are shown in **Fig. 3.3**, p. 48 and **Fig. 3.4**, p. 49.

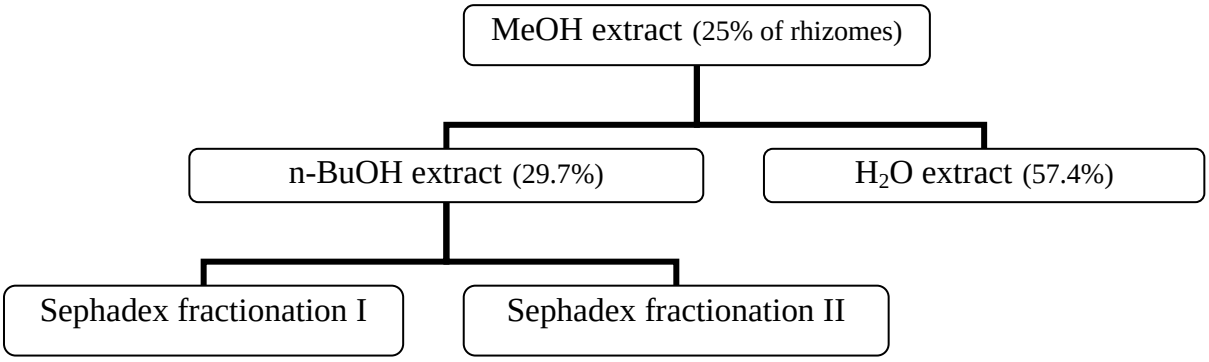

Fig. 3.2: Main fractionation pathway of the MeOH extract and yields (mass %, rest of the MeOH extract was lost or distributed into emulsion phase between organic and water fraction during the liquid-liquid chromatography, Materials & Methods, p. 32).

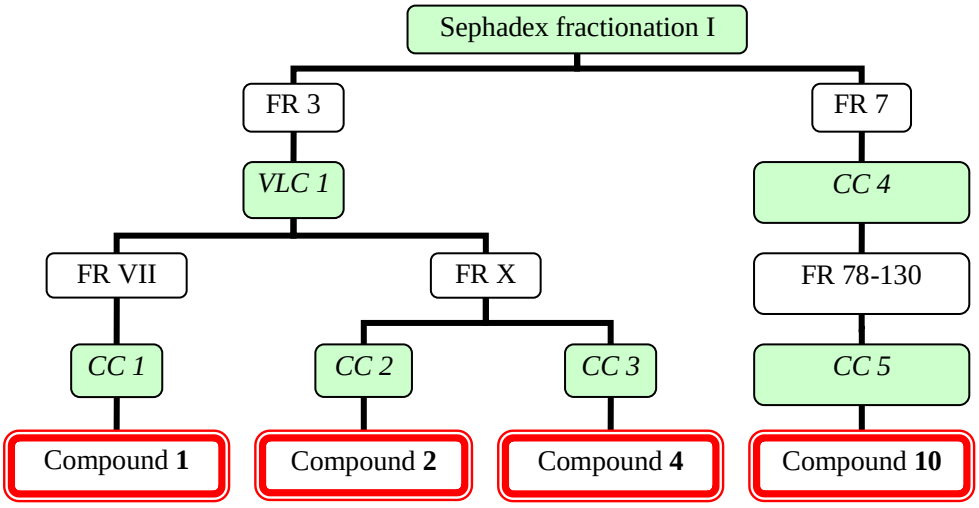

Fig. 3.3: *Sephadex fractionation I* pathway leading to the isolation of **1**, **2**, **4** and **10**. Methods used are marked light green (see Materials & Methods for explanation).

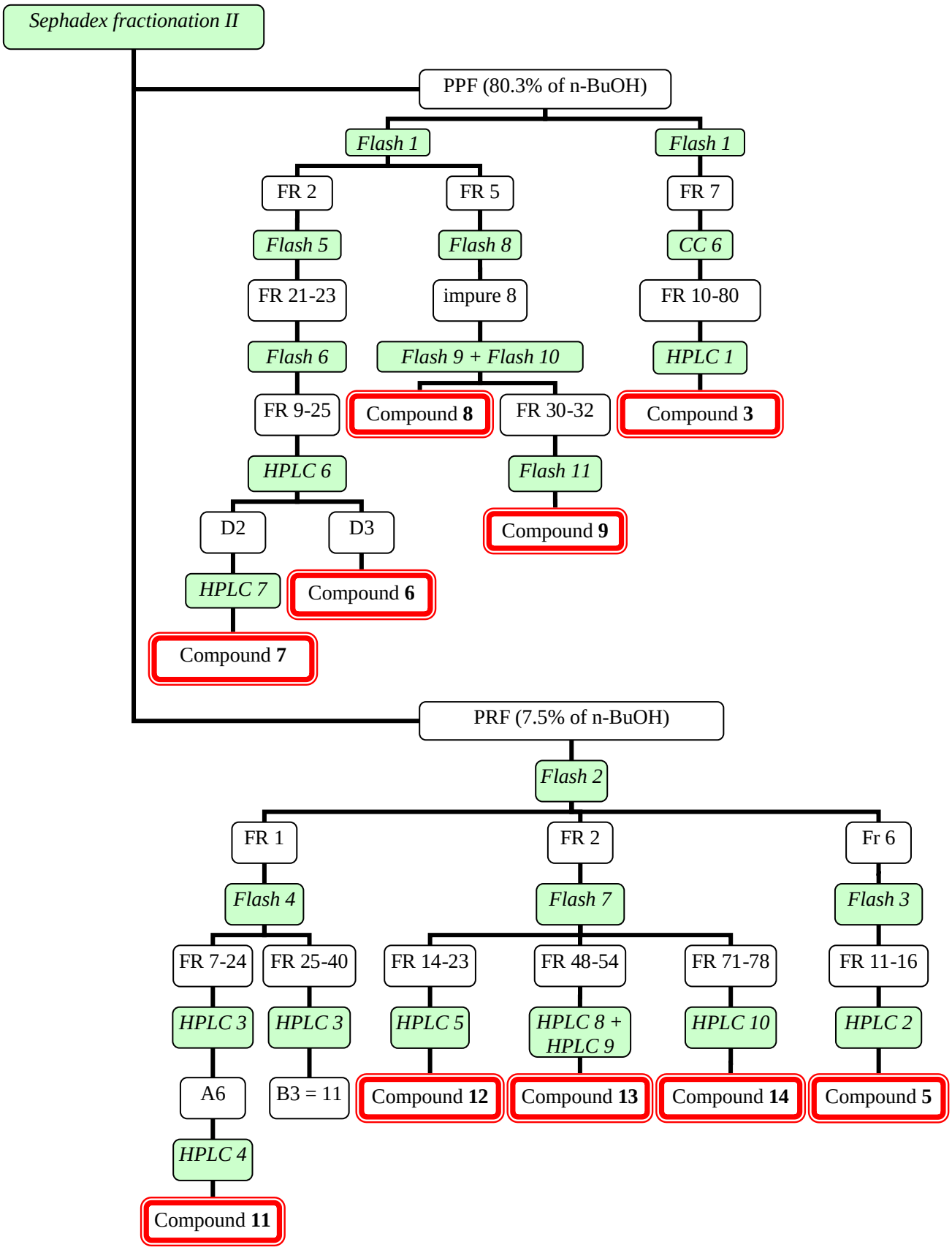

Fig. 3.4: *Sephadex fractionation II* pathway leading to the isolation of **3**, **5**, **6**, **7**, **8**, **9**, **11**, **12**, **13** and **14**. Methods used are marked light green (see Materials and Methods for explanation).

3.1.2 Structure elucidation

Isolated compounds were submitted for the NMR analysis which is the most common and powerful tool for structure elucidation. Beside classical ^{1}H and ^{13}C experiments, also 2D measurements were performed. HSQC gave information about $^{1}J_{H,C}$ correlations, meaning, that we were able to determine protons connected directly to a specific carbon. In HMBC $^{2}J_{H,C}$ and $^{3}J_{H,C}$ in some cases also $^{4}J_{H,C}$ correlations were determined. COSY is a very useful experiment where geminal and vicinal protons are detected. It is especially helpful in the structure elucidation of saponins due to the presence of several -CH_2- and -CH- groups. For correlation between protons through space, ROESY experiments were performed.

As the supporting experiments to the NMR, ESI-MS (electro spray ionisation) spectra were measured to get molecular weight of isolated compounds. ESI-MS is a very mild method ionisation method meaning that compounds remain intact forming most prominently pseudomolecular ions. Occasionally, bigger fragments, such as sugars, can be detached from the compound. On the other hand, EI-MS experiments cause ionisation to smaller fragments of the compound. Both experiments give helpful information for easier structure elucidation.

HR-MS (high resolution MS) is a special experiment, where exact mass of compounds can be measured. With this method, we can also predict the chemical formula of the compound.

To get even more information about the compounds, optical rotation and UV spectra were measured (Materials & Methods p. 29).

With the above described methods, it was possible to determine the structures with their relative stereochemistry. To determine the absolute stereochemistry of sugars, they were detached from the glycoside and transformed into their diastereisomers with *S*-(-)-1-phenylethylamine. By comparising with reference sugars, absolute stereochemistry of the sugars was determined using CE (Materials & Methods p. 30).

Detailed information about structure elucidation is described in following chapters.

3.1.3 Identification of steroid saponins

3.1.3.1 Compound **1** (Deglucoruscine)

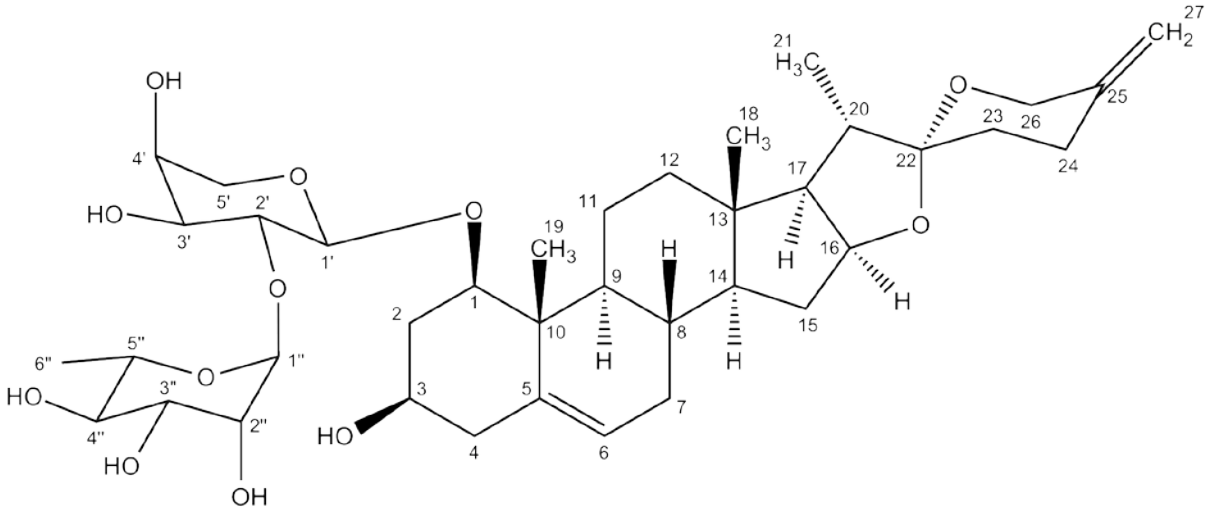

Compound **1** was isolated (25.7 mg) and identified as deglucoruscine (isolation scheme, p. 32). TLC chromatograms sprayed with anisaldehyde reagent gave typical green coloration which was observed as red fluorescence spot under UV at 366 nm (Rf = 0.65 in standard system, p. 28). ^{1}H NMR experiment confirmed a saponin structure with characteristic signals for the aglycone between approx 1 - 3 ppm and for the sugar moieties at around 3.5 - 5 ppm (**Table 3.1**, p. 53 and **Fig 3.5**, p.54). Most common signals were the methyl groups of the aglycone, H_3-18 at δ = 0.84 ppm (s), H_3-19 at δ = 1.44 ppm (s) and H_3-21 at δ = 1.03 ppm (d). In ^{13}C experiment several signals were suggesting a neoruscogenin aglycon. C-27 exo-methylene group signal was found at δ = 108.7 ppm. Signals at δ = 139.6 ppm, δ = 124.7 ppm and δ = 144.5 ppm were typical for C-5, C-6 and C-25. Carbon at δ = 83.6 ppm that showed correlation to a proton at δ = 3.83 ppm (dd) in HSQC was identified as C-1 and is also a very characteristic signal for neoruscogenin (Mimaki *et al.* 1998 a/b/c, 1999, 2003, 2008). With these signals as a starting point for structure elucidation, aglycone was identified as neoruscogenin using COSY and HMBC. Correlations from C-1 to C-4 and C-6 to C-20 followed by correlations from C-23 to C-24 were observed, meaning, that most of the signals were assigned using COSY. Position of quaternary carbons was determined via HMBC.

Absolute stereochemistry was confirmed via ROESY, where C-19 was set to β position (Hänsel & Sticher).

Two signals at δ = 100.4 ppm and δ = 101.8 ppm correlating with protons at δ = 4.71 ppm (d) - H-1' and δ = 6.34 ppm (d) - H-1" suggested the presence of two anomeric protons of two sugars. With aglycone structure elucidated, remaining unassigned 11 carbons confirmed two sugars, a pentose and a hexose. Sugar signals were assigned using COSY and HMBC where H-1' was identified as the anomeric proton of the arabinose and H-1" as the anomeric proton of the rhamnose. HMBC correlation between H-1' and C-1 clearly proved that arabinose is attached to the aglycone at C-1 (**Fig. 3.6**, p. 54). Correlation between H-2' and C-1" signified that the rhamnose was attached to the arabinose at C-2' (**Fig. 3.7**, p. 55).

Compound **1** showed a pseudomolecular ion peak at *m/z*: 705 $[M-H]^-$ in negative-ion ESI-MS which confirmed the proposed structure from NMR analysis.

Capillary electrophoresis confirmed the presence of L-arabinose and L-rhamnose (Materials & Methods p. 30 and CE results p. 101). Normal L-arabinose chair conformation is $^4C_1$. Therefore $^3J_{H\text{-}1'/H\text{-}2'}$ = 7.3 Hz signifies the presence of α-L-arabinose. In the case of β-L-arabinose a very small $^3J_{H\text{-}1'/H\text{-}2'}$ value would be observed (Markham 1989). Stable conformation of L-rhamnose is a $^1C_4$ chair conformation. Therefore, a small $^3J_{H\text{-}1''/H\text{-}2''}$ = 1.0 Hz value confirmed the presence of α-L-rhamnose.

The optical rotation of **1** was measured $[\alpha]_D^{24}$ = -78.3 (c = 0.1, MeOH) and UV maximum at 202 nm (0.1 mg/mL, ε = 7413 L/mol cm).

With all these facts gathered, the structure of deglucoruscin was confirmed and identical to literature data (Mimaki *et al.* 1998 b).

Nr.	**C**	Nr.	**H**
1	83.6	1	3.83 dd (11.9, 3.9)
2	37.4	2	2.73 m*
			2.35 q (11.9)
3	68.2	3	3.87 m*
4	43.9	4	2.69 m*
			2.57 m
5	139.6	5	
6	124.7	6	5.57 m
7	32.0	7	1.87 m*
			1.52 m*
8	33.2	8	1.56 m*
9	50.4	9	1.50 m*
10	42.9	10	
11	24.1	11	2.97 m
			1.62 m*
12	40.3	12	1.51 m*
			1.26 m*
13	40.2	13	
14	56.8	14	1.10 m*
15	32.4	15	1.99 m
			1.42 m*
16	81.5	16	4.50 m*
17	63.0	17	1.70 m*
18	16.7	18	0.84 s
19	15.1	19	1.44 s
20	41.8	20	1.90 m*
21	15.0	21	1.03 d (7.0)
22	109.5	22	
23	33.2	23	1.74 m*
24	29.0	24	2.69 m*
			2.22 m
25	144.5	25	
26	65.0	26	4.44 d (12.1)
			4.00 d (11.9)
27	108.7	27	4.79 s
			4.75 s
1’	100.4	1’	4.71 d (7.3)
2’	75.2	2’	4.59 t (8.1)
3’	76.0	3’	4.14 m*
4’	70.2	4’	4.14 m*
5’	67.4	5’	4.26 dd (12.4, 0.1)
			3.65 d (12.1)
1’’	101.8	1’’	6.34 d (1.0)
2’’	72.6	2’’	4.73 s broad
3’’	72.7	3’’	4.64 dd (9.2, 2.7)
4’’	74.3	4’’	4.32 t (9.4)
5’’	69.5	5’’	4.85 m
6’’	19.1	6’’	1.74 d (6.2)

Table 3.1: ^{1}H and ^{13}C NMR data for compound **1** (δ in ppm, J in Hz, 600 MHz for ^{1}H and 150 MHz for ^{13}C, 298 K, in pyridine d-5, * - overlapping signals)

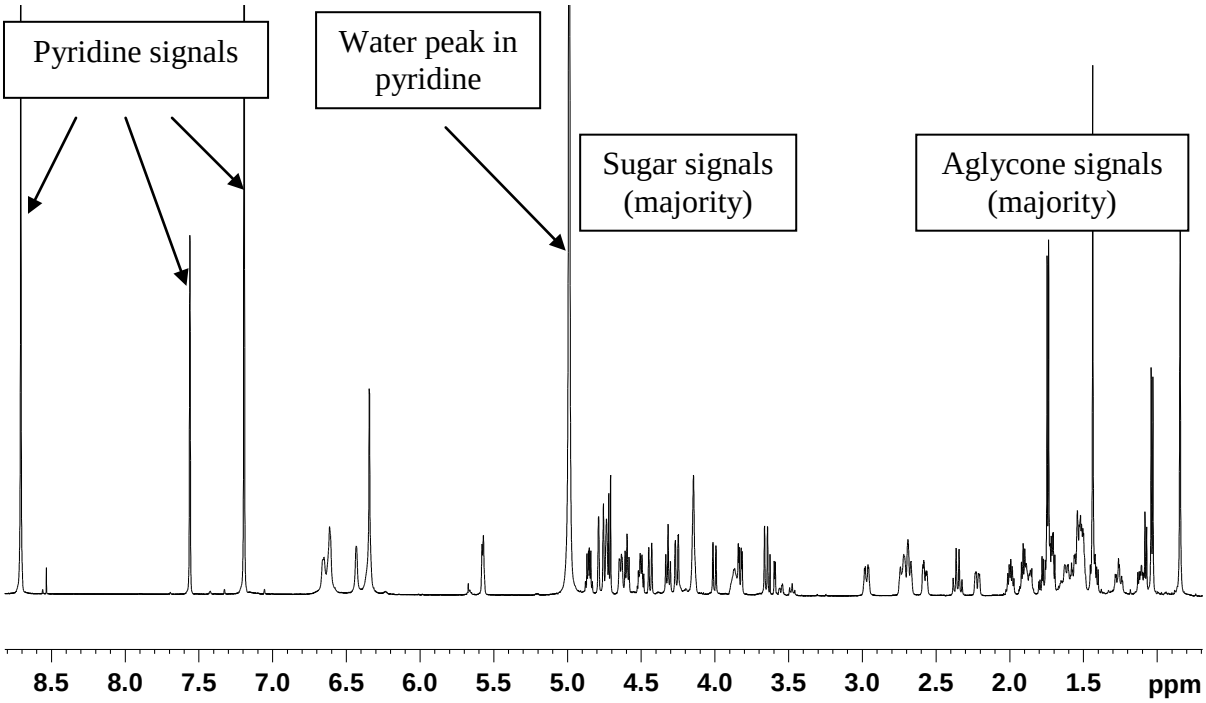

Fig. 3.5: ^{1}H spectrum (pyridine d-5, 600 MHz) of **1** with clearly separated areas of sugar and aglycone signals.. Solvent signals at 7.2 ppm, 7.6 ppm and 8.7 ppm together with water signal in pyridine at 4.9 ppm.

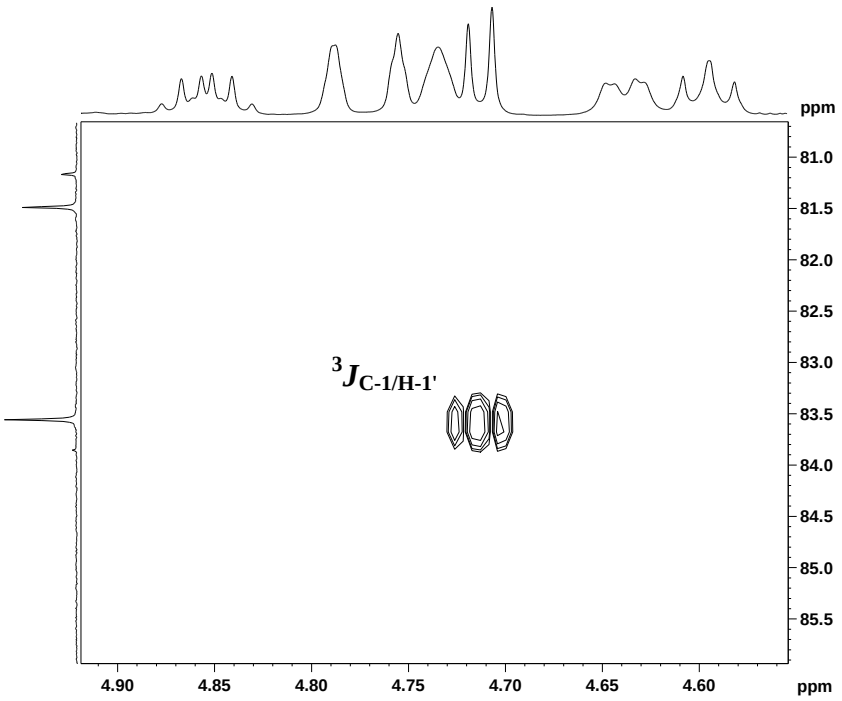

Fig. 3.6: HMBC correlation between C-1 (δ = 83.6 ppm) and H-1' (δ = 4.71 ppm) of **1**, confirming the position of arabinose at C-1 of the aglycone.

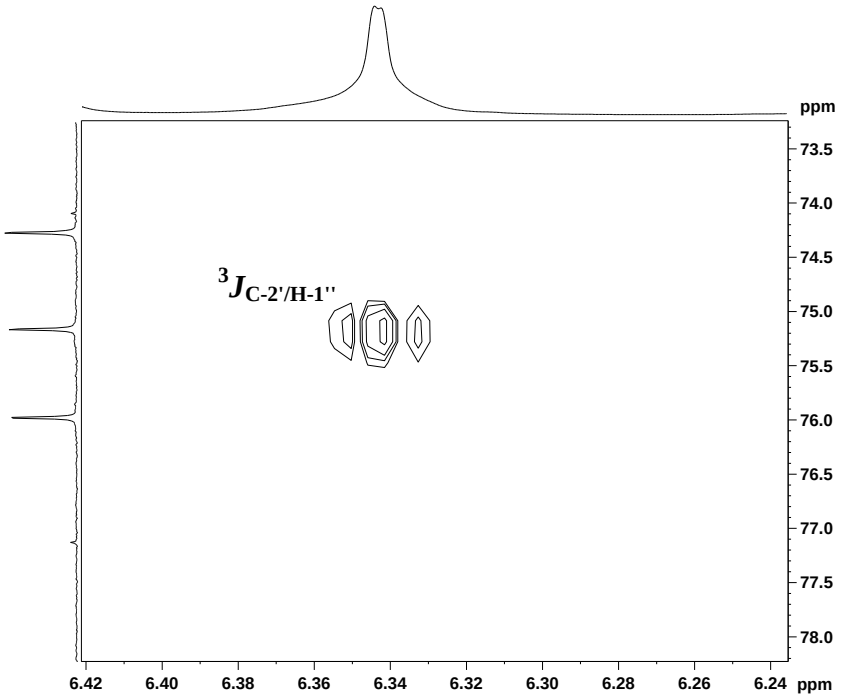

Fig. 3.7: HMBC correlation between C-2' (δ = 75.2 ppm) and H-1" (δ = 6.34 ppm) of **1**, confirming that rhamnose is attached to arabinose at position C-2'.

3.1.3.2 Compound **2** (22-O-methyldeglucoruscoside)

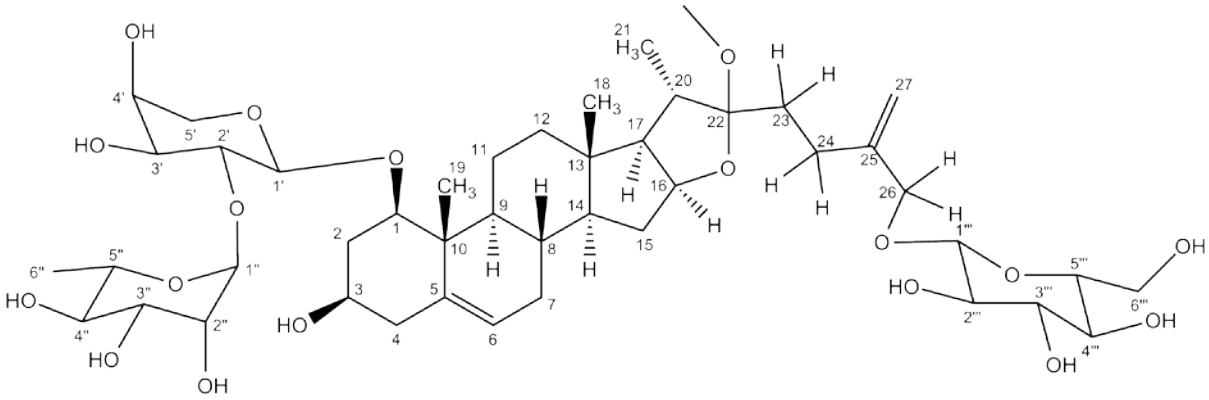

Compound **2** was isolated (227.5 mg) and identified as 22-O methoxylated deglucoruscoside (isolation scheme p. 32). Spots on the TLC chromatograms detected with anisaldehyde reagent were coloured green and exhibited fluorescence spots at 366 nm, which was typical for saponins (Rf = 0.23 in standard system, p. 28).

^{1}H NMR experiment confirmed a saponin structure with characteristic signals for the aglycone between approx 1 - 3 ppm and for the sugar moieties at around 3.5 - 5 ppm. As in all steroid saponins isolated from *Ruscus*, most common signals were the methyl groups of the aglycone. With the *m/z*: 899 $[M-H]^-$ in negative-ion ESI-MS and with data from the literature (Mimaki *et al.* 1998 b), we concluded that the isolated compound is 22-O-methyldeglucoruscoside. Before running the complete 2D NMR analysis, **2** was submitted for freeze drying. During the process of freezing in water and drying on the freeze dryer, **2** decomposed over night into two saponins. Following ESI-MS experiment gave two *m/z* signals, one for original compound at 899 $[M-H]^-$ and one at 885 $[M-H]^-$. After investigating the structure of **2** and considering Kite *et al*., final conclusion was that **2** got de-methylated in water at the position C-22. ^{13}C and 2D NMR spectra of the mixture were performed, but no signal assignments were done due to highly overlapping signals. In order to investigate this transformation process, further testing was planned. (Origin of C-22 hydroxylated and methoxylated compounds p. 38 and p. 112).

3.1.3.3 Compound **3** (Deglucoruscoside)

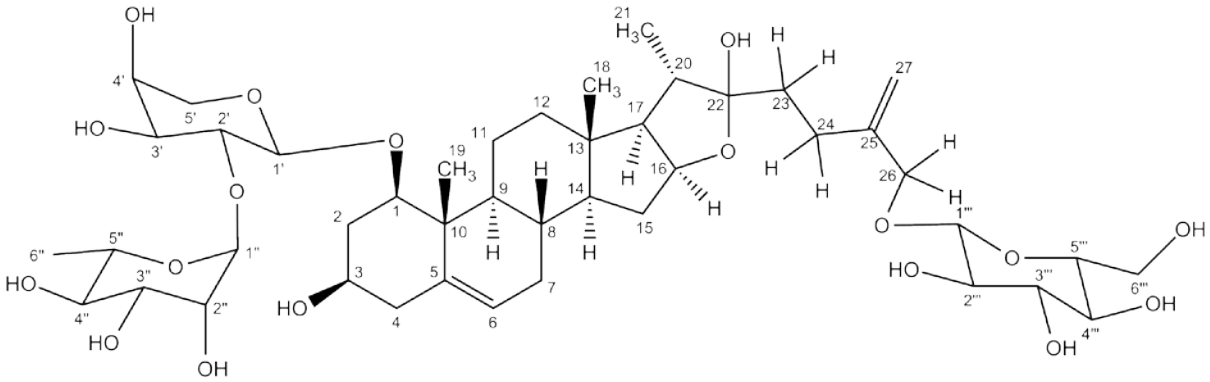

Compound **3** was isolated (10.6 mg) and identified as deglucoruscoside (isolation scheme p. 32). TLC chromatograms sprayed with anisaldehyde reagent gave typical green coloration which was observed as red fluorescence spot under UV at 366 nm (Rf = 0.18 in standard system, p. 28).

^{1}H NMR experiment confirmed a saponin structure with characteristic signals for the aglycone between approx. 1 - 3 ppm and for the sugar moieties at around 3.5 - 5 ppm (**Table 3.2**, p. 59 and **Fig 3.8**, p. 60). Typical signals, such as methyl groups of the aglycone, H_3-18 at δ = 0.90 ppm (s), H_3-19 at δ = 1.44 ppm (s) and H_3-21 at δ = 1.26 ppm (d) were found. Similar to **1**, several signals in ^{13}C experiment also suggested the presence of a neoruscogenin aglycon. C-27 exhibited an exo-methylene group signal resonating at δ = 110.6 ppm. Signals at δ = 139.6 ppm, δ = 124.8 ppm and δ = 147.3 ppm were typical for C-5, C-6 and C-25. Carbon at δ = 83.5 ppm showed correlation to a proton at δ = 3.83 ppm (dd) and was identified as C-1. On the other hand some significant chemical shifts were noted for carbons from C-19 to C-27 in comparison to compound **1**, indicating a different substructure. After analysis of the above mentioned carbon skeleton, using HMBC spectral data, an open ring structure has been confirmed. First clue was the non-present HMBC correlation between C-22 and H-26, which was observed in HMBC of compound **1**. Second fact leading to the final conclusion was a HMBC correlation between C-26 and an anomeric proton, later assigned as H-1'''. An open ring system of the furostanols is only stable with terminal sugar connected to C-26, therefore this signal was crucial for the confirmation of the structure (**Fig. 3.11**, p. 61).

Two more anomeric carbons at δ = 100.4 ppm and δ = 101.8 ppm correlating with protons at δ = 4.71 ppm (d) and δ = 6.34 ppm (s) suggested the presence of two more sugars. Comparing the signals with those from compound **1**, it was expected that arabinose and rhamnose is connected to aglycone at C-1. Sugar signals were assigned using COSY and HMBC where H-1' was identified as the anomeric proton of the arabinose and H-1" as the anomeric proton of the rhamnose. A correlation between H-1' and C-1 in HMBC experiment unambiguously proved that arabinose is attached to the aglycone at C-1 (**Fig. 3.9**, p. 60). Correlation between H-2' and C-1" confirmed the assumption that the rhamnose was attached to the arabinose at C-2' (**Fig. 3.10**, p. 61). Sugar bound to the terminal C-26 carbon was identified as glucose. **3** was confirmed as deglucoruscoside by pseudomolecular ion peak at *m/z*: 885 $[M-H]^-$ in negative-ion ESI-MS and data comparison to literature (Mimaki *et al.* 1998 b).

Absolute stereochemistry via CE showed the presence of L-arabinose, L-rhamnose and D-glucose which were identified as α-L-arabinose, α-L-rhamnose and β-D-glucose after analysing the $^3J_{H\text{-}1'/H\text{-}2'}$ values. $^3J_{H\text{-}1'/H\text{-}2'}$ = 7.4 Hz signified the presence of α-L-arabinose and a very small $^3J_{H\text{-}1''/H\text{-}2''}$ value (could not be measured, therefore H-1' assigned as singlet) confirmed the presence of α-L-rhamnose. $^3J_{H\text{-}1'''/H\text{-}2'''}$ = 7.7 Hz value confirmed the presence of β-D-glucose. For α-D-glucose the *J* value would be much smaller.

Compound **3** was submitted for further analysis concerning the stability and kinetics of C-22 methoxy- and hydroxy- compounds (Origin of C-22 hydroxylated and methoxylated compounds p. 38).

Nr.	**C**	Nr.	**H**
1	83.5	1	3.83 dd (11.9, 3.8)
2	37.4	2	2.73 m*
			2.35 q (11.9)
3	68.2	3	3.86 m*
4	43.9	4	2.69 m*
			2.56 dd (12.7, 3.8)
5	139.6	5	
6	124.8	6	5.56 d (5.7)
7	32.1	7	1.87 m*
			1.49 m*
8	33.2	8	1.53 m*
9	50.4	9	1.50 m*
10	43.0	10	
11	24.1	11	2.98 m
			1.64 m*
12	40.4	12	1.58 m*
			1.29 m*
13	40.5	13	
14	56.8	14	1.12 m*
15	32.7	15	1.99 m
			1.43 m*
16	81.3	16	4.90 m*
17	63.9	17	1.85 m*
18	16.9	18	0.90 s
19	15.1	19	1.44 s
20	40.7	20	2.21 m*
21	16.4	21	1.26 d (6.9)
22	110.4	22	
23	38.0	23	2.21 m*
24	28.4	24	2.68 m*
25	147.3	25	
26	72.1	26	4.58 d (13.3)
			4.31 d (10.7)
27	110.6	27	5.31 s
			5.02 s
1’	100.4	1’	4.72 d (7.4)
2’	75.2	2’	4.60 m*
3’	76.0	3’	4.15 m*
4’	70.2	4’	4.15 s broad
5’	67.4	5’	4.25 d (11.9)
			3.65 d (12.0)
1’’	101.8	1’’	6.34 s
2’’	72.6	2’’	4.74 s broad
3’’	72.7	3’’	4.64 dd (9.3, 3.1)
4’’	74.3	4’’	4.32 m
5’’	69.5	5’’	4.85 m*
6’’	19.1	6’’	1.74 d (6.2)
1’’’	104.0	1’’’	4.87 d (7.7)
2’’’	75.2	2’’’	4.04 m*
3’’’	78.6	3’’’	4.23 m*
4’’’	71.7	4’’’	4.23 m*
5’’’	78.6	5’’’	3.91 m*
6’’’	62.8	6’’’	4.53 d (11.6) br.
			4.37 m*

Table 3.2: ^{1}H and ^{13}C NMR data for compound **3** (δ in ppm, J in Hz, 600 MHz for ^{1}H and 150 MHz for ^{13}C, 298 K, in pyridine d-5, * - overlapping signals)

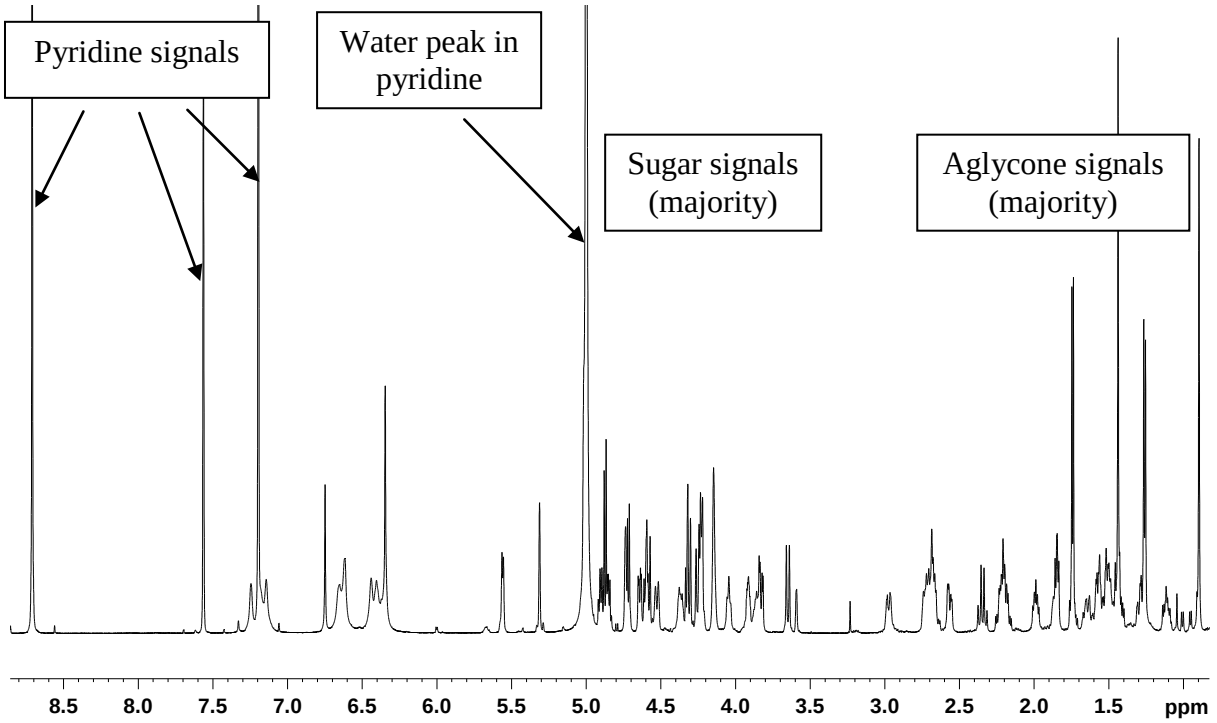

Fig. 3.8: ^{1}H spectrum (pyridine d-5, 600 MHz) of **3** with clearly separated areas of sugar and aglycone signals.

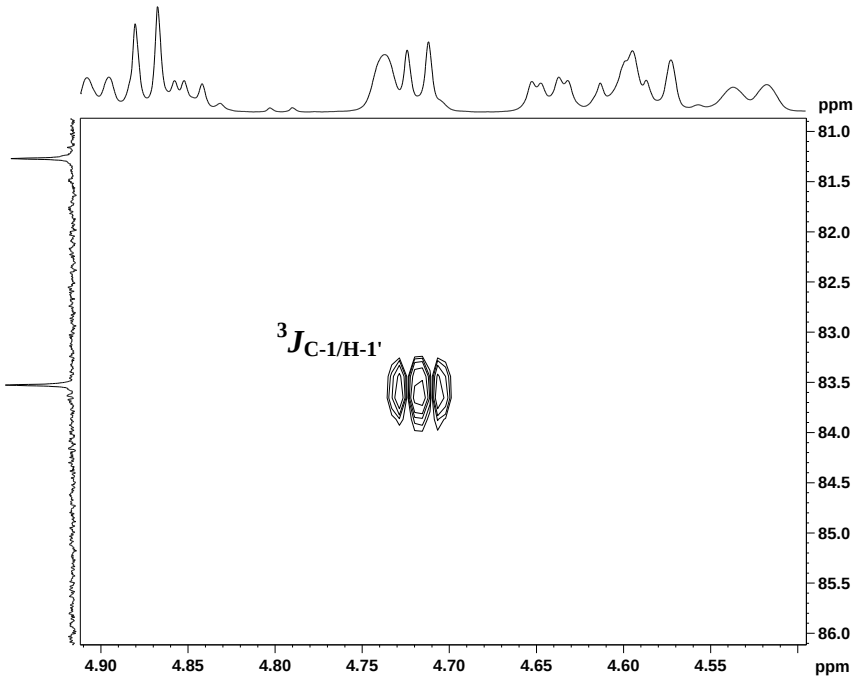

Fig. 3.9: HMBC correlation between C-1 (δ = 83.5 ppm) and H-1' (δ = 4.72 ppm) of **3**, signifying the position of arabinose at position C-1 of the aglycone.

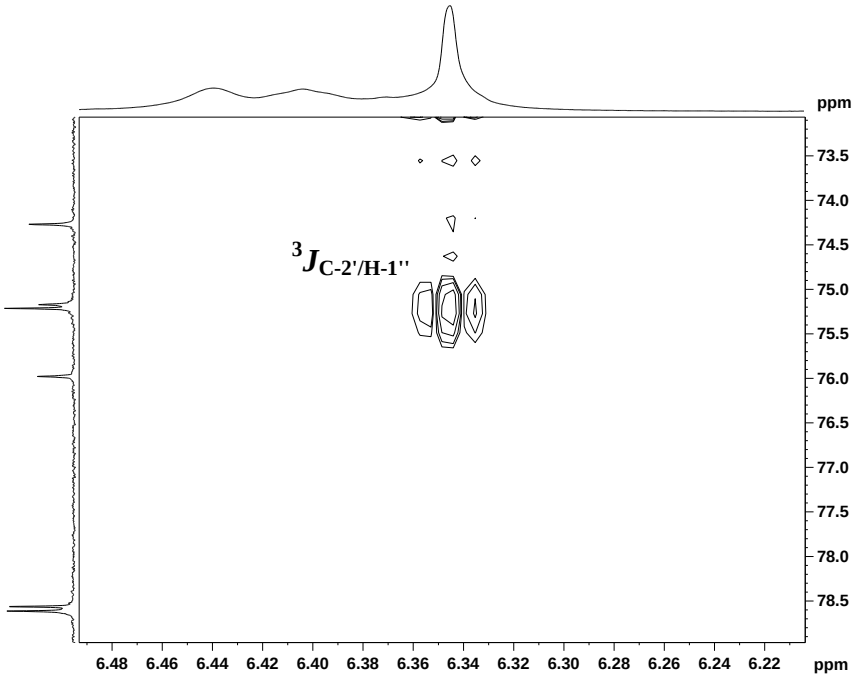

Fig. 3.10: HMBC correlation between C-2' (δ = 75.2 ppm) and H-1" (δ = 6.34 ppm) of **3**, signifying that rhamnose is attached to arabinose at position C-2'.

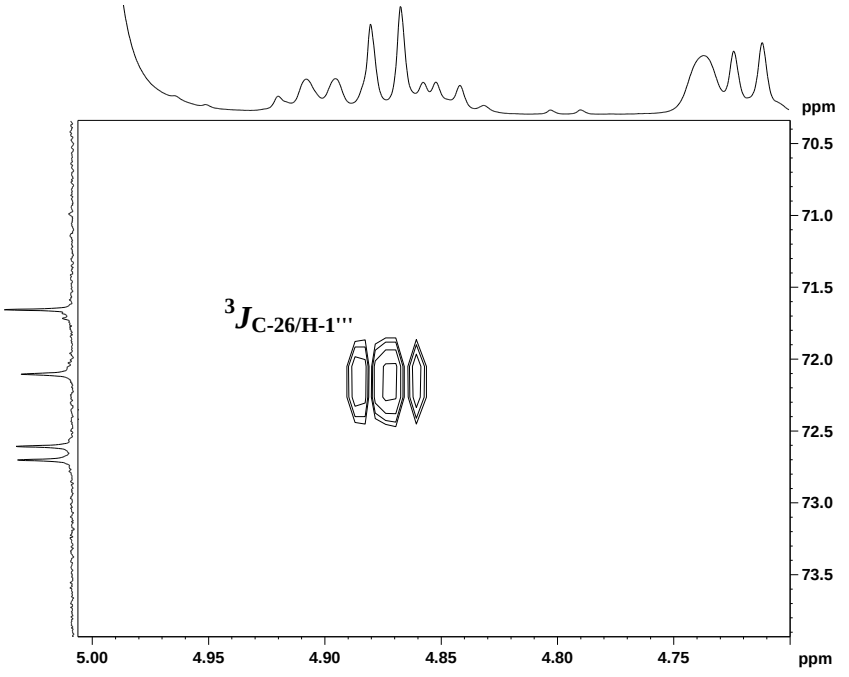

Fig. 3.11: HMBC correlation between C-26 (δ = 72.1 ppm) and H-1''' (δ = 4.87 ppm) of **3**, signifying that glucose is attached to the aglycone at C-26.

3.1.3.4 Compound **4** (3'-O-acetyl-4'-O-sulfodeglucoruscin)

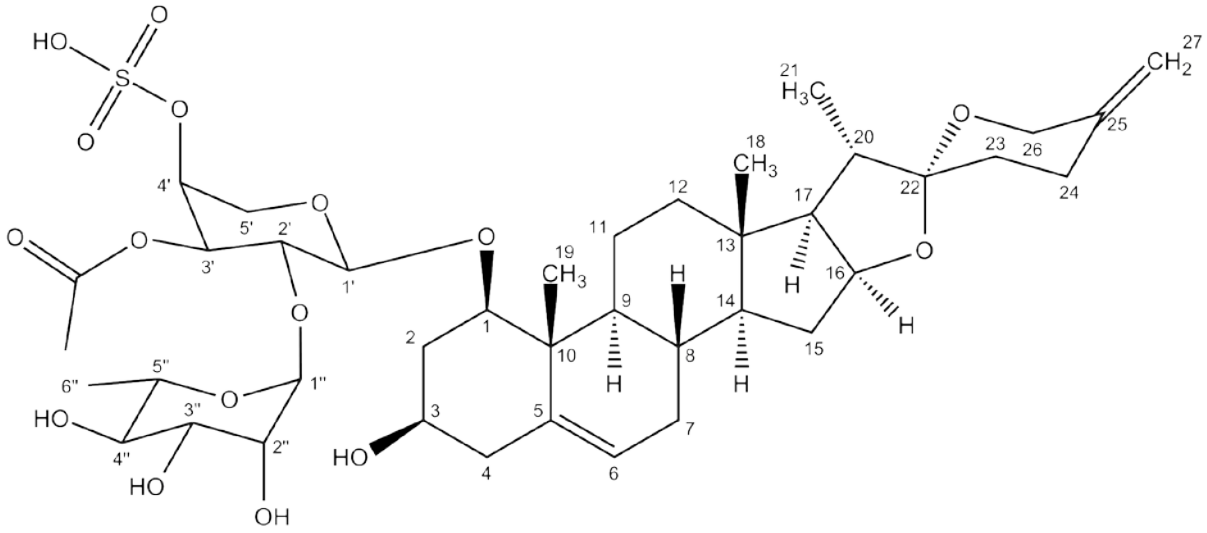

Compound **4** (3.7 mg) was identified as a new saponin and has not been found in nature so far (Rf = 0.63 in standard system, p. 28, colored green after derivatization with anisaldehyde reagent). Several other sulfated and acetylated saponins have been reported and therefore used as a comparison for this compound (Mimaki *et al.* 1998 b).

Like in other saponins, two major signal areas were observed in ^{1}H NMR experiment, the aglycone area ranging between 1 - 3 ppm and the sugar area at around 3.5 - 5 ppm. As for **1**, aglycone was identified to be neoruscogenin with typical methyl groups, C-1, C-5, C-6, C-25 and exo-methylene C-27 carbon. Neoruscogenine skeleton was confirmed via COSY and HMBC experiments as for **1**.

Same as in ^{13}C NMR spectrum of **1**, two signals, at δ = 99.6 ppm and δ = 102.0 ppm, correlating with protons at δ = 4.85 ppm (d) and δ = 5.78 ppm (s) in HSQC, suggested the presence of two sugar moieties. In comparison to proton spectrum of compound **1** a notable shift for some signals of the sugar part have been observed. This was the first hint for structural deviation from **1**.

As in **1**, sugars were identified as rhamnose attached to arabinose (C-2' correlation to H-1" in HMBC, **Fig. 3.14**, p. 66), which is connected to C-1 of the aglycone (C-1 correlation to H-1' in HMBC, **Fig. 3.13**, p. 65). Capillary electrophoresis confirmed the presence of L-arabinose and L-rhamnose (Materials & Methods p. 30 and CE results p. 101). A relatively large $^{3}J_{\text{H-1'/H-}}$

$_{2'}$ value at 6.4 Hz signified the presence of α-L-arabinose and a very small $^{3}J_{\text{H-1''/H-2''}}$ value (could not be measured, therefore H-1' was assigned as singlet) confirmed the presence of α-L-rhamnose.

Carbon signal at δ = 171.0 ppm correlated with methyl group at δ = 21.1 ppm indicated the presence of an acetyl group. Position of the acetyl at C-3' was confirmed via HMBC.

Compound **4** gave a pseudomolecular ion peak at *m/z*: 827 $[M-H]^-$ in negative-ion ESI-MS. Mass (M = 828) was compared to the so far elucidated acetylated deglucoruscin, M = 748. A difference of 81 (calculated for a fragment bound to an hydroxyl group) indicated the presence of a sulfate group. HR-MS for compound **4** showed exact mass of $[M+H]^+$ *m/z* 829.3680 calculated for $C_{40}H_{61}O_{16}S_1$, which confirmed the assumption concerning the sulfate group. A high field shift of the C-4' suggested that the sulfate was bound to this carbon. Due to the fact that C-1' was connected to the aglycone, C-2' to the rhamnose, C-3' with the acetyl group and that C-5' was a methylene group, it was obvious that the sulfate group was bound to the C-4'. Signals for the rhamnose were comparable to those from the literature (Mimaki *et al.* 1998 a/b/c, 1999, 2003, 2008).

The optical rotation of **4** was measured $[\alpha]_D^{24}$ = -93.4 (c = 0.1, MeOH) and UV maximum at 202 nm (0.1 mg/mL, ε = 7634 L/mol cm).

Nr.	**C**	Nr.	**H**
1	83.9	1	3.76 dd (11.9, 3.8)
2	37.4	2	2.67 m*
			2.24 q*
3	68.0	3	3.84 m*
4	43.9	4	2.66 m*
			2.56 m
5	139.4	5	
6	125.0	6	5.56 d (5.6)
7	32.0	7	1.86 m*
			1.52 m*
8	33.2	8	1.54 m*
9	50.2	9	1.42 m*
10	43.0	10	
11	24.1	11	2.83 m
			1.58 m*
12	39.7	12	1.42 m*
			1.17 m*
13	40.1	13	
14	56.6	14	1.07 m*
15	32.4	15	1.98 m
			1.40 m*
16	81.5	16	4.48 m
17	62.8	17	1.65 m*
18	16.6	18	0.82 s
19	15.0	19	1.38 s
20	41.9	20	1.88 m*
21	14.9	21	0.99 d (7.0)
22	109.4	22	
23	33.2	23	1.73 m*
24	29.0	24	2.68 m*
			2.20 m*
25	144.6	25	
26	65.0	26	4.43 d (12.1)
			3.99 d (12.1)
27	108.6	27	4.78 s
			4.74 s
1’	99.6	1’	4.85 d (6.4)
2’	73.5	2’	4.62 m
3’	74.8	3’	5.48 m*
4’	71.5	4’	5.48 m*
5’	64.8	5’	4.72 dd*
			3.80 d*
1’’	102.0	1’’	5.78 s
2’’	72.3	2’’	4.57 m
3’’	72.4	3’’	4.53 dd (9.3, 3.3)
4’’	74.0	4’’	4.29 t (9.4)
5’’	70.2	5’’	4.69 m*
6’’	19.0	6’’	1.75 d (6.1)
-CO-	171.0		
$-CH_3$	21.1		1.98 s
$-HSO_3$			

Table 3.3: ^{1}H and ^{13}C NMR data for compound **4** (δ in ppm, J in Hz, 600 MHz for ^{1}H and 150 MHz for ^{13}C, 298 K, in pyridine d-5, * - overlapping signals)

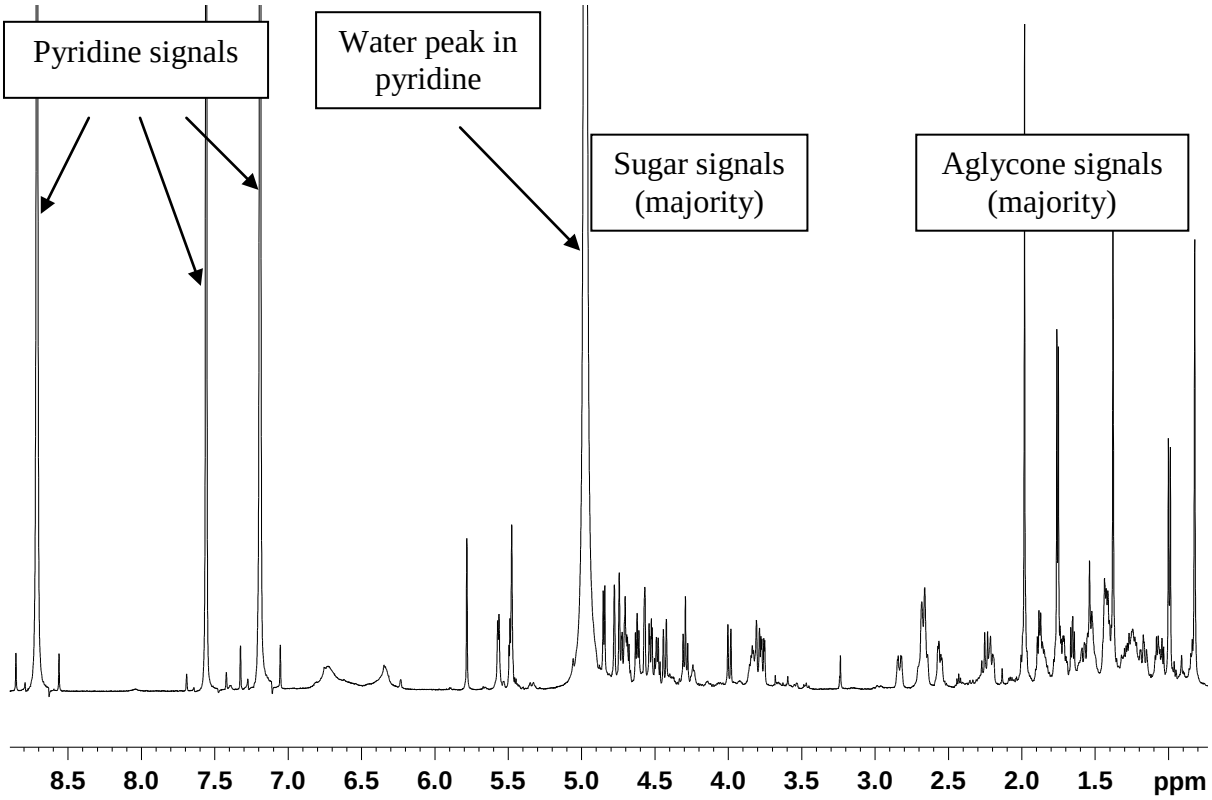

Fig. 3.12: ^{1}H spectrum (pyridine d-5, 600 MHz) of **4** with clearly separated areas of sugar and aglycone signals

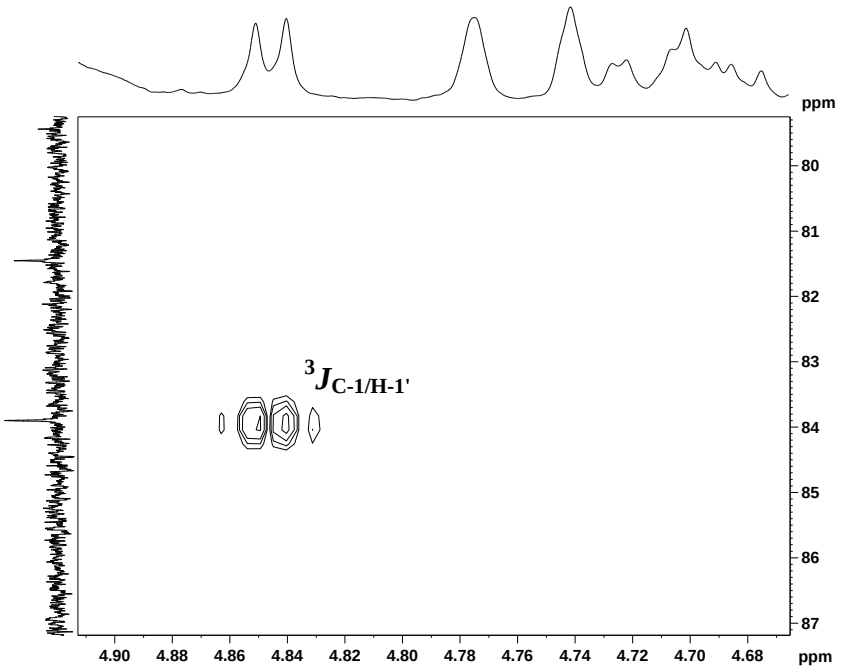

Fig. 3.13: HMBC correlation between C-1 (δ = 83.9 ppm) and H-1' (δ = 4.85 ppm) of **4**, confirming the position of arabinose at position C-1 of the aglycone.

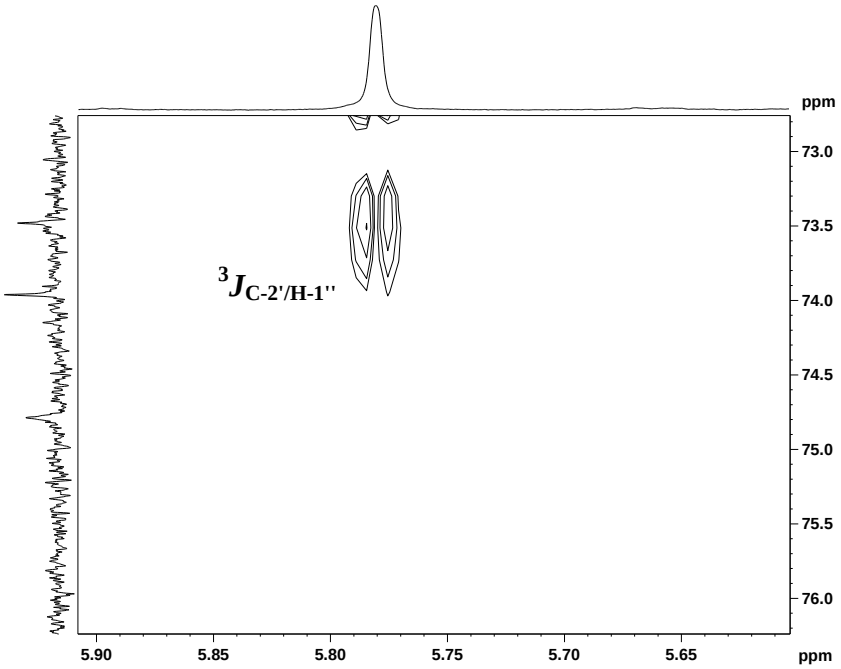

Fig. 3.14: HMBC correlation between C-2' (δ = 73.5 ppm) and H-1" (δ = 5.78 ppm) of **4**, confirming that rhamnose is attached to arabinose at position C-2'.

3.1.3.5 Compound **5** (1-O-sulfo-ruscogenin)

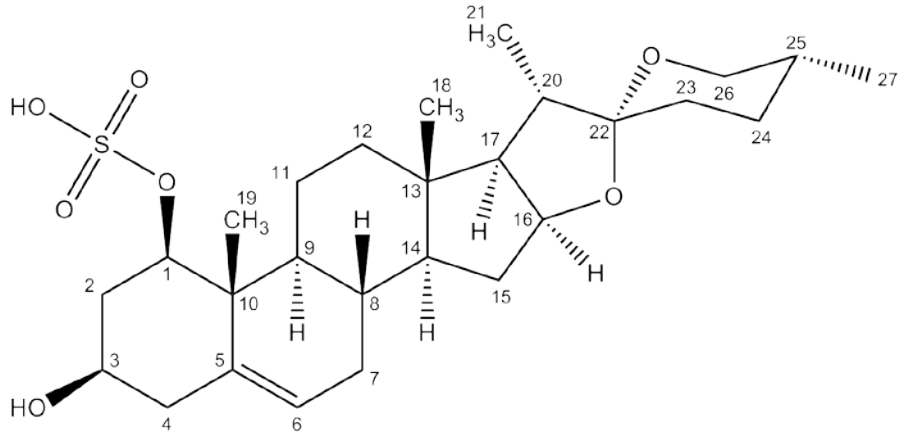

A 1-O sulfated saponin has been isolated and assigned as compound **5** (14.0 mg). ^{1}H NMR experiment confirmed the presence of an aglycone and surprisingly no signals of sugar moieties between 3.5 - 5 ppm. Rf value of **5** on TLC (Rf = 0.55 in standard system, p. 28, colored green after derivatization with anisaldehyde reagent) was similar to those from other isolated saponins indicating that this compound was not an unsubstituted aglycone. This assumption was confirmed by ESI-MS where M = 510 was approved by the pseudomolecular ion at *m/z*: 509 $[M-H]^-$) which is higher in comparison to the molecular weight of neoruscogenin (M = 428).

NMR analysis of the aglycone showed the presence of ruscogenin. In ^{13}C experiment no exo-methylene group was found at around 109 ppm. Additionally, an extra methyl group resonating at δ = 0.67 ppm (d) in proton spectrum and correlated with C-25 in HMBC, was detected. COSY correlation between this methyl group and C-25 suggested ruscogenin skeleton. After comparing the signals with literature (Mimaki *et al.* 1998 a/b/c, 1999, 2003, 2008) and thorough COSY and HMBC analysis of the aglycone, the presence of ruscogenin was confirmed (**Table 3.4**, p. 68 and **Fig 3.15**, p. 69).

Molecular weight of ruscogenin is M = 430, leaving a total mass of 81 (510-(430-1)) for the attached substituent. Several sulfated compounds have already been isolated from *R. aculeatus* and therefore the presence of an O-sulfo ruscogenin was taken into consideration. A very pronounced downfield shift of C-1 (δ = 84.2 ppm), comparable to 1-O glycosides, signified that the sulfate was connected to the ruscogenin via C-1.

A potassium salt of **5** has already been found and published. (Oulad-Ali *et al.* 1996)

Optical rotation of **5** was measured $[\alpha]_D^{24}$ = -53.2 (c = 0.1, MeOH) and UV maximum at 202 nm (0.1 mg/mL, ε = 4702 L/mol cm).

Nr.	**C**	Nr.	**H**
1	84.2	1	4.75 dd (11.9,4.2)
2	39.8	2	3.52 m*
			2.29 q (11.9)
3	68.0	3	3.88 m
4	43.7	4	2.65 m
			2.54 m
5	139.0	5	
6	125.2	6	5.55 d (5.8)
7	31.9	7	1.83 m*
			1.45 m*
8	33.1	8	1.54 m*
9	49.9	9	1.70 m*
10	43.2	10	
11	23.7	11	3.06 m
			1.61 m*
12	40.7	12	1.67 m*
			1.32 m*
13	40.2	13	
14	56.7	14	1.07 m*
15	32.4	15	1.99 m*
			1.42 m*
16	81.1	16	4.5 m
17	63.1	17	1.70 m*
18	16.7	18	0.83 s
19	14.8	19	1.29 s
20	41.9	20	1.89 m*
21	15.1	21	1.08 d (7.0)
22	109.3	22	
23	31.9	23	1.66 m*
			1.61 m*
24	29.3	24	1.54 m*
25	30.6	25	1.55 m*
26	66.8	26	3.55 m*
			3.48 m*
27	17.3	27	0.67 d (5.6)

Table 3.4: ^{1}H and ^{13}C NMR data for compound **5** (δ in ppm, J in Hz, 600 MHz for ^{1}H and 150 MHz for ^{13}C, 298 K, in pyridine d-5, * - overlapping signals)

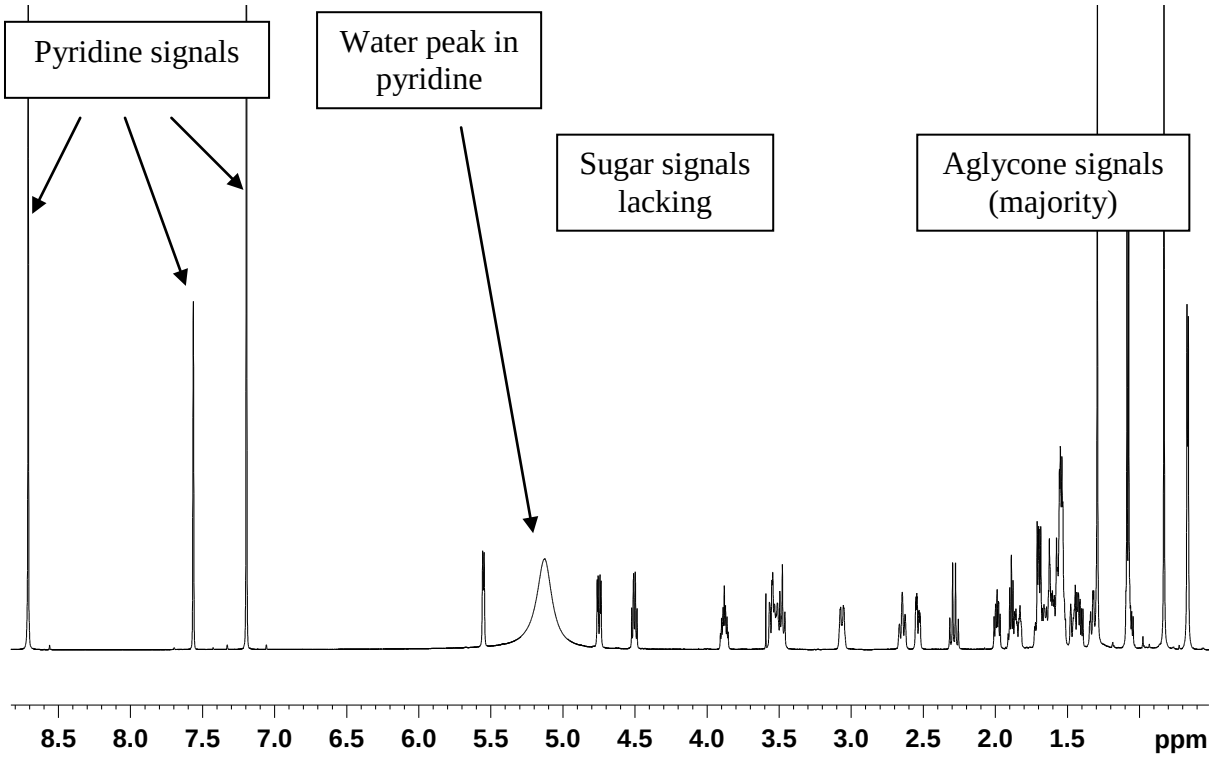

Fig. 3.15: ^{1}H spectrum (pyridine d-5, 600 MHz) of **5** with signals of the aglycone part and missing sugar signals in comparison to compound **1**.

3.1.3.6 Compound **6** (4'-O-(2-hydroxy-3-methylpentanoyl)-deglucoruscin)

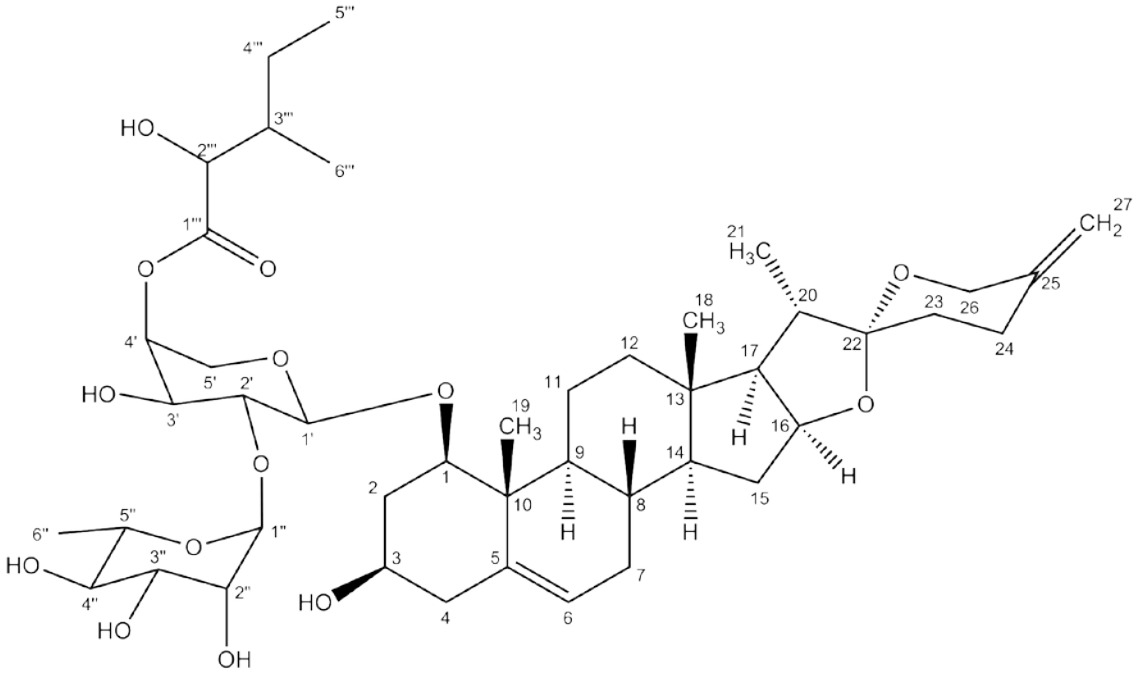

Compound **6** (13.4 mg) was found to be a new steroidal saponin (Rf = 0.68 in standard system, p. 28, colored green with anisaldehyde reagent). Signals in ^{13}C experiment indicated the presence of a neoruscogenin aglycone with two sugars attached (**Table 3.5**, p. 71 and **Fig. 3.16**, p. 72). Further NMR analysis (see **1**, p. 51) showed the presence of rhamnose attached to arabinose (C-2' correlation to H-1" in HMBC, **Fig. 3.18**, p. 73), which is connected to C-1 of the aglycone (C-1 correlation to H-1' in HMBC, **Fig. 3.17**, p. 72). CE showed the presence of L-arabinose and L-rhamnose (p. 30 and 101). A relatively large $^{3}J_{H\text{-}1'/H\text{-}2'}$ was observed, but could not be determined due to overlapping, signified the presence of α-L-arabinose. A very small $^{3}J_{H\text{-}1''/H\text{-}2''}$ value (could not be measured, therefore H-1' assigned as singlet) confirmed the presence of α-L-rhamnose. Additional aliphatic side chain was considered due to presence of additional carbons not belonging to a sugar skeleton. Hydroxylated carbons exhibited normally chemical shift values between δ = 70 - 75 ppm in ^{13}C spectrum with anomeric carbons resonating at around δ = 100 ppm. A low field signal at δ = 175.1 ppm suggested the presence of an acetyl group. COSY and HMBC were used to determine the side chain as a 2-hydroxy-3-methylpentanoat connected to the arabinose via C-4' (**Fig. 3.19**, p. 73). Negative-ion ESI-MS gave *m/z*: 819 $[M\text{-}H]^-$. Optical rotation of **6** was measured $[\alpha]_D^{24}$ = -34.7 (c = 0.1, MeOH) and UV maximum at 202 nm (0.1 mg/mL, ε = 6396 L/mol cm).

Nr.	**C**	Nr.	**H**
1	83.0	1	3.82 dd (12.0, 3.8)
2	37.3	2	2.67 m*
			2.35 q (12.0)
3	68.2	3	3.86 m
4	43.8	4	2.69 m*
			2.58 dd (12.7, 3.5)
5	139.5	5	
6	124.7	6	5.58 d (5.7)
7	31.9	7	1.89 m*
			1.52 m*
8	33.1	8	1.59 m
9	50.3	9	1.53 m*
10	42.8	10	
11	24.3	11	2.99 m
			1.74 m*
12	40.6	12	1.90 m*
			1.43 m*
13	40.4	13	
14	57.0	14	1.13 m*
15	32.4	15	2.01 m
			1.46 m*
16	81.5	16	4.51 m
17	63.1	17	1.81 m*
18	16.9	18	0.95 s
19	15.0	19	1.43 s
20	41.9	20	2.01 m
21	15.0	21	1.16 d (7.0)
22	109.5	22	
23	33.3	23	1.79 m
24	29.0	24	2.71 m*
			2.23 m
25	144.5	25	
26	65.0	26	4.45 d (12.2)
			4.00 d (12.1)
27	108.7	27	4.79 s
			4,76 s
1’	99.9	1’	4.70 d*
2’	75.3	2’	4.41 dd (9.1, 7.8)
3’	73.7	3’	4.28 m*
4’	73.1	4’	5.53 s
5’	64.6	5’	4.13 dd (13.0, 1.9)
			3.67 d (12.8)
1’’	102.1	1’’	6.22 s
2’’	72.5	2’’	4.69 m
3’’	72.7	3’’	4.59 dd*
4’’	74.3	4’’	4.31 t (9.5)
5’’	69.6	5’’	4.82 m
6’’	19.2	6’’	1.76 d (6.2)
1’’’	175.1	1’’’	
2’’’	75.8	2’’’	4.6 m*
3’’’	39.7	3’’’	2.28 m
4’’’	24.7	4’’’	2.07 m
			1.62 m*
5’’’	16.1	5’’’	1.27 d (6.8)
6’’’	12.2	6’’’	1.07 d (7.4)

Table 3.5: ^{1}H and ^{13}C NMR data for compound **6** (δ in ppm, J in Hz, 600 MHz for ^{1}H and 150 MHz for ^{13}C, 298 K, in pyridine d-5, * - overlapping signals)

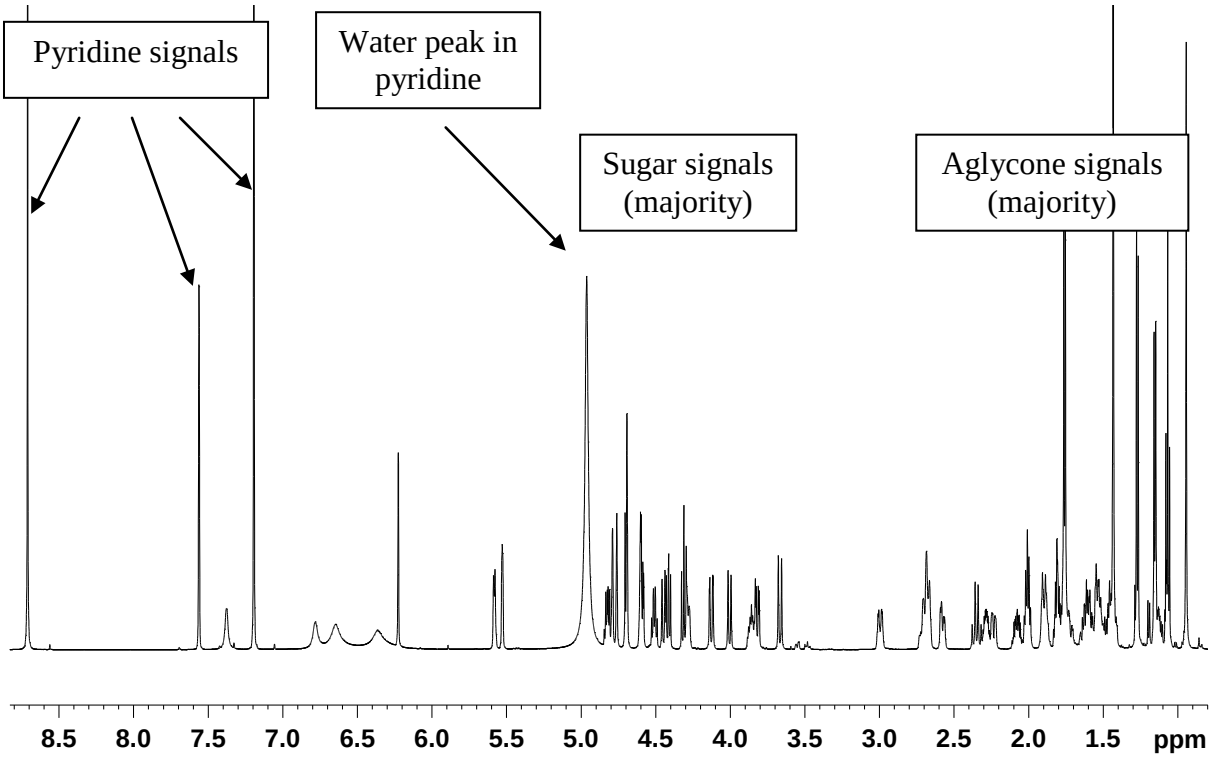

Fig. 3.16: ^{1}H spectrum (pyridine d-5, 600 MHz) of **6** with clearly separated areas of sugar and aglycone signals.

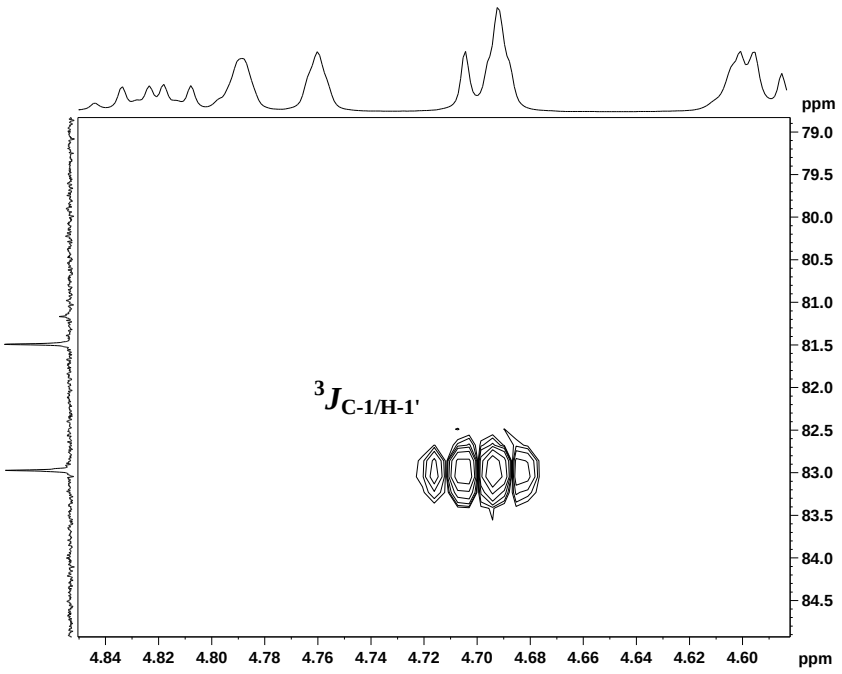

Fig. 3.17: HMBC correlation between C-1 (δ = 83.0 ppm) and H-1' (δ = 4.70 ppm) of **6**, signifying the position of arabinose at position C-1 of the aglycone.

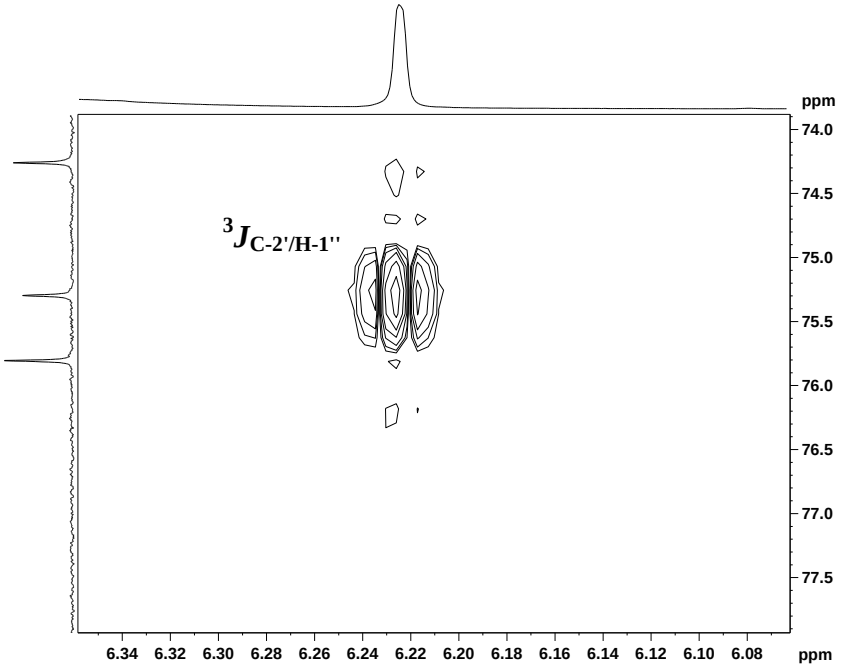

Fig. 3.18: HMBC correlation between C-2' (δ = 75.3 ppm) and H-1" (δ = 6.22 ppm) of **6**, signifying that rhamnose is attached to arabinose at position C-2'.

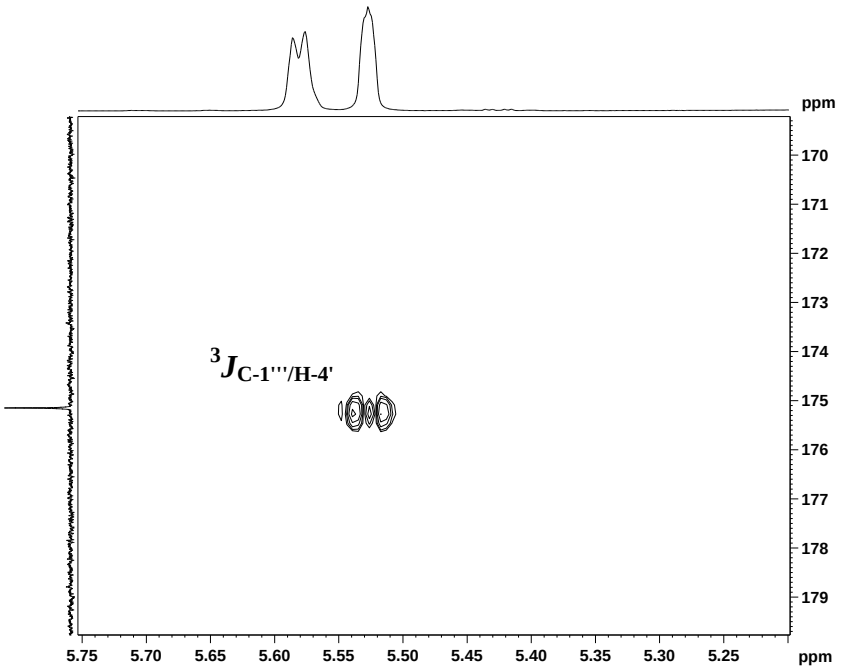

Fig. 3.19: HMBC correlation between C-1''' (δ = 175.1 ppm) and H-4' (δ = 5.53 ppm) of **6**, signifying that 2-hydroxy-3-methylpentanoat is connected to the arabinose via C-4'.

3.1.3.7 Compound **7** (4'-O-acetyl-deglucoruscin)

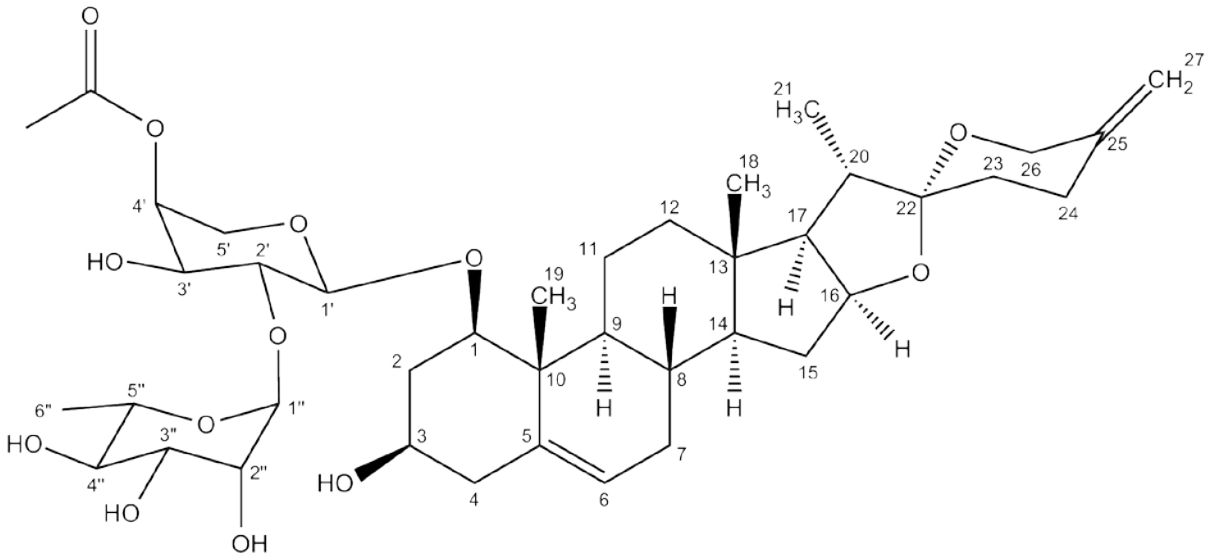

Compound **7** (1.8 mg) has been reported for the first time (Rf = 0.68 in standard system, p. 28, colored green after derivatization with anisaldehyde reagent). Carbon spectrum was compared to the spectrum of **1** (see **1**, p. 51) and suggested the presence of neoruscogenin as aglycone. The structure of neoruscogenine exhibiting a typical signal pattern in ^{13}C and ^{1}H NMR spectrum (see **1**, p. 51) was confirmed via COSY and HMBC experiments. Thorough NMR analysis showed the presence of rhamnose attached to arabinose (C-2' correlation to H-1" in HMBC, **Fig. 3.22**, p. 77), which is connected to C-1 of the aglycone (C-1 correlation to H-1' in HMBC, **Fig. 3.21**, p. 76). Capillary electrophoresis confirmed this assumption by showing the presence of L-arabinose and L-rhamnose (Materials & Methods p. 30 and CE results p. 101). A relatively large $^{3}J_{\text{H-1'/H-2'}}$ at 7.4 Hz signified the presence of α-L-arabinose and a very small $^{3}J_{\text{H-1"/H-2"}}$ value (too small to be visible in the ^{1}H NMR spectrum, therefore H-1' was assigned as singlet) indicated the presence of α-L-rhamnose.

Carbon at 170.9 ppm showing correlations with the protons of the methyl group resonating at 1.98/21.0 ppm in HMBC experiment showed the presence of an acetyl group (**Fig. 3.23**, p. 77). Due to low amount of **7**, no clear correlation between carboxyl group (δ = 170.9 ppm) and H-4' was found. Position of acetyl group at C-4' was assigned due to high shift of H-4' in proton spectrum. With the negative-ion ESI-MS with *m/z*: 747 $[M-H]^-$ a 4'-O acetylated deglucoruscin structure was confirmed. Optical rotation of **7** $[\alpha]_D^{24}$ = -39.5 (c = 0.1, MeOH) and UV maximum at 202 nm (0.1 mg/mL, ε = 6725 L/mol cm) were measured.

Nr.	**C**	Nr.	**H**
1	83.2	1	3.79 dd (12.1, 3.8)
2	37.5	2	2.66 m*
			2.38 q (12.0)
3	68.2	3	3.86 m
4	43.7	4	2.68 m*
			2.58 dd (12.5, 3.8)
5	139.4	5	
6	124.3	6	5.58 d (5.3)
7	31.9	7	1.89 m*
			1.54 m*
8	33.1	8	1.58 m*
9	50.3	9	1.54 m
10	42.6	10	
11	24.4	11	2.96 m
			1.68 m*
12	40.5	12	1.74 m*
			1.34 m*
13	40.3	13	
14	57.1	14	1.13 m
15	32.3	15	2.01 m*
			1.46 m*
16	81.4	16	4.51 m*
17	63.1	17	1.75 m*
18	16.9	18	0.92 s
19	15.0	19	1.43 s
20	41.8	20	1.96 m*
21	14.9	21	1.07 d (6.9)
22	109.5	22	
23	33.2	23	1.76 m*
24	29.0	24	2.70 m*
			2.23 m
25	144.4	25	
26	65.0	26	4.45 d* (12.4) 4.01 d (12.1)
27	108.6	27	4.78 d (19.2)
1’	100.0	1’	4.67 d (7.4)
2’	75.3	2’	4.47 m*
3’	73.7	3’	4.25 m*
4’	73.2	4’	5.38 s
5’	64.3	5’	4.22 dd (13.1, 1.8)
			3.63 d (12.9)
1’’	102.0	1’’	6.31 s
2’’	72.5	2’’	4.71 s (Br)
3’’	72.7	3’’	4.60 dd (9.3, 3.0)
4’’	74.2	4’’	4.32 t (9.4)
5’’	69.6	5’’	4.86 m*
6’’	19.2	6’’	1.78 d (6.1)
-CO-	170.9		
$-CH_3$	21.0		1.98 s

Table 3.6: ^{1}H and ^{13}C NMR data for compound **7** (δ in ppm, J in Hz, 600 MHz for ^{1}H and 150 MHz for ^{13}C, 298 K, in pyridine d-5, * - overlapping signals)

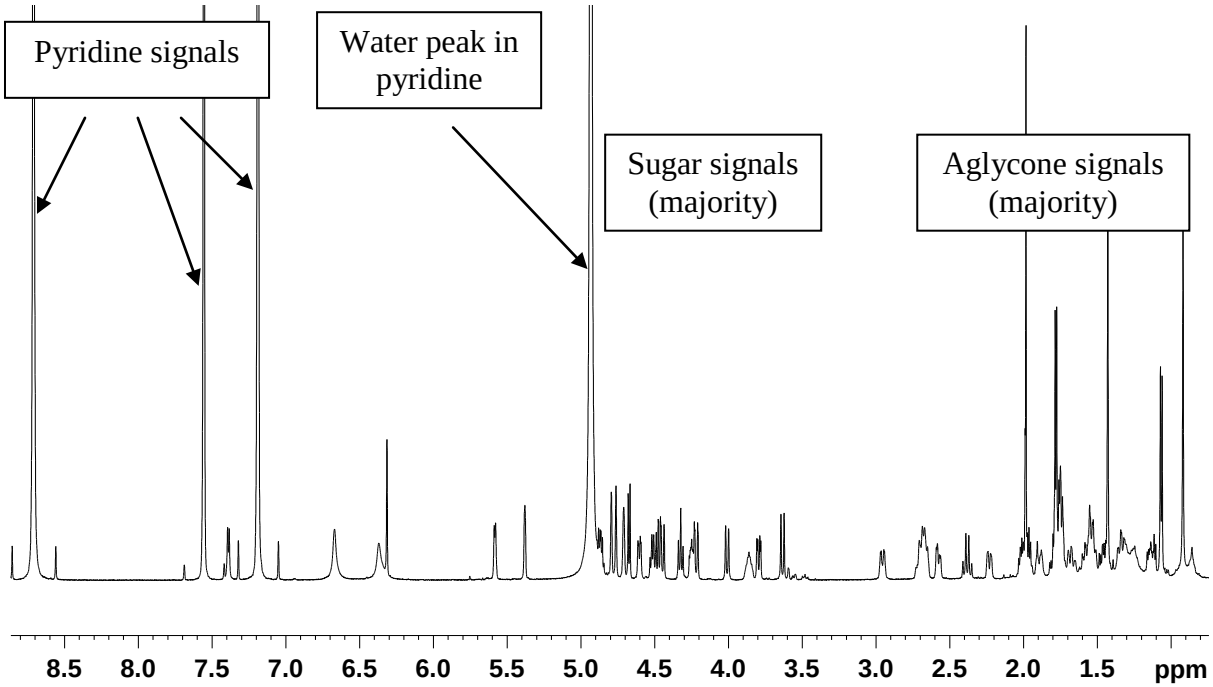

Fig. 3.20: ^{1}H spectrum (pyridine d-5 600 MHz) of **7** with clearly separated areas of sugar and aglycone signals.

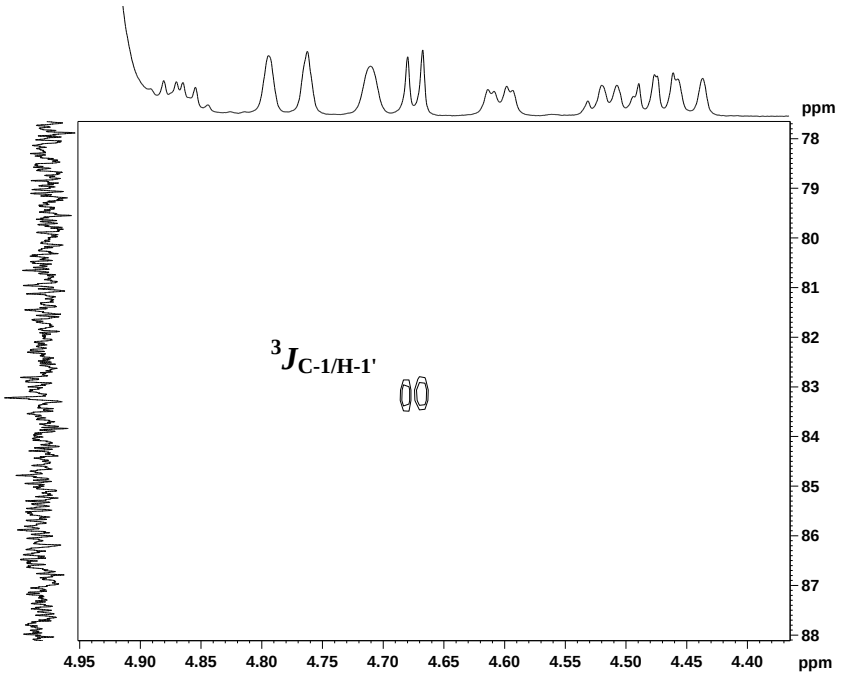

Fig. 3.21: HMBC correlation between C-1 (δ = 83.2 ppm) and H-1' (δ = 4.67 ppm) of **7**, confirming the position of arabinose at position C-1 of the aglycone.

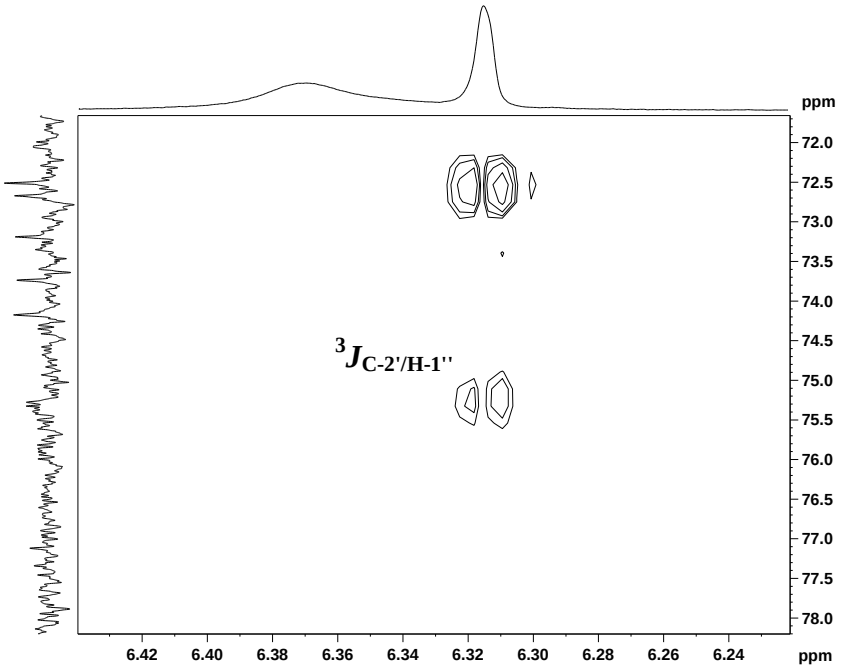

Fig. 3.22: HMBC correlation between C-2' (δ = 75.3 ppm) and H-1" (δ = 6.31 ppm) of **7**, confirming that rhamnose is attached to arabinose at position C-2'.

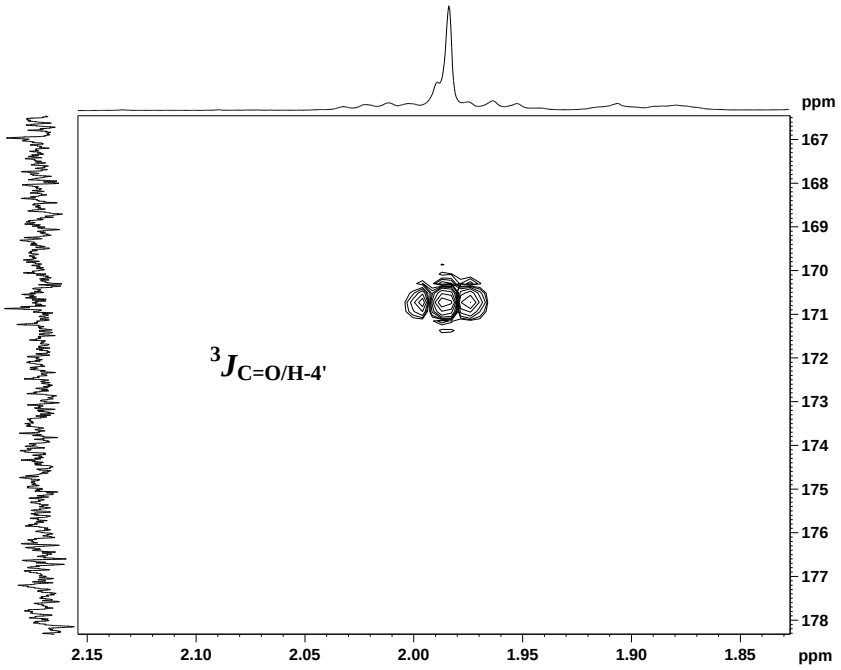

Fig. 3.23: HMBC correlation between carboxyl group (δ = 170.9 ppm) and methyl group (δ = 1.98 ppm) of **7**.

3.1.3.8 Compound **8** (Ruscin)

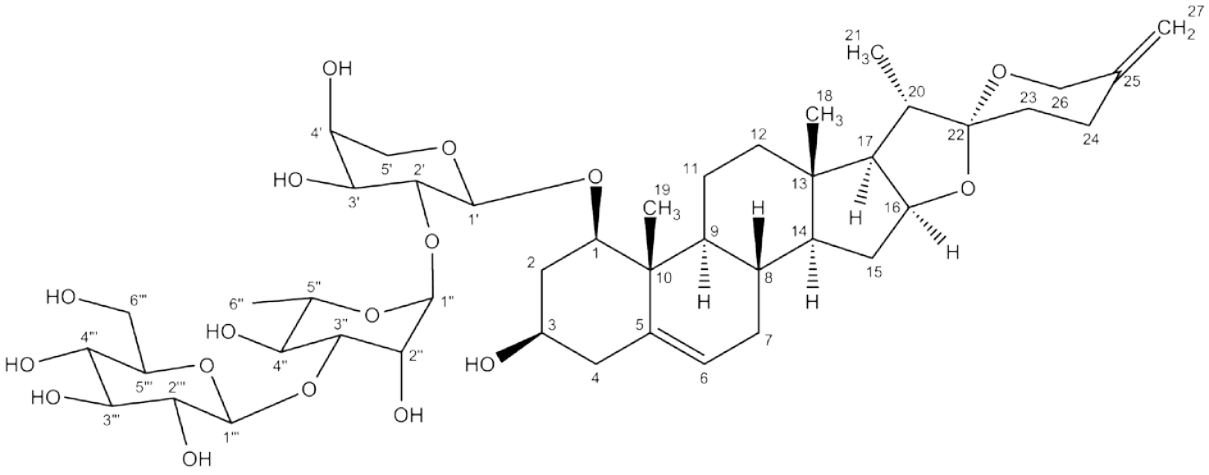

Compound **8** (87.4 mg) was identified as one of the most abundant steroid saponins from *R. aculeatus*, namely ruscin (Rf = 0.39 in standard system, p. 28, colored green after derivatization with anisaldehyde reagent). As in **1**, aglycone was identified as the neoruscogenine. Typical signals, such as methyl groups of the aglycone, H_3-18 at δ = 0.83 ppm (s), H_3-19 at δ = 1.45 ppm (s) and H_3-21 at δ = 1.07 ppm (d) were found in ^{1}H spectrum. In the ^{13}C spectrum a signal an exo-methylene group was found at δ = 110.6 ppm belonging to C-27. Signals at δ = 139.5 ppm, δ = 124.8 ppm and δ = 144.5 ppm are typical for C-5, C-6 and C-25. A carbon resonating at δ = 84.8 ppm that showed correlation to a proton at δ = 3.73 ppm (dd) in HSQC was identified as C-1 and is also a very characteristic signal for neoruscogenin (Mimaki *et al.* 1998 b).

Three signals, at δ = 101.2 ppm, at δ = 101.3 ppm and at δ = 106.6 ppm, correlating with protons at δ = 4.60 ppm (d), δ = 6.36 ppm (s) and δ = 5.65 ppm (d), most likely belong to anomeric protons and carbons and suggested the presence of three sugars. As 27 carbons belong to the neoruscogenin skeleton, the remaining 17 signals also indicated the presence of three sugars, two hexoses and one pentose. Further NMR analysis (see **1**, p. 51) showed the presence of glucose attached to rhamnose (C-3" correlation to H-1'" in HMBC, **Fig. 3.27**, p. 82) attached to arabinose (C-2' correlation to H-1" in HMBC, **Fig. 3.26**, p. 82), which is connected to C-1 of the aglycone (C-1 correlation to H-1' in HMBC, **Fig. 3.25**, p. 81). Capillary electrophoresis confirmed the presence of L-arabinose, L-rhamnose and D-glucose (Materials & Methods p. 30 and CE results p. 101). A relatively large $^{3}J_{\text{H-1'/H-2'}}$ was observed

(not measured due to overlapping), which indicated the presence of α-L-arabinose and a very small $^{3}J_{H\text{-}1''/H\text{-}2''}$ value (not visible in the ^{1}H NMR spectrum, therefore H-1' was assigned as singlet) signified α-L-rhamnose. $^{3}J_{H\text{-}1'''/H\text{-}2'''} = 7.9$ confirmed the presence of β-D-glucose.

A pseudomolecular ion peak at *m/z*: 867 $[M\text{-}H]^-$ in negative-ion ESI-MS confirmed compound **8** as ruscin (Hänsel & Sticher 2007).

Optical rotation of **8** $[\alpha]_D^{24}$ = -91.0 (c = 0.1, MeOH) and UV maximum at 201 nm (0.1 mg/mL, ε = 10364 L/mol cm) were measured.

Nr.	**C**	Nr.	**H**
1	84.8	1	3.73 dd (11.9, 4.0)
2	38.1	2	2.75 m*
			2.45 q (11.9)
3	68.2	3	3.85 m
4	43.8	4	2.69 m*
			2.55 dd (12.8, 3.1)
5	139.5	5	
6	124.8	6	5.55 d (5.7)
7	32.0	7	1.85 m*
			1.51 m*
8	33.0	8	1.54 m*
9	50.5	9	1.47 m*
10	42.9	10	
11	23.9	11	2.96 m
			1.59 m*
12	40.3	12	1.49 m*
			1.25 dt (6.4, 3.5)
13	40.2	13	
14	56.8	14	1.09 m
15	32.3	15	1.98 m
			1.42 m*
16	81.4	16	4.49 m*
17	63.0	17	1.71 m*
18	15.0	18	0.83 s
19	16.7	19	1.45 s
20	41.8	20	1.89 m*
21	15.1	21	1.02 d (7.0)
22	109.4	22	
23	33.2	23	1.74 m*
24	28.9	24	2.68 m*
			2.21 m
25	144.5	25	
26	64.9	26	4.43 d (12.2)
			4.00 d (12.1)
27	108.6	27	4.76 d (19.9)
1’	101.2	1’	4.60 d*
2’	74.2	2’	4.57 m*
3’	76.2	3’	4.09 m*
4’	78.3	4’	4.12 m*
5’	67.7	5’	4.24 d*
			3.63 d (11.8)
1’’	101.3	1’’	6.36 s
2’’	72.1	2’’	4.95 m
3’’	82.7	3’’	4.87 dd (9.5, 2.9)
4’’	73.3	4’’	4.52 m*
5’’	69.3	5’’	4.90 m*
6’’	18.7	6’’	1.66 d (6.2)
1’’’	106.6	1’’’	5.65 d (7.9)
2’’’	76.1	2’’’	4.09 m*
3’’’	78.3	3’’’	4.23 m*
4’’’	71.7	4’’’	4.23 m*
5’’’	70.2	5’’’	4.12 m*
6’’’	62.5	6’’’	4.48 m*
			4.43 m*

Table 3.7: ^{1}H and ^{13}C NMR data for compound **8** (δ in ppm, J in Hz, 600 MHz for ^{1}H and 150 MHz for ^{13}C, 298 K, in pyridine d-5, * - overlapping signals)

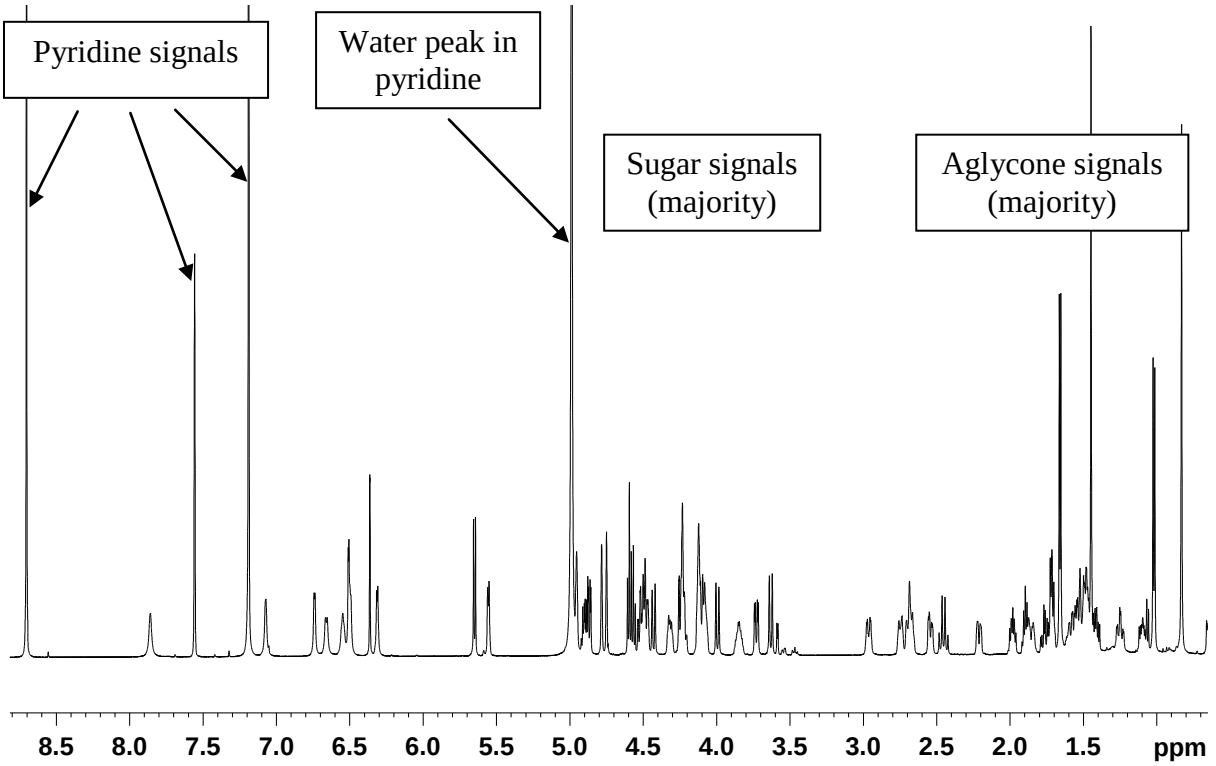

Fig. 3.24: ^{1}H spectrum (pyridine d-5, 600 MHz) of **8** with clearly separated areas of sugar and aglycone signals.

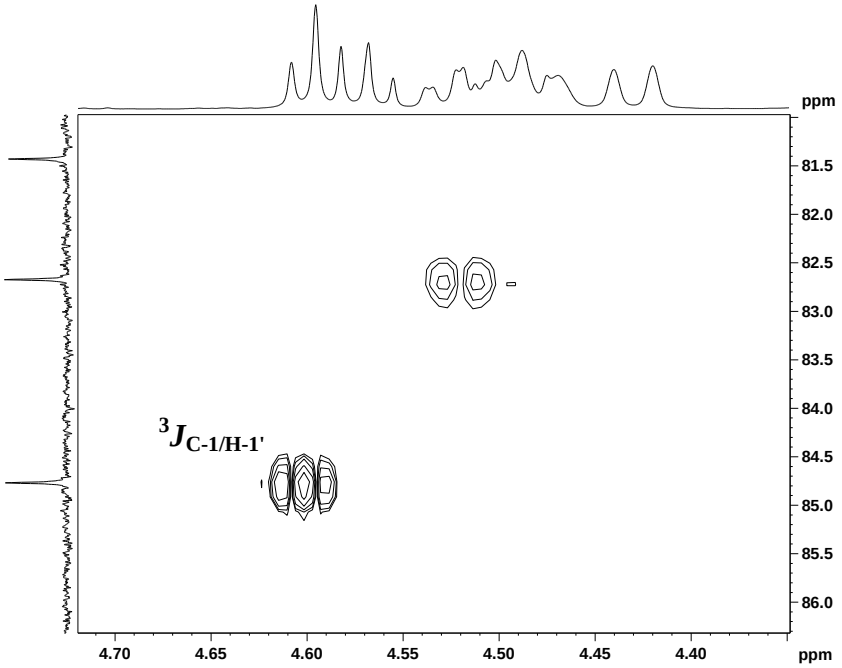

Fig. 3.25: HMBC correlation between C-1 (δ = 84.8 ppm) and H-1' (δ = 4.60 ppm) of **8**, confirming the position of arabinose at C-1 of the aglycone.

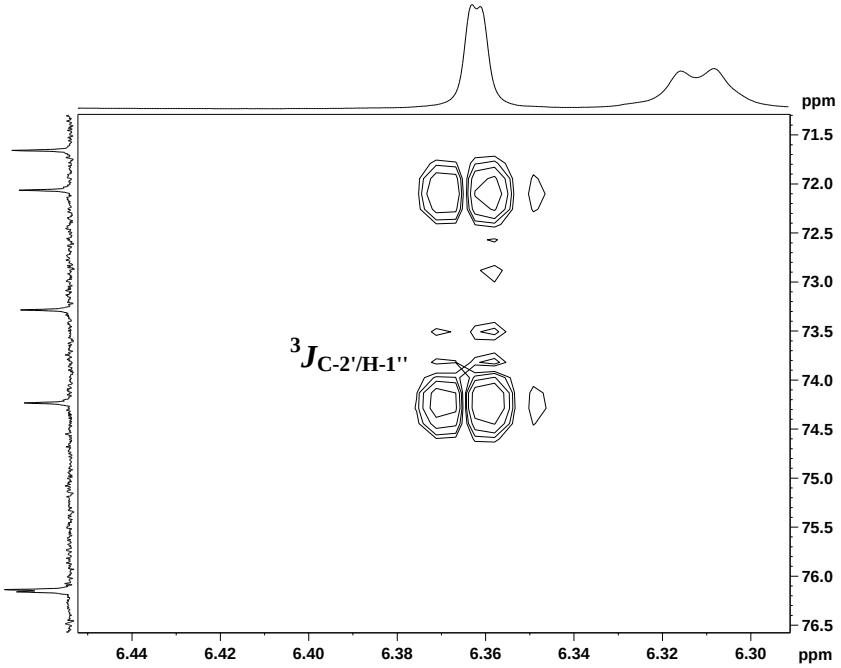

Fig. 3.26: HMBC correlation between C-2' (δ = 74.2 ppm) and H-1" (δ = 6.36 ppm) of **8**, confirming that rhamnose is attached to arabinose at position C-2'.

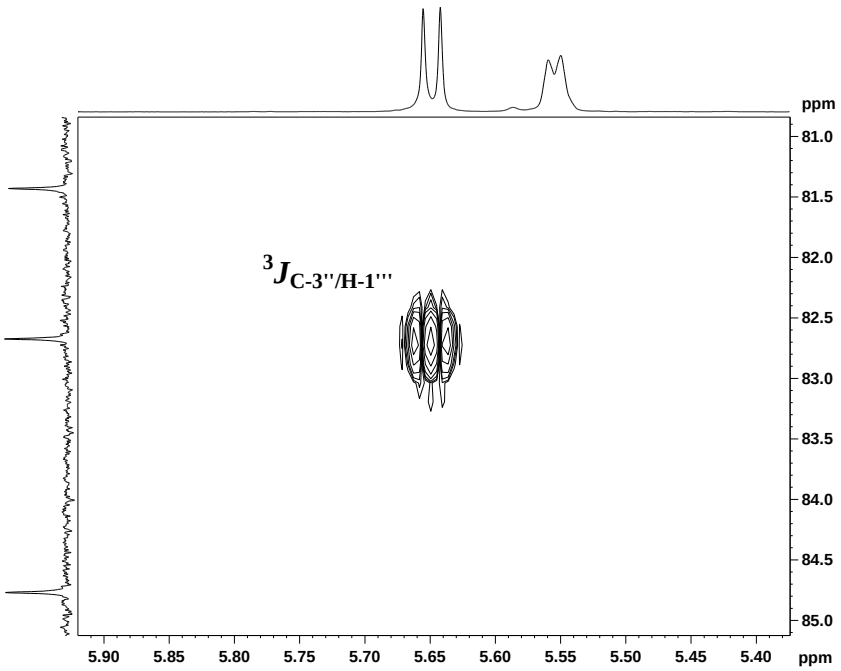

Fig. 3.27: HMBC correlation between C-3" (δ = 82.7 ppm) and H-1'" (δ = 5.65 ppm) of **8**, confirming that glucose is attached to the rhamnose at C-3".

3.1.3.9 Compound **9** (Ruscogenin-1-O-(O-α-L-rhamnopyranosyl-(1 → 2)-β-D-galactopyranoside))

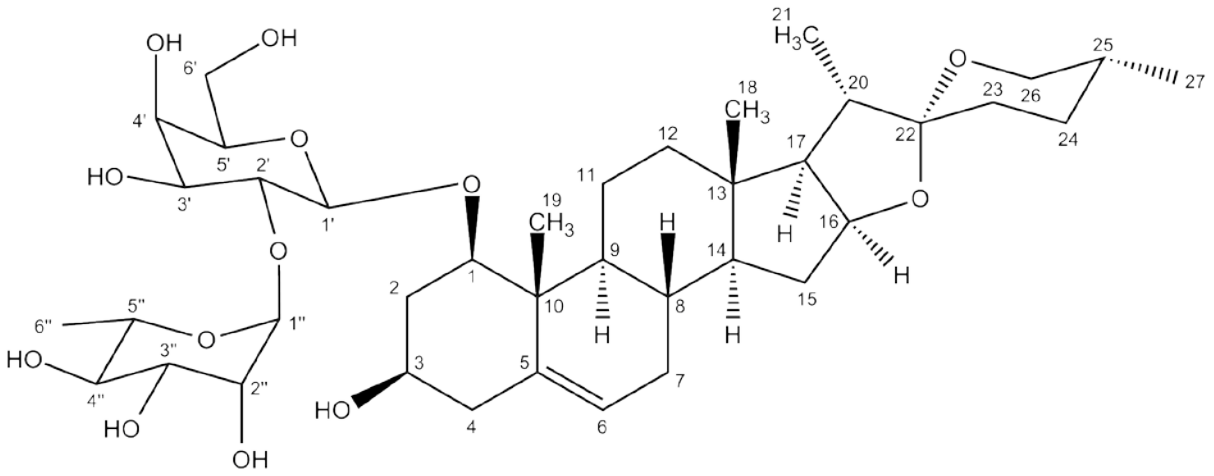

Compound **9** (11.1 mg) was identified as a known ruscogenin-type saponin (Rf = 0.43 in standard system, p. 28, colored green after derivatization with anisaldehyde reagent) and described by Mimaki *et al.* 1998 a. In ^{13}C experiment no exo-methylene group resonated around 109 ppm and an extra methyl group at δ = 0.67 ppm (d) in proton spectrum, correlating with C-25 in HMBC, indicated a C-27 methyl group. COSY correlation between this methyl group and C-25 also suggested the presence of a ruscogenin skeleton. After comparing the signals with literature (Mimaki *et al.* 1998 a/b/c, 1999, 2003, 2008) and further COSY and HMBC analysis of the aglycone, presence of ruscogenine was confirmed (**Table 3.8**, p. 85 and **Fig. 3.28**, p. 86).

Two signals at δ = 100.7 ppm and δ = 101.7 ppm correlating with protons at δ = 4.77 ppm (d) assigned as H-1' and δ = 6.38 ppm (d) assigned as H-1" and typical for anomeric protons and carbons suggested the presence of two sugars. Sugar signals were assigned using COSY and HMBC where H-1' was identified as the anomeric proton of the galactose and H-1" as the anomeric proton of the rhamnose. HMBC correlation between H-1' and C-1 confirmed that galactose is attached to the aglycone at C-1 (**Fig. 3.29**, p. 86). Correlation between H-2' and C-1" pointed out that the rhamnose is attached to the galactose at C-2' (**Fig. 3.30**, p. 87).

Capillary electrophoresis confirmed the presence of D-galactose and L-rhamnose (Materials & Methods p. 30 and CE results p. 101). A relatively large $^{3}J_{H\text{-}1'/H\text{-}2'}$ value at 7.7 Hz signified

the presence of β-D-galactose and a very small $^{3}J_{\text{H-1"/H-2"}}$ value at 0.9 Hz proved the presence of α-L-rhamnose.

A pseudomolecular ion peak at *m/z* 737 $[M-H]^-$ in negative-ion ESI-MS and comparison literature data confirmed the presence of already published compound.

Optical rotation of **9** $[\alpha]_D^{24}$ = -102.0 (c = 0.1, MeOH) and UV maximum at 202 nm (0.1 mg/mL, ε = 5756 L/mol cm) was measured.

Nr.	**C**	Nr.	**H**
1	84.3	1	3.83 dd (12.0, 4.1)
2	38.0	2	2.69 m*
			2.41 q (12.0)
3	68.2	3	3.80 m*
4	43.9	4	2.68 m*
			2.55 ddd (12.7, 0.1, 0.9)
5	139.6	5	
6	124.8	6	5.56 d (5.8)
7	32.0	7	1.86 m*
			1.53 m*
8	33.1	8	1.57 m*
9	50.6	9	1.57 m*
10	42.9	10	
11	24.1	11	3.02 m*
			1.58 m*
12	40.5	12	1.60 m*
			1.37 m*
13	40.2	13	
14	57.1	14	1.15 m
15	32.4	15	2.00 m
			1.43 m*
16	81.2	16	4.46 m*
17	63.0	17	1.76 dd*
18	16.9	18	0.86 s
19	15.1	19	1.43 s
20	42.0	20	1.90 m*
21	15.0	21	1.03 d (7.0)
22	109.3	22	
23	31.8	23	1.66 m*
			1.61 m*
24	29.3	24	1.54 m*
25	30.7	25	1.55 m*
26	66.9	26	3.56 m
			3.47 m
27	17.4	27	0.67 d (5.6)
1’	100.7	1’	4.77 d (7.7)
2’	75.0	2’	4.63 dd (9.2, 7.8)
3’	76.8	3’	4.18 m
4’	70.5	4’	4.49 m*
5’	76.4	5’	3.93 t (6.4)
1’’	62.0	1’’	4.49 m*
			4.34 m*
1’’	101.7	1’’	6.38 d (0.9)
2’’	72.6	2’’	4.75 m*
3’’	72.7	3’’	4.65 dd*
4’’	74.3	4’’	4.31 t (9.5)
5’’	69.3	5’’	4.91 m
6’’	19.1	6’’	1.75 d (6.2)

Table 3.8: ^{1}H and ^{13}C NMR data for compound **9** (δ in ppm, J in Hz, 600 MHz for ^{1}H and 150 MHz for ^{13}C, 298 K, in pyridine d-5, * - overlapping signals)

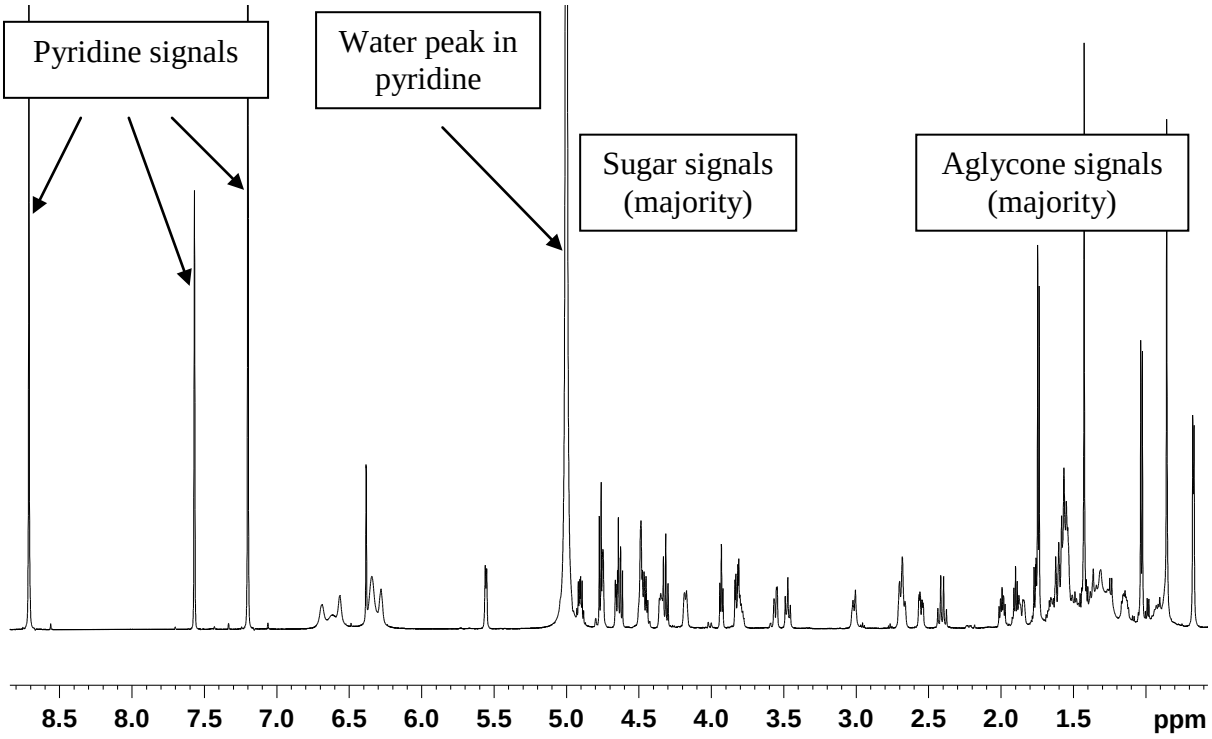

Fig. 3.28: ^{1}H spectrum (pyridine d-5, 600 MHz) of **9** with clearly separated areas of sugar and aglycone signals.

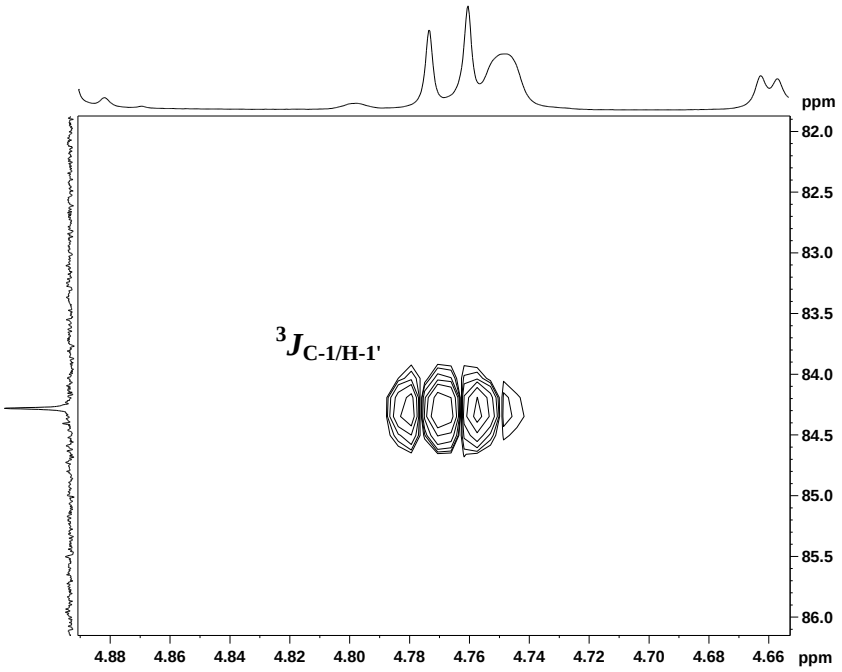

Fig. 3.29: HMBC correlation between C-1 (δ = 84.3 ppm) and H-1' (δ = 4.77 ppm) of **9**, confirming the position of galactose at C-1 of the aglycone.

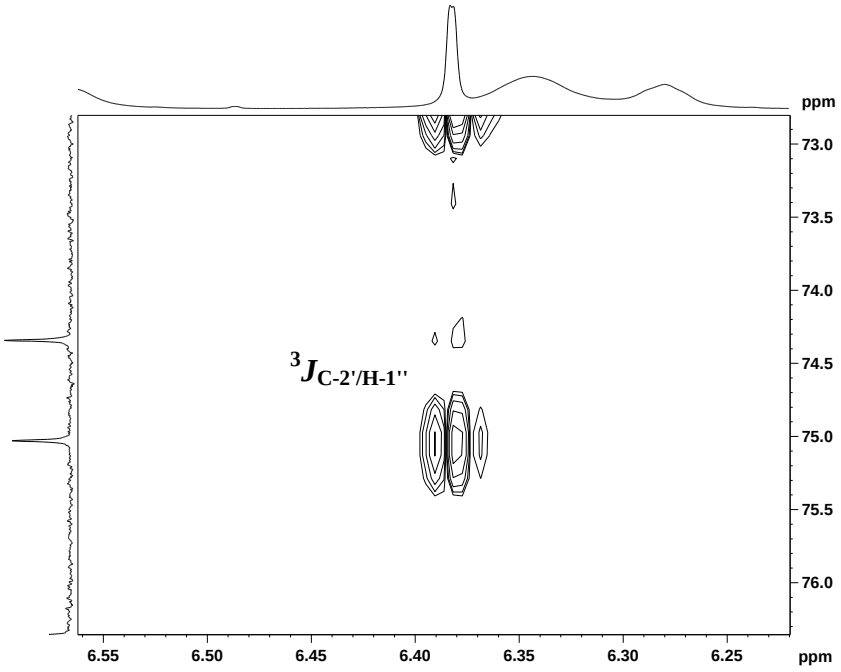

Fig. 3.30: HMBC correlation between C-2' (δ = 75.0 ppm) and H-1'' (δ = 6.38 ppm) of **9**, confirming that rhamnose is attached to galactose at position C-2'.

3.1.4 Identification of phenolic compounds

3.1.4.1 Compound **10** (Esculin)

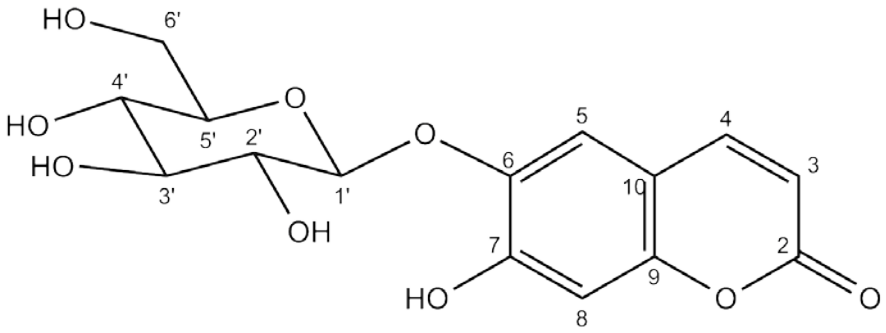

Compound **10** (< 1 mg) was identified as the well known and widespread coumarin esculin. Nevertheless, this is the first report of esculin isolated from *R. aculeatus*.

On a TLC plate, **10** was observed as a very intensive blue fluorescence spot, suggesting the presence of a caffeic acid derivative (Rf = 0.54 in standard system, p. 28, colored fluorescent blue under UV at 366 nm). NMR proton spectrum showed the presence of a sugar and only 4 aromatic protons belonging to the aglycone (**Fig. 3.31**, p. 89). A signal at δ = 164.2 in ^{13}C experiment indicated the presence of a carbonyl group. Four other quaternary carbons were also found with the help of HMBC spectra. Furthermore, position of two benzene ring protons (singlets) were assigned in 1,4 position. HMBC experiment also showed that the sugar (**Fig. 3.32**, p. 90), is attached to the coumarin at C-6. Two other aromatic carbons resonated at 145.3 ppm and 153.0 ppm suggesting the presence of hydroxyl or alkoxy groups. With all this fragments identified and further HMBC and COSY correlations, structure of esculin was proposed and confirmed by ESI-MS giving a *m/z* 339 $[M-H]^-$ for the pseudomolecular ion. Sugar was identified as glucose. Due to a very low weight (< 1 mg), no further experiments were conducted on compound **10**.

Nr.	**C**	Nr.	**H**
2	164.2	2	
3	111.8	3	6.15 d (9.4)
4	146.3	4	7.81 d (9.4)
5	116.2	5	7.35 s
6	145.3	6	
7	156.0	7	
8	104.8	8	6.75 s
9	111.8	9	
10	153.0	10	
1’	104.3	1’	4.81 d (7.6)
2’	74.8	2’	3.51 m*
3’	77.6	3’	3.47 m*
4’	71.4	4’	3,38 m
5’	78.5	5’	3.46 m*
6’	62.6	6’	3.93 dd (12.0, 2.1)
			3.71 dd (12.0, 6.0)

Table 3.9: ^{1}H and ^{13}C NMR data for compound **10** (δ in ppm, J in Hz, 600 MHz for ^{1}H and 150 MHz for ^{13}C, 298 K, in MeOD d-4, * - overlapping signals)

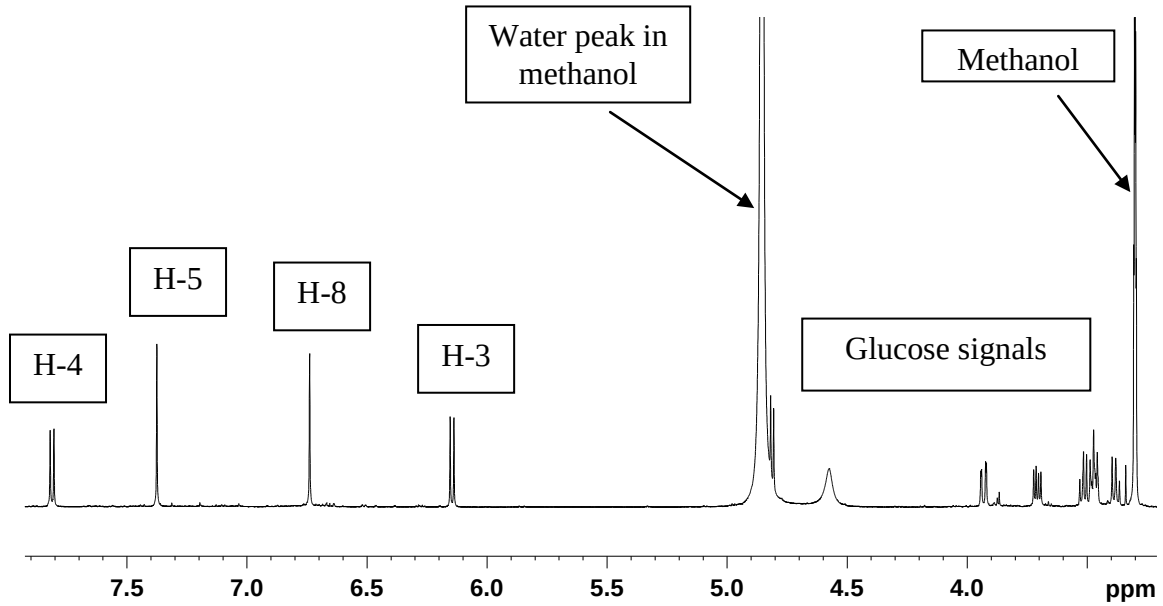

Fig. 3.31: ^{1}H spectrum (methanol d-4, 600 MHz) of **10** with signals of glucose and aglycone.

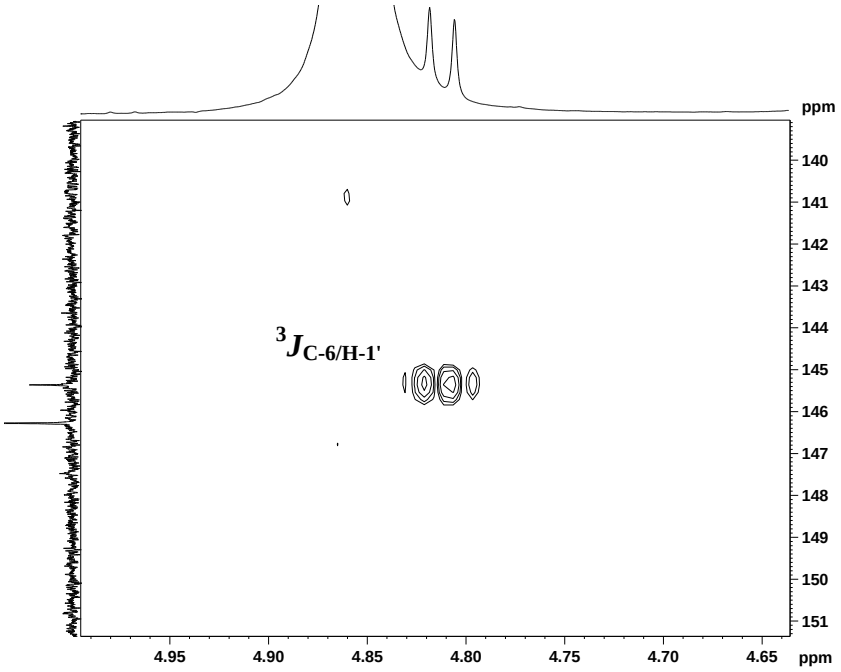

Fig. 3.32: HMBC correlation between C-6 (δ = 145.3 ppm) and H-1' (δ = 4.81 ppm) of **10**, confirming the position of glucose at C-6 of the aglycone.

3.1.4.2 Compound **11** (Ruscozepine A)

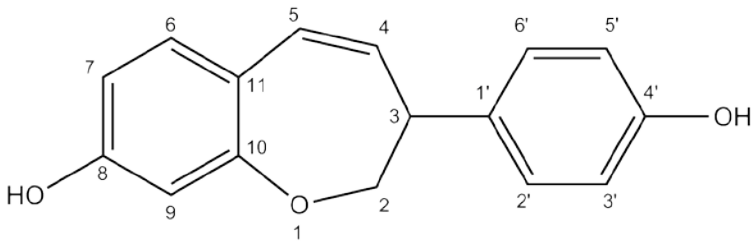

Compound **11** (0.3 mg) was found to be a compound with a novel skeleton and its synthesis via one of the classical biosynthetic pathway for aromatic compounds is hard to explain. TLC chromatograms sprayed with anisaldehyde reagent gave purple coloration for **11** at VIS (Rf = 0.41 developed in DCM:MeOH:H_2O = 90:10:1 on RP-18 plate).

Several signals in ^{1}H NMR experiment indicated the presence of a phenolic compound with two phenolic ring ssystems (**Fig. 3.33**, p. 92). Three low field shifted signals in ^{13}C NMR spectrum suggested three hydroxy groups attached to the aromatic rings. Two carbon signals at 130.4 ppm and 116.2 ppm coupled in HSQC with protons at 7.04 and 6.71 ppm, which were integrated by 2 and correlating in COSY (**Fig. 3.34**, p. 93), pointed to the presence of a p-substituted benzene ring. A HMBC experiment confirmed via a correlation of H-3 (3.83 ppm) and C-1′ (133.5 ppm) that C-1' was attached to C-3 resonating at 50.7 ppm and that C-4' was hydroxylated (δ = 157.4 ppm). A correlation between H-3/H-2 (showing for H-2 the typical shift value and signal pattern of a oxygen substituted methylene group in a ring system, δ = 4.20 ppm, ddd, J = 11.6, 3.2, 0.8 and 4.04 dd, J = 11.7, 6.7) and between H-3/H-4 (showing the typical shift value of a methin proton belonging to a double bond, δ = 5.76 ppm, dd J = 11.8, 4.0) was found in the COSY experiment and allowed one important step to the building of the seven-membered ring system. Presence of the methylene character of C-2 was shown in the HSQC experiment. Its low field shift at 76.4 ppm in ^{13}C confirmed that it is bound to oxygen. Furthermore, H-4 is correlated to H-5 in COSY and a HMBC correlation between H-5 and aromatic C-11 indicated thar the seven-membered ring is annelated to one of the phenolic rings. This was also confirmed by a HMBC correlation between H-2 and C-10. Since the aromatic C-10 resonated down field shifted (δ = 161.7 ppm) it was clear that both

C-10 and C-2 were bound to the same oxygen. With HMBC and COSY, it was possible to assign the rest of the signals where C-8 (δ = 158.8 ppm) was carrying the second hydroxyl group.

Structure was confirmed by a HR-MS giving a molecular ion with exact mass of *m/z* 254.0943 [M^+] calculated for $C_{16}H_{14}O_3$.

Due to low amount, compound **11** was not submitted for any further testing. UV maxima at 222, 267 and 300 nm (in MeOH) were measured.

Nr.	**C**	Nr.	**H**
2	76.4	2	4.20 ddd (11.6, 3.2, 0.8)
			4.04 dd (11.7, 6.7)
3	50.7	3	3.83 m
4	131.1	4	5.76 dd (11.8, 4.0)
5	128.9	5	6.35 dd*
6	134.8	6	7.05 m*
7	111.0	7	6.45 dd (8.4, 2.5)
8	158.8	8	
9	107.3	9	6.34 d* (2.5)
10	161.7	10	
11	120.0	11	
1’	133.5	1’	
2’	130.4	2’	7.04 m*
3’	116.2	3’	6.71 m*
4’	157.4	4’	
5’	116.2	5’	6.71 m*
6’	130.4	6’	7.04 m*

Table 3.10: ^{1}H and ^{13}C NMR data for compound **11** (δ in ppm, *J* in Hz, 600 MHz for ^{1}H and 150 MHz for ^{13}C, 298 K, in MeOD d-4, * - overlapping signals)

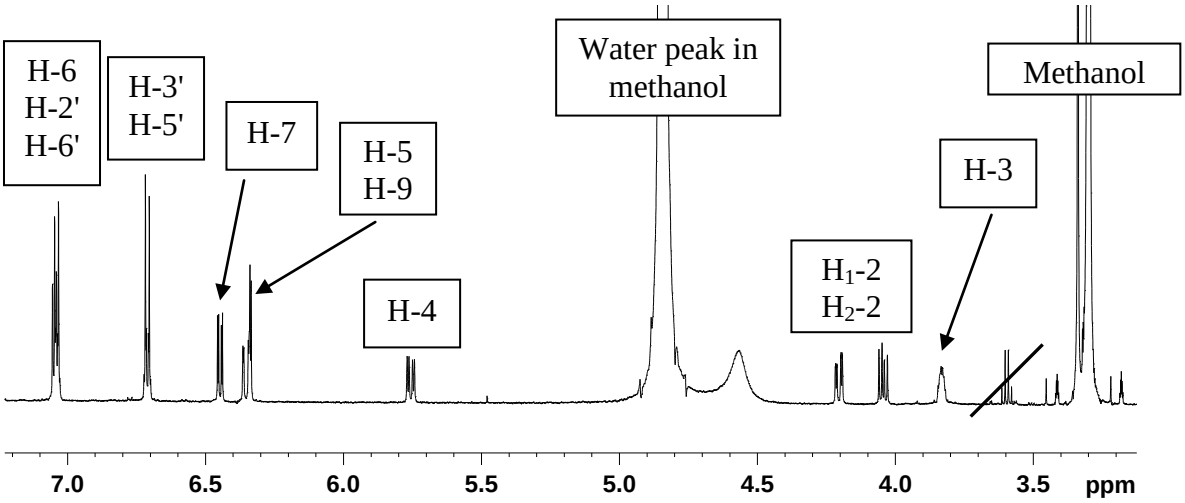

Fig. 3.33: ^{1}H spectrum (methanol d-4, 600 MHz) of **11**.

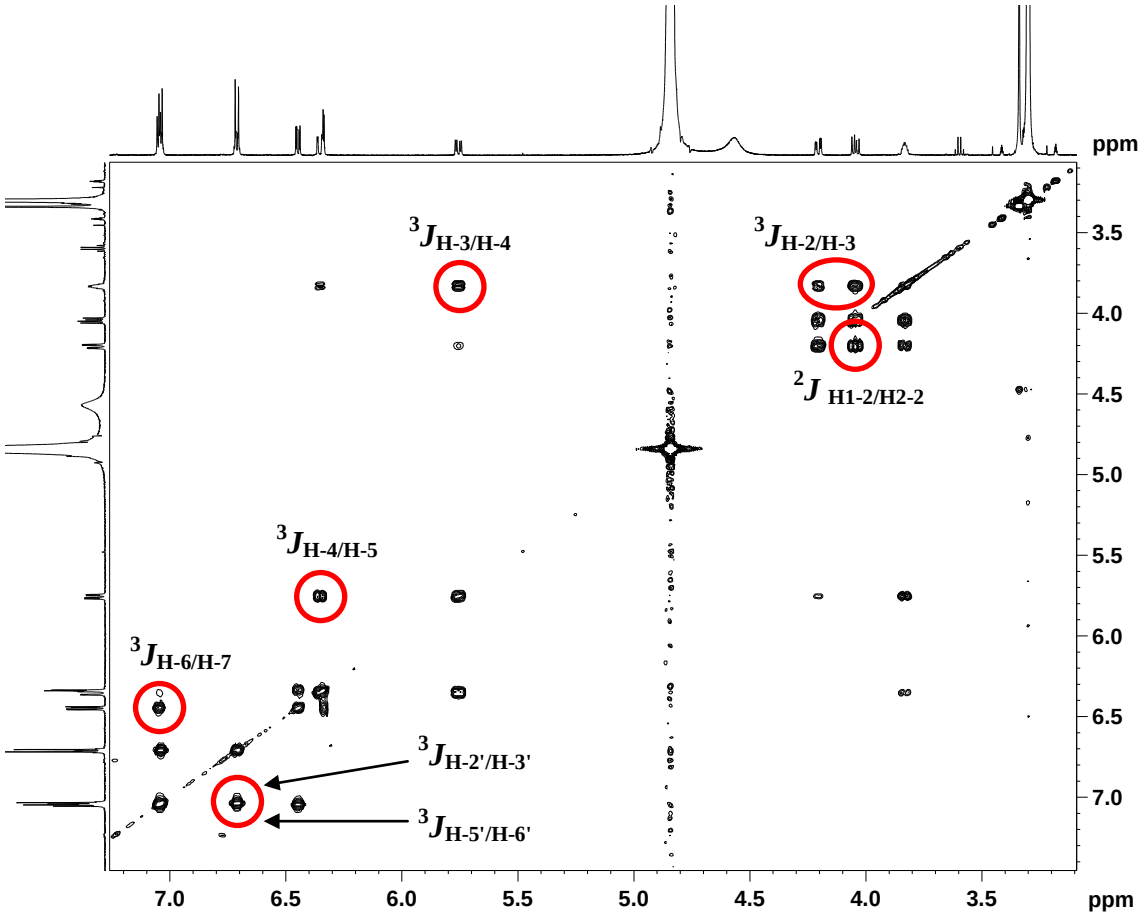

Fig. 3.34: COSY spectrum of compound **11** with highlighted key correlations.

3.1.4.3 Compound **12** (1-(2- hydroxyethyl)-3,4-dihydroxy benzene)

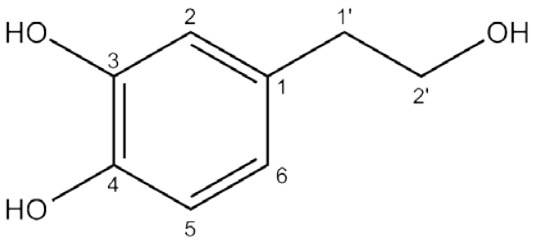

Compound **12** was identified as already known compound. Its consistency was found to be very oily and therefore difficult to weight exactly (around 7 mg, Rf = 0.25 developed in DCM:MeOH:H_2O = 90:10:1).

^{1}H NMR spectrum indicated the presence of a simple phenolic compound (**Fig. 3.35**, p.95). The presence of six aromatic and two aliphatic carbons was confirmed in ^{13}C experiment. Two of the aromatic carbons (δ = 146.1 ppm and (δ = 144.6 ppm) downfield shifted, suggesting two hydroxyl groups. Alifatic signals were assigned as hydroxyethyl due to the presence of two methylene groups and a downfield shift of C-2' (δ = 64.6 ppm). Positions of all substituents were confirmed via HMBC and COSY.

Structure was confirmed by ESI-MS giving a *m/z*: 153 $[M-H]^-$ for the pseudomolecular ion.

Due to characteristics of **12** (oily and hydrophilic and therefore impossible to get an exact weight), no further experiments were performed.

UV maxima at 224 and 279 nm (in MeOH) were measured.

Nr.	C	Nr.	H
1	131.8	1	
2	117.1	2	6.64 d (1.9)
3	146.1	3	
4	144.6	4	
5	116.3	5	6.66 d (8.0)
6	121.2	6	6.51 dd (8.1, 2.0)
1’	39.7	1’	2.65 t (7.2)
2’	64.6	2’	3.66 t (7.3)

Table 3.11: ^{1}H and ^{13}C NMR data for compound **12** (δ in ppm, J in Hz, 600 MHz for ^{1}H and 150 MHz for ^{13}C, 298 K, in MeOD d-4, * - overlapping signals)

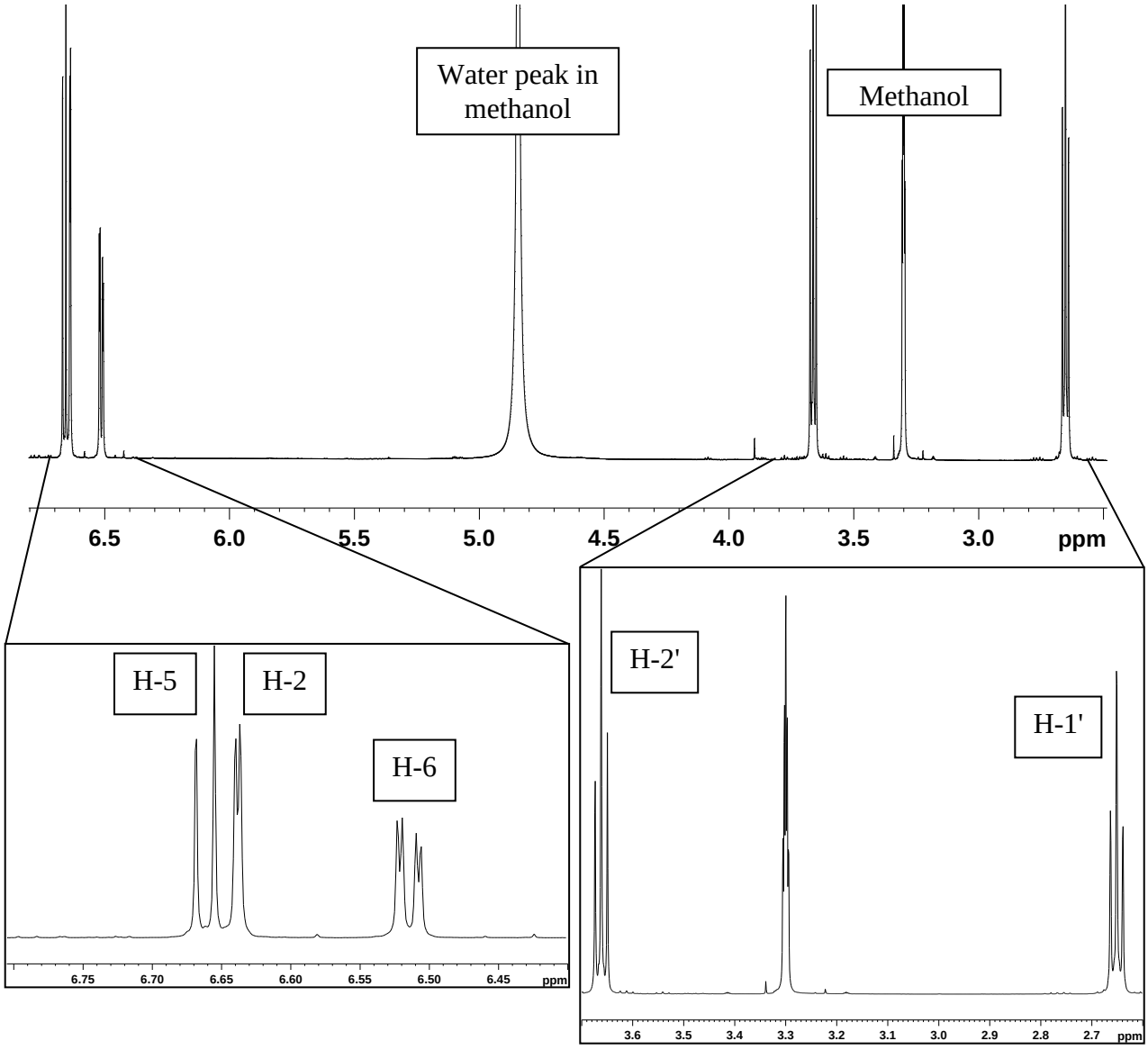

Fig. 3.35: ^{1}H spectrum (methanol d-4, 600 MHz, 298 K) of **12** with expansions.

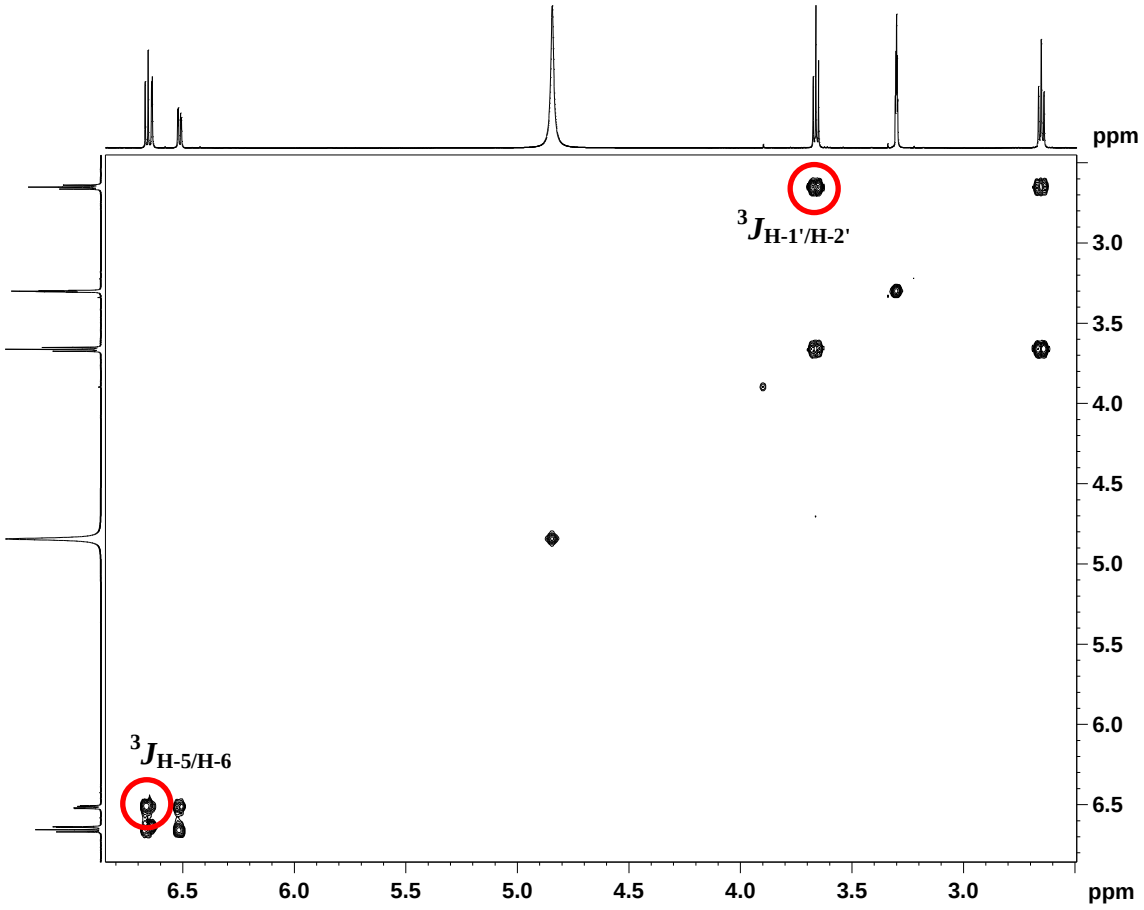

Fig. 3.36: COSY spectrum of compound **12** with highlighted key correlations.

3.1.4.4 Compound **14** (Ruscozepine B)

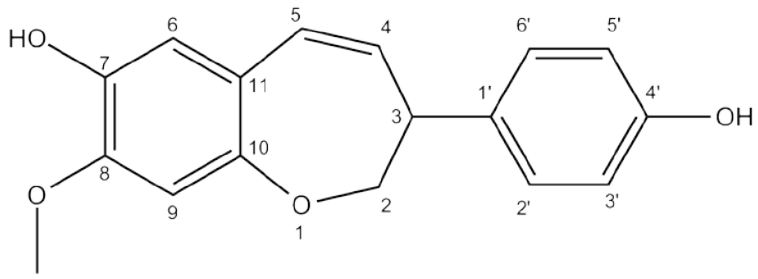

Compound **14** (1.2 mg) was also found to be a new compound with a novel skeleton and being structurally related to **11**. TLC chromatograms sprayed with anisaldehyde gave purple coloration for **14** at VIS (Rf = 0.36 developed in MeOH:H_2O = 7:3 on RP-18 plate).

Signal pattern of **14** was very similar to the one from compound **11**. The main difference was observed in additional methyl group (δ = 56.4 ppm in carbon and δ = 3.80 ppm (s) in proton spectrum, **Table 3.12**, p. 98 and **Fig. 3.37**, p. 99) and a possible extra hydroxyl group due to a downfield shift of C-7 (111.0 ppm for **11** and 142.5 ppm for **14**). A downfield shifted methyl group indicated the presence of a methoxy group, which was confirmed by a missing aromatic proton (H-7 in compound **11**). The other benzene ring had exactly the same chemical shifts as the ring in **11**. Position of the methoxy group was confirmed by HMBC. As in compound **11**, structure was assigned using COSY and HMBC and confirmed by HR-MS with the exact mass signal 284.1049 [M+] calculated for $C_{17}H_{16}O_4$.

Optical rotation of **14** $[\alpha]_D^{24}$ = -98.9 (c = 0.1, MeOH) and UV maxima at 230 nm, 273 nm and 307 nm (0.1 mg/mL, ε = 3300 at 307 nm) were measured.

Nr.	**C**	Nr.	**H**
2	76.7	2	4.18 dd (11.3, 3.6)
			4.03 dd (11.6, 6.7)
3	50.9	3	3.83 m
4	128.6	4	5.81 dd (11.9, 4.1)
5	132.5	5	6.28 dd (11.9, 1.9)
6	119.1	6	6.66 s
7	142.5	7	
8	148.7	8	
9	104.7	9	6.52 s
10	154.3	10	
11	120.3	11	
1’	133.5	1’	
2’	130.4	2’	7.04 m*
3’	116.2	3’	6.71 m*
4’	157.4	4’	
5’	116.2	5’	6.71 m*
6’	130.4	6’	7.04 m*
-OMe	56.4	-OMe	3.80 s

Table 3.12: ^{1}H and ^{13}C NMR data for compound **14** (δ in ppm, J in Hz, 600 MHz for ^{1}H and 150 MHz for ^{13}C, 298 K, in MeOD d-4, * - overlapping signals)

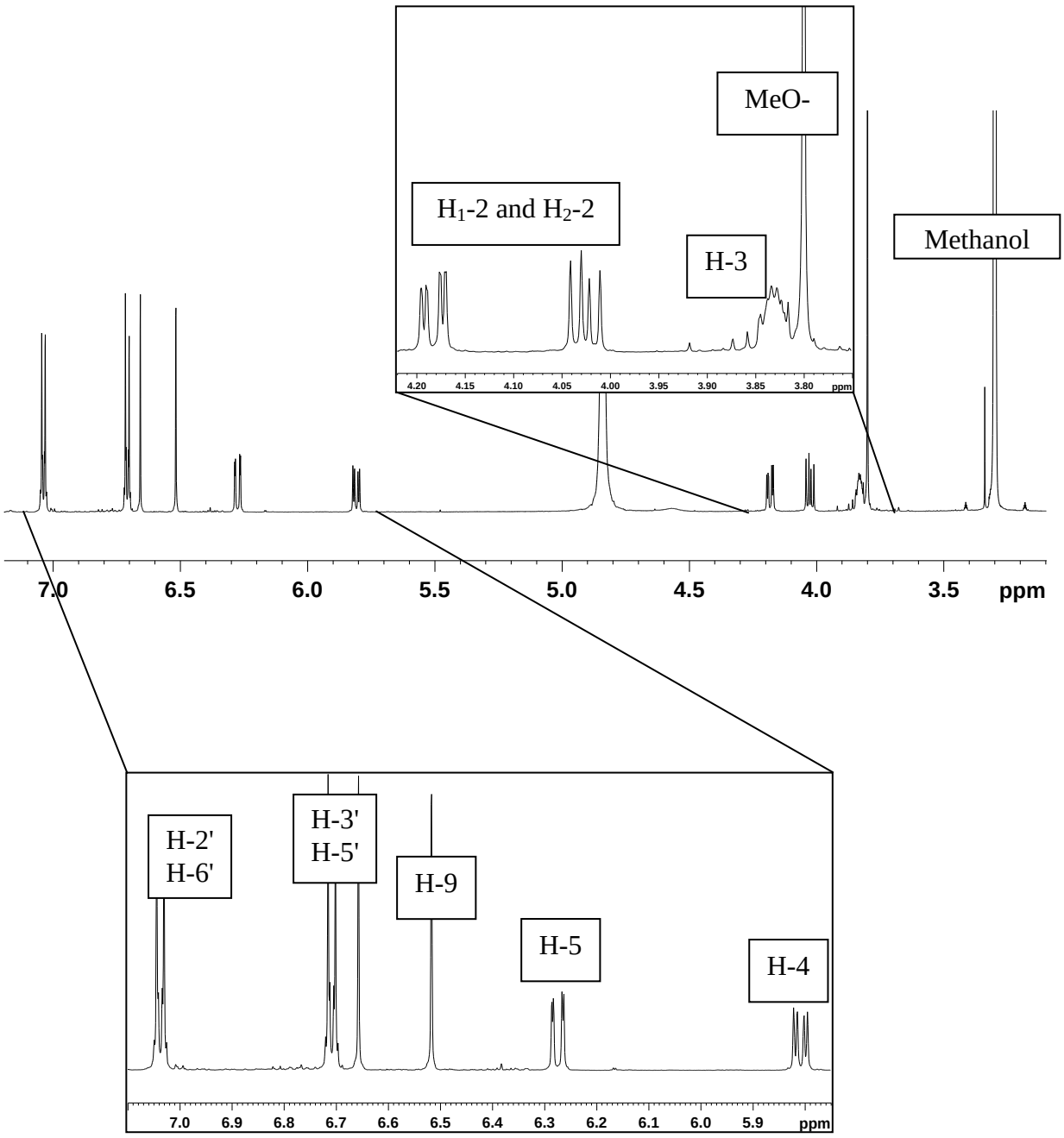

Fig. 3.37: ^{1}H spectrum (methanol d-4, 600 MHz, 298 K) of **14** with expansion.

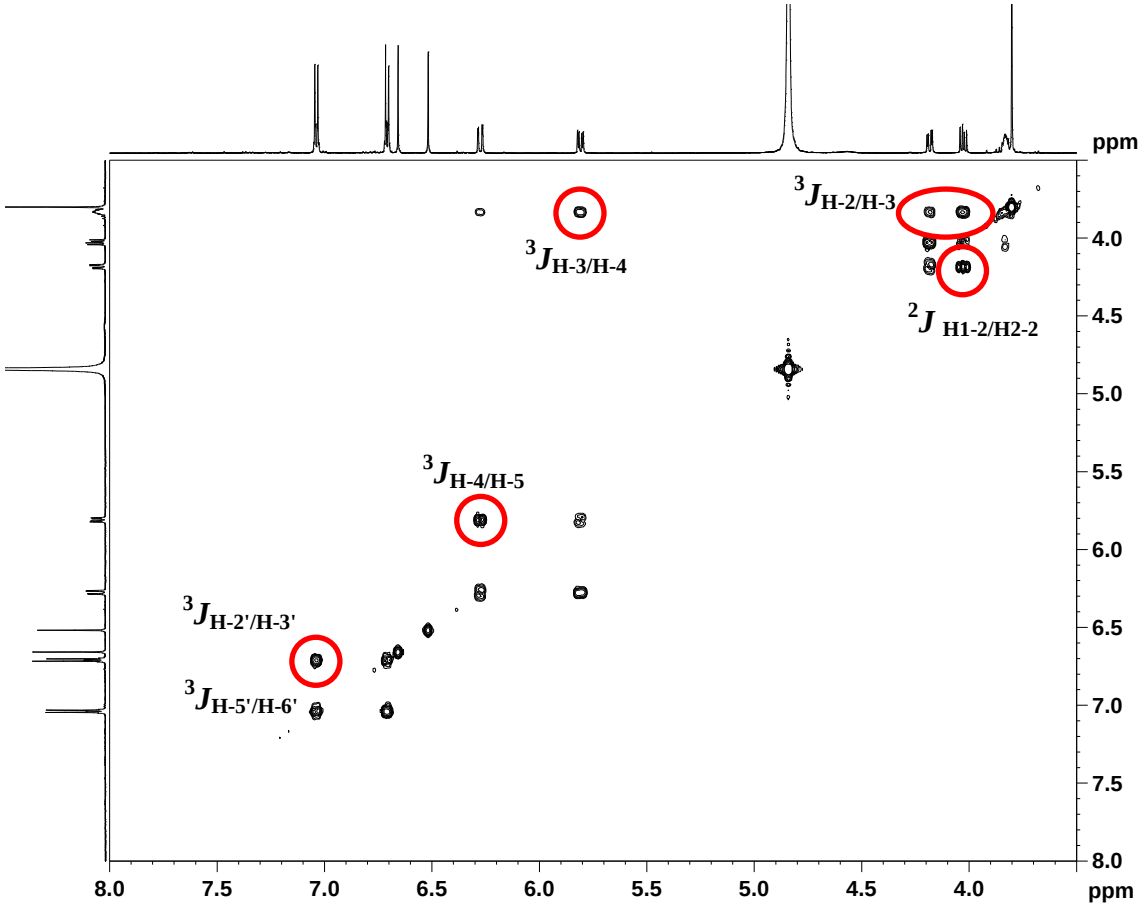

Fig. 3.38: COSY spectrum of compound **14** with highlighted key correlations.

3.1.5 Absolute stereochemistry of sugars determined by CE

Absolute stereochemistry of the sugars present in compounds isolated from *R. aculeatus* was determined via capillary electrophoresis according to Noe & Freissmuth 1995. This method separates compounds based on their size and charge in a fused silica capillary. Capillaries of different size are connected with two buffer containers and electrodes, where detector, normally based on UV, is placed on the cathode side. All compounds travel into same direction due to the electroosmotic flow (EOF) and are separated due to their electrophoretic mobility. Positive ions travel to the cathode faster than negatively charged. Uncharged particles normally migrate together with EOF.
Voltages up to 35 kV can be applied. For the use of voltages higher that 20 kV a change of cooling system is recommended. Water cooling can cause sparkling through the capillary wall, which eventually leads to very high electrical currents and breakdown of electroosmosis. Detector, normally UV detector, sends signals to the computer, where the separation can be observed in a form of a plot called electropherogram.

In order to determine the absolute stereochemistry of the sugars in glycosides, they need to be hydrolysed from aglycone. This needs exposition to acidic conditions at high temperatures. In order to separate L and D enantiomers, a transformation into diastereoisomers must be performed. In this work, *S*-(-)-1-phenylethylamin has been used to derivatize the sugars. Samples as well as commercially available and with phenyletylamin derivatized reference sugars were applied to CE. Signals in electropherogram were assigned by addition of the authentic sugars (spiking) to the mixture of all sugars.
A mixture of reference sugars was injected to get a clean plot of the authentic compounds (**Fig. 3.39**, p. 102). Sugar type was determined by injection and analysis of the sugar mixture obtained from the hydrolysis of the isolated compounds (**Fig. 3.40**, p. 103 and **Fig. 3.42**, p. 104). With this experiment, we have also proven that separation of investigated sugars occurred. In order to confirm the type of the sugar and to assign absolute stereochemistry of the sugars from isolated compounds, the mixture of reference sugars was spiked with sugars from isolated compounds (**Fig. 3.41**, p. 103 and **Fig. 3.43**, p. 104). For derivatization, only compound **8** and **9** were used, due to the low yield of the other glycosides. They contain all types of monosaccharides that were found in compounds isolated during this thesis. It is most likely that the same monosaccharide enantiomer is part of the other glycosides present in Rusci rhizoma. As reference, all D and L enantiomers were used, except for rhamnose. The

only commercially available rhamnose enantiomer was the L-rhamnose. Thereby, it could not be proven that L and D rhamnose signals would be separated using this CE method. The electropherogram of all seven references showed a very good base-line separation. Therefore, it is most likely that a D-rhamnose would show at least a minimal separation from the L diastereoisomer, to allow the determination of the absolute stereochemistry. Jürgenliemk 2000 demonstrated different migration times of L-rhamnose and synthesised D-rhamnose, under the same CE conditions.

CE can not only be considered as a very strong, but unfortunately also as a relatively interference-prone analytical method. It can be observed (see CE figures), that migration times vary quite a lot making the direct comparison of single runs not reasonable. This problem has been solved by spiking of the samples with known compounds.

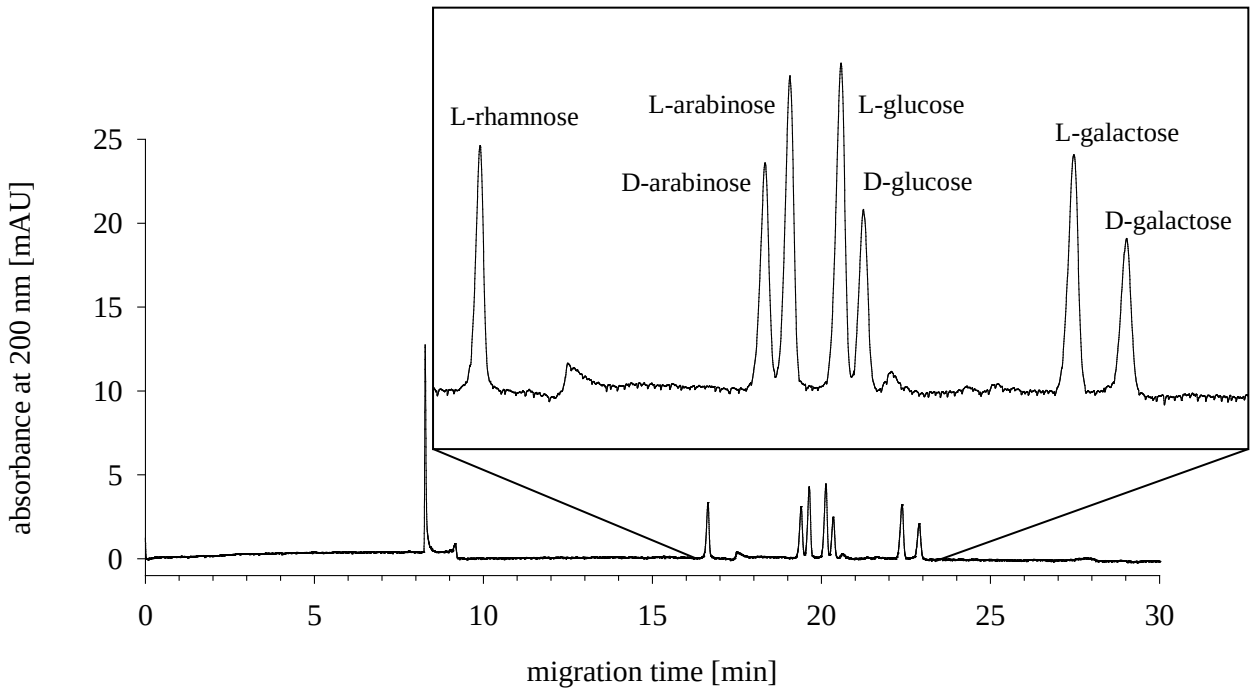

Fig. 3.39: Electropherogram of the reference sugar mixture (L-rhamnose, D-arabinose, L-arabinose, L-glucose, D-glucose, L-galactose and D-galactose)

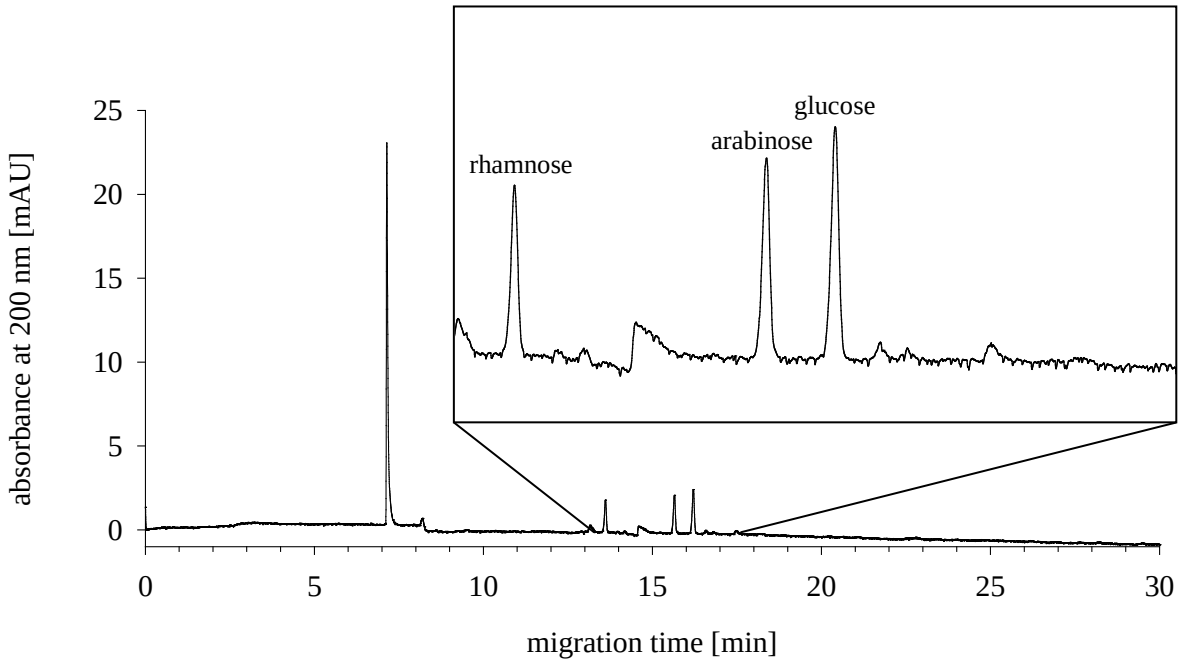

Fig. 3.40: Electropherogram of the monosaccharides, after hydrolysis of compound **8** and derivatisation, signifying the presence of rhamnose, arabinose and glucose

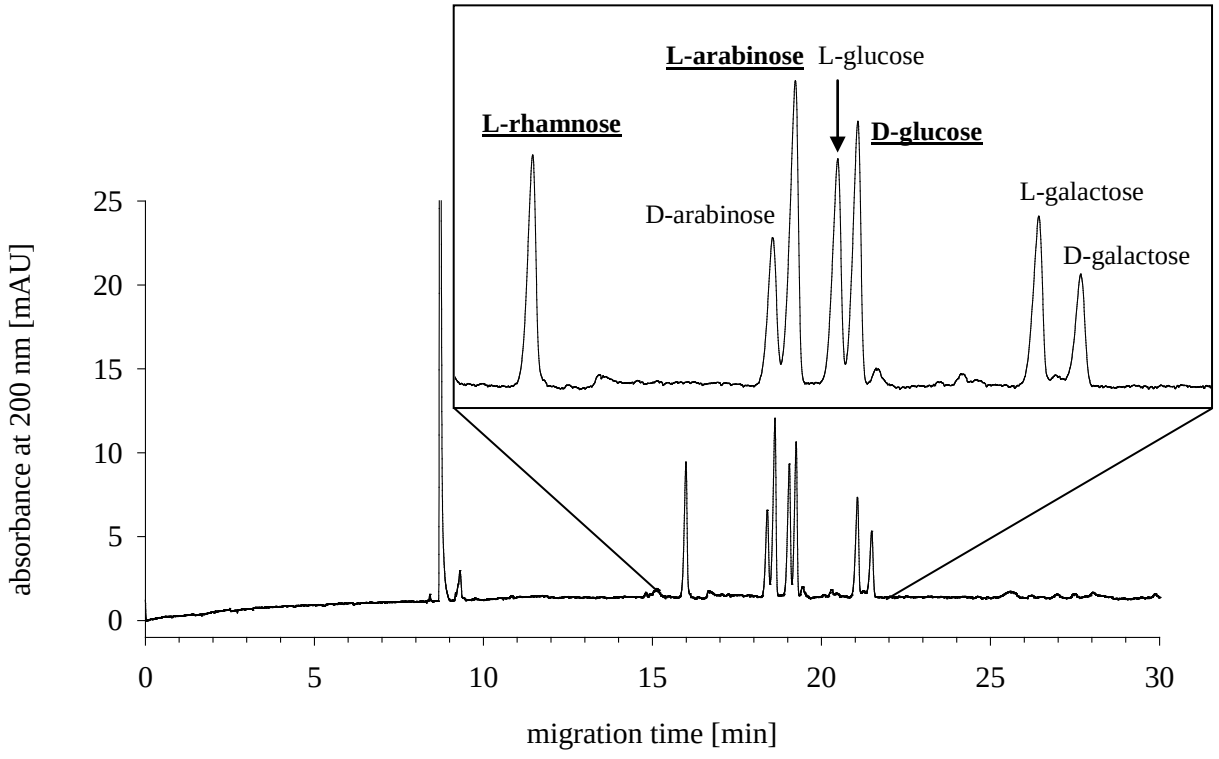

Fig. 3.41: Electropherogram of the reference sugar mixture spiked with derivatized sugars obtained after hydrolysis of compound **8**, confirming the presence of L-rhamnose, L-arabinose and D-glucose in compound **8**.

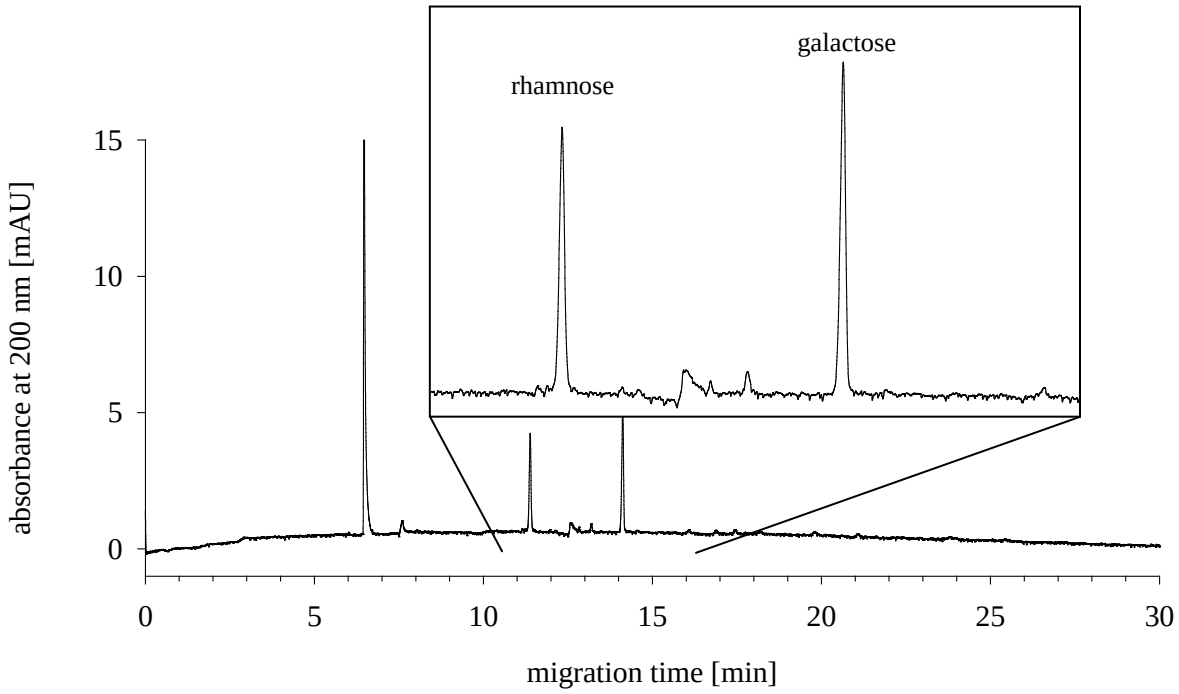

Fig. 3.42: Electropherogram of the monosaccharides, after hydrolysis of compound **9** and derivatisation, signifying the presence of rhamnose and galactose

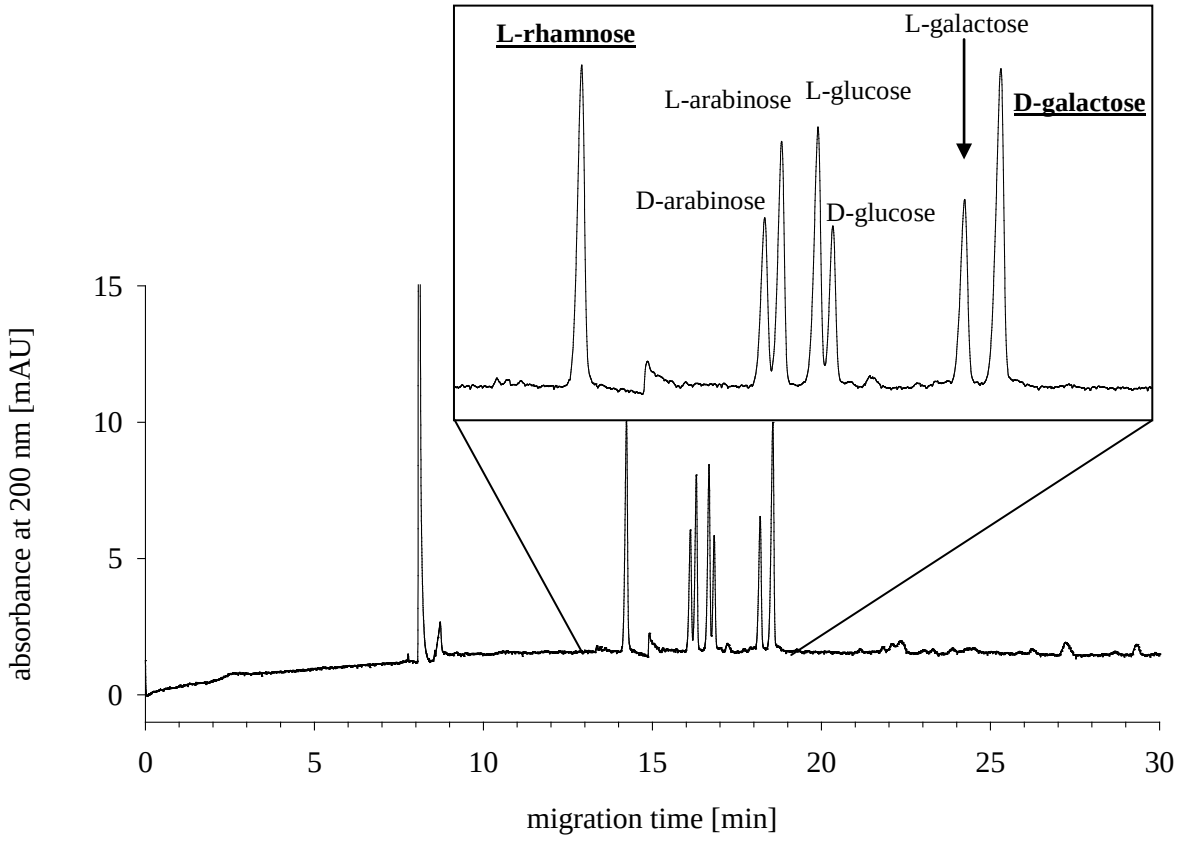

Fig. 3.43: Electropherogram of the reference sugar mixture spiked with derivatized sugars from compound **9**, signifying the presence of L-rhamnose and D-galactose in compound **9**.

3.2 Summary and short discussion on isolation and structure elucidation

Thirteen pure compounds have been isolated from the rhizomes of *R. aculeatus*, nine steroidal saponins and four phenolic compounds.

It is known that main constituents of the rhizomes from Butcher's Broom are steroidal saponins. Therefore, it was expected that mainly this type of natural products would be isolated during this research. Several compounds from all types of steroidal saponins (ruscogenin-type, neoruscogenin-type, ruscoside-type) have already been reported in several papers by Mimaki *et al*. 1998 a/b/c, 1999, 2003, 2008. Although the spectrum of these compounds was considered to be very broad, it was not primarily expected that new saponins from *R. aculeatus* would be isolated. The goal of this study was to isolate as many as possible to get a certain database of the saponins which should then be tested in various cell assays. Nevertheless, three new saponines have been isolated (see compounds **4**, **6** and **7**). Therefore, a possibility of finding some other new compounds should be taken into account.

Several problems occurred during the isolation process, mainly because of the presence of the high number of different compounds. This is also the key reason, for making so many isolation steps necessary, in order to get pure saponins (isolation procedure, p. 36).

Compound **2** (p. 56) was found to be a 22-O-methoxy derivative of **3** (p. 57). After isolation of **2** (isolation procedure, p. 36), the compound was freeze-dried in order to obtain a water-free powder. After dissolving it in water, freezing and application to the freeze dryer, **2** was dried over night to get a white amorphous powder. A TLC of the dried product was made where two clear spots, the original and a lower one, were observed and thus the compound must have de-composed during the freeze-drying process.

Due to a very high amount of saponins in the extracts from the rhizomes of Butcher's Broom, isolation of other constituents, such as phenols, has been neglected up to now. Single reports on the identification of phenolics can be found in literature (El Sohly *et al.* 1975), but no thorough analysis or isolations have been performed so far.

Four pure phenolic compounds have been isolated during this work. Two of them were identified as novel constituents with an unusual skeleton. According to IUPAC, this skeleton should be named as a 3-phenyl-2,3-dihydrobenzoxepin. Since the base structure is classified as a new biosynthetic product found in *R. aculeatus*, a combined name 'ruscozepines' was selected for this new type of compounds (see compounds **11** and **14**). Yet, absolute stereochemistry of **11** and **14** has still to be determined via CD spectroscopy. A possible

biosynthetic pathway of ruscozepines could be a dimerisation of two phenethyl alcohols as indicated in **Fig. 3.44**, p. 106. The isolation of compound **12** can support this theory.

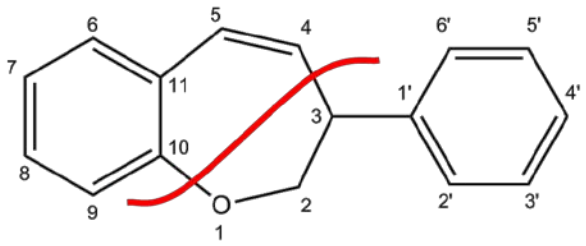

Fig. 3.44: General ruscozepine structure indicating a possible coupling of two phenethyl alcohols.

Compound **10** (esculin) is a well known and relatively widespread coumarin which is also present in Horse chestnut (*Aesculus hippocastanum*) and Sweet Clover (*Melilotus officinalis*). Interestingly, all three plants are used in treatment of CVDs. This was the first report of esculin in Butcher's Broom. Presence of esculin in our fractions was determined very easily, due to the intensive light blue fluorescence under UV at 366 nm.

To summarize, reinvestigation of compounds from *R. aculeatus* are still a new and very interesting field of research. A variety of further compounds have also been detected during the fractionation of PRF. Therefore, it would be reasonable to focus on the isolation of phenolic compounds from *R. aculeatus* to broaden the marginal knowledge about this group. For further thorough analysis and isolation a higher amount of the starting material is absolutely necessary.

All isolates with analytical data from this research work have been gathered in **Table 3.13**, p.107.

Compound	Anisaldehyde coloration	MS data	UV_{max}[nm]	$[\alpha]_D^{24}$ [^{0}]
1, deglucoruscin	green	705 $[M-H]^-$	202	-78.3
2, 22-O-methyldeglucoruscoside	green	899 $[M-H]^-$	n/a	n/a
3, deglucoruscoside	green	885 $[M-H]^-$	n/a	n/a
4, 3'-O-acetyl-4'-O-sulfo deglucoruscine	green	827 $[M-H]^-$	202	-93.4
5, 1-O-sulfo ruscogenin	green	509 $[M-H]^-$	202	-53.2
6, 4'-O-(2-hydroxy-3-methylpentanoyl)-deglucoruscin	green	819 $[M-H]^-$	202	-34.7
7, 4'-O-acetyl-deglucoruscin	green	747 $[M-H]^-$	202	-39.5
8, ruscin	green	867 $[M-H]^-$	201	-91.0
9 *	green	737 $[M-H]^-$	202	-102.0
10, esculin	yellow	339 $[M-H]^-$	n/a	n/a
11, ruscozepine A	purple	254.0943 $[M^+]$ **	222 267 300	n/a
12, 1-(2- hydroxyethyl)-3,4-dihydroxy benzene	brown	153 $[M-H]^-$	224 279	n/a
14, ruscozepine B	purple	284.1049 $[M^+]$ **	230 273 307	-98.9

***

Table 3.13: Overview of compounds isolated from *Ruscus aculeatus* with some analytical data. * - full name see p., ** - HR-MS data, *** - Compound **13** was excluded since it was identified as a mixture of diastereoisomers.

3.3 Quantification of the extracts and fractions

3.3.1 Saponin quantification

Quantification of the saponins in extract and fractions from Butcher's Broom was performed according to European Pharmacopoeia (Ph. Eur.).

Weights used for the quantification procedure were chosen considering the sample to starting material (rhizomes) ratio. MeOH extract represented 25% of the rhizomes dried weight, therefore 0.5 g of MeOH extract (instead of 2 g of rhizomes according to Ph. Eur.) were used for quantification of the methanolic extract. After liquid/liquid partitioning of the methanolic extract, for n-BuOH fraction 0.15 g (29.7% of MeOH) and for water fraction 0.29 g (57.4% of MeOH) were used. 0.12 g of PPF (80.3% of n-BuOH) and 0.01 g of PRF (7.5% of n-BuOH) were also quantified concerning their saponin content.

Content of saponins was calculated as ruscogenins (neoruscogenin and ruscogenin) and was determined by the comparison of the peak areas after HPLC analysis. Ruscogenins *CRS* (5 mg/100 ml MeOH; 3.02 mg neoruscogenin and 1.91 mg ruscogenin) were used as an external reference. Saponin content of the MeOH extract (2.91 g saponins/100 g MeOH extract) was set as the 100% value. Part of the saponins was lost during the liquid-liquid chromatography.

Results of the saponin quantifications are summarized in **Fig. 3.45** and **Fig. 3.46**.

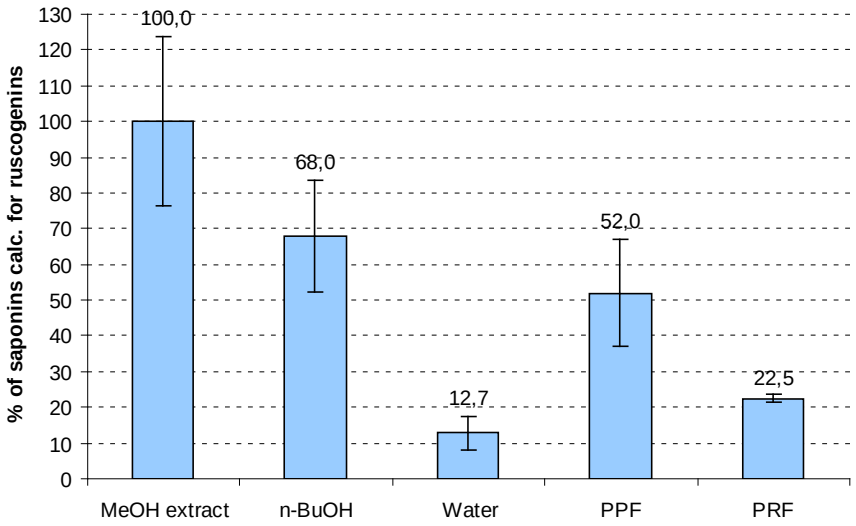

Fig. 3.45: % of saponins calculated as ruscogenins (ruscogenin + neoruscogenin) and expressed as the percent of saponins determined in MeOH extract (2.91 g/100 g of MeOH extract); n = 3; mean ± SD.

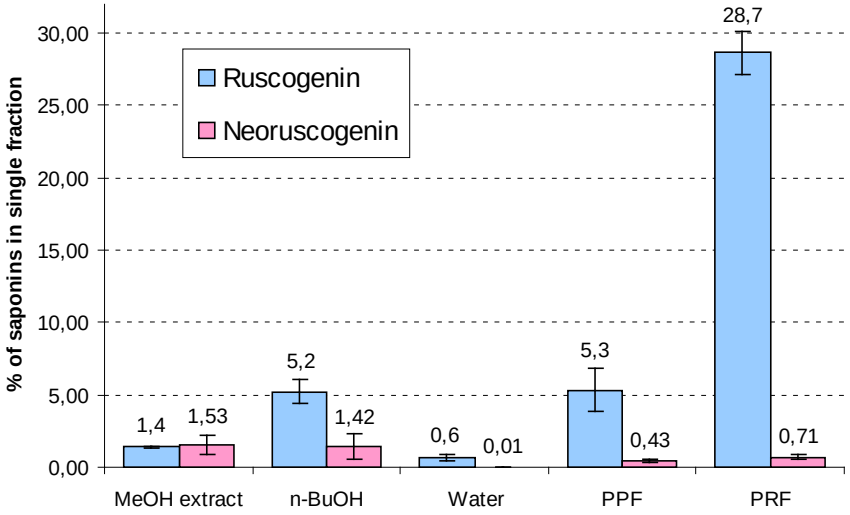

Fig. 3.46: % of saponins calculated as ruscogenin and neoruscogenin and expressed as the percent of saponins determined in single fractions; n = 3; mean ± SD.

From **Fig. 3.45**, p. 108, it is clear that most of the saponins from the methanolic extract stayed in the n-BuOH fraction after the liquid-liquid partitioning. As observed on a TLC plate (**Fig. 3.1**, p. 46), most of the steroid saponins from the n-BuOH fraction accumulated in fraction PPF after Sephadex fractionation II (p. 33). Therefore, fraction PPF was used for the isolation of steroid saponins. Nevertheless, the content of the saponins in PRF was relatively high (22.5%). But considering the high molecular weights of saponins and a very low yield of fraction PRF (7.5% of n-BuOH), it can be concluded, that steroid saponins with a high molecular weight most probably contribute to the total weight of fraction PRF. This was confirmed by TLC analysis (**Fig. 3.1**, p. 46) of fraction PRF, where only few typical red spots were observed under UV after derivatization with anisaldehyde reagent.

The initial MeOH extract showed the presence of both ruscogenin and neoruscogenin-type saponins. The content of neoruscogenin-type was slightly higher in comparison to ruscogenin-type saponins (**Fig. 3.46**, p. 109). Interestingly, all fractions produced from the initial methanolic extract showed much higher percent of ruscogenin-type saponins, which got even higher with further fractionation. On the other hand, during this thesis, we were able to isolate mainly neoruscogenin-type saponins. Due to this phenomenon, some problems should be considered. It is not only very difficult to isolate compounds from unstable extracts, but also makes extraction, fractionation and isolation under different conditions questionable and irreproducible. It is possible that the use of modified methods leads to completely different

fractions and even compounds. In order to standardize such procedures, exact analytical conditions should be specified.

3.3.2 Quantification of total phenolic compounds

Quantification of all phenolic compounds was peformed according to quantification of the phenols in Ph. Eur. monography of Tormentillae rhizoma (Ph. Eur. modified by Glasl 1983).
Same as for saponins, approximate weights of the analysed samples were determined by the sample to starting material (rhizomes) ratio (Quantification of saponins, p. 108). Results of the quantification of phenolic compounds are gathered in **Fig. 3.47** and **Fig. 3.48**.
As for saponins, most of the phenolic compounds were found in n-BuOH extract after the liquid-liquid partition from MeOH extract. Further fractionation of n-BuOH fraction to PPF and PRF gave an equal distribution of phenolics with a slightly higher content in PRF. It is important to know that fraction PRF was described as 'rich on phenolics' due to higher amount of such compounds in single fractions (**Fig. 3.48**, p. 111). As described before (quantification of saponins, p. 108), there are major differences between the weight of PPF and PRF. Same amount of phenolics in much smaller fraction PRF means that percentage of these compounds is much higher than in PPF, which can be observed in **Fig. 3.48**.

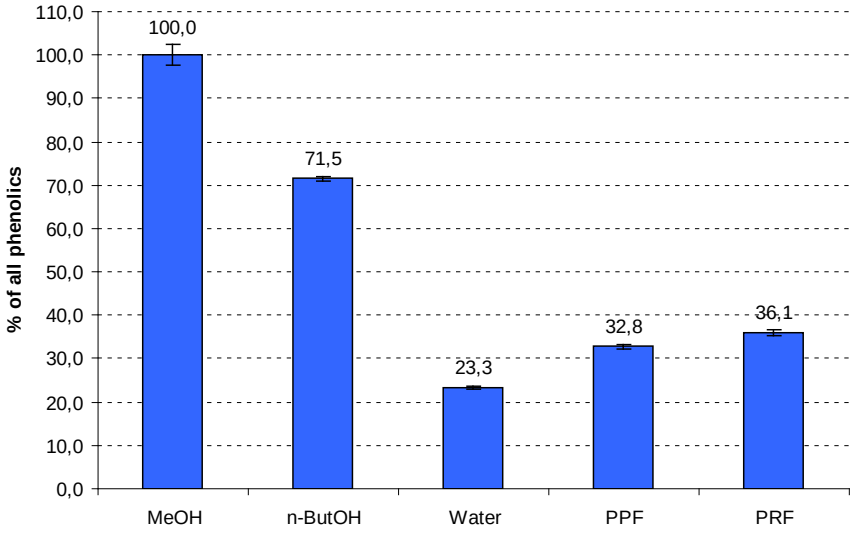

Fig. 3.47: % of all phenolic compounds expressed as the percentage of the phenolic compounds determined in MeOH extract (1.50 g/100 g of MeOH extract); n = 3; mean ± SD.

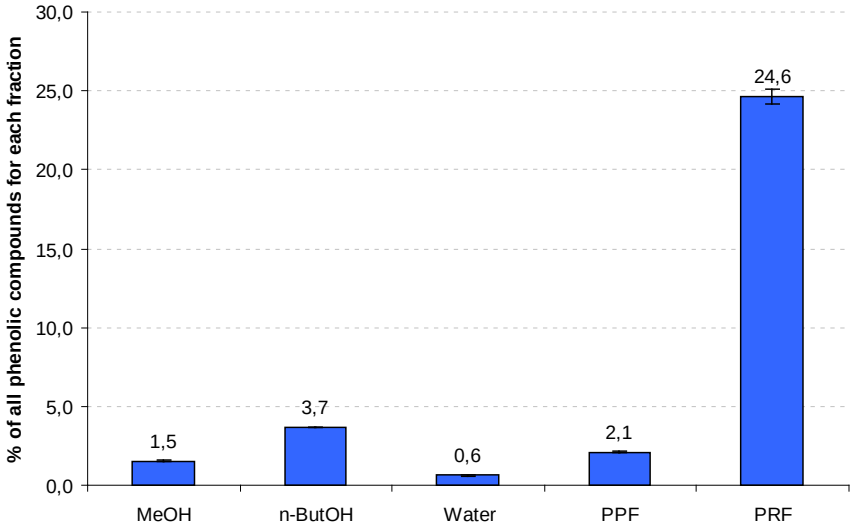

Fig. 3.48: % of all phenolic compounds expressed as the percentage of the phenolic compounds determined in single fractions; n = 3; mean ± SD.

3.4 Investigation of origin of C-22 hydroxy- and methoxylated compounds

As described for compound **2** (p. 56) NMR experiment of decomposed **2** confirmed the presence of two very similar compounds. ESI-MS experiment of this mixture gave two signals: 885 $[M-H]^-$ and 899 $[M-H]^-$ suggesting that original compound **2** has been de-methylated to **3**, resulting in a mixture of **2** and **3**. Same phenomenon has been observed by Kite *et al*. If the transformation from C-22-methoxy- to more stable C-22-hydroxy- compound occurs in a neutral and low-energy environment, a very important question needs to be answered. Why should *R. aculeatus* synthesise unstable C-22-methoxy compounds and prevent demethylation to hydroxyl derivatives in aqueous solution? Therefore, several reports about C-22-methoxylated products (Mimaki *et al.* 1998 b) need to be re-analyzed, due to the high probability that reported compounds are only artefacts of the isolation process. MeOH, as one of the main solvents used for extraction and chromatography, could be the reason for the generation of artefacts. In order to investigate this phenomenon, further analysis including compound **3** and extracts from *R. aculeatus* have been performed.

3.4.1 Inert extraction and LC-MS analysis of the extracts

In order to avoid influence of the solvent on the compounds from theButcher's Broom extract and thereby avoiding artefacts, rhizomes were extracted with solvents replacing MeOH and water (Materials & Methods, p. 38).

Extracts (n-BuOH, H_2O) were analysed using LC-MS (ESI-MS) coupled experiment. Due to previous reports about chromatographic problems using extracts from Butcher's Broom (Kite *et al.* 2007), three different HPLC methods (p. 39) were tested to optimize the quality of separation on the RP-18 column. First, acetic acid was used to acidify solvents used for liquid chromatography (H_2O/ACN). Due to poor separation, 1% of acetic acid was exchanged by 0.1% of formic acid without further change of the HPLC method. A better, but still not satisfactory separation had been observed. Therefore, the second method was optimized by increasing the flow and extending the gradient from 25 to 40 min. Method *MS 3* (p. 39) was by far the best method used for LC-MS analysis of the extracts.

To analyse, whether extracts from *R. aculeatus* originally contain both C-22 methoxylated and hydroxylated furostanols, extracts were analyzed concerning the presence of ions with

m/z 886 for C-22 hydroxy- and 900 for C-22 methoxy-compound. Since acetic acid and formic acid were used as modifiers in this experiment, *m/z* signals of adducts [M + CH_3COO^-] and [M + $HCOO^-$] were expected. Interesting molecular weights for the pseudomolecular ions, when using formic acid, were therefore *m/z* 931 and 932 for compound **3** as well as *m/z* 945 and 946 for compound **2**. With acetic acid as modifier, relevant peaks were *m/z* 945 and 946 for compound **3** and *m/z* = 959 and 960 for compound **2**.

In all experiments, including all three HPLC methods, only the presence of compound **3** could be observed. When using acetic acid as the modifier, *m/z* 945 [M + CH_3COO^-] together with appropriate pseudomolecular ion at *m/z* 885 $[M-H]^-$ were found. With formic acid *m/z* 931 [M + $HCOO^-$] together with appropriate pseudomolecular ion at 885 $[M-H]^-$ were detected. No trace of compound **2** was found in any of the extracts using all three methods (see figures from **Fig. 3.49**, p. 113 to **Fig. 3.56**, p. 117)

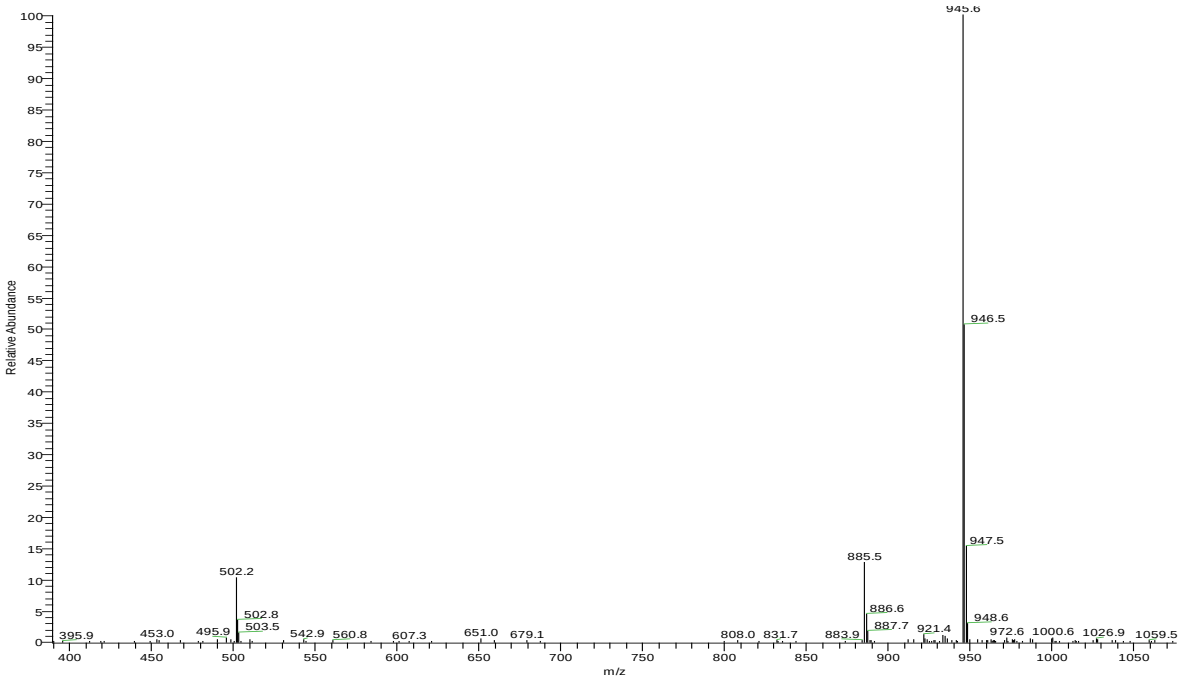

Fig. 3.49: ESI-MS signals for compound **2** ($[M-H]^-$ and [M + CH_3COO^-]) after HPLC-MS analysis using *MS 1*, showing the presence of compound **2** in n-BuOH and H_2O extract.

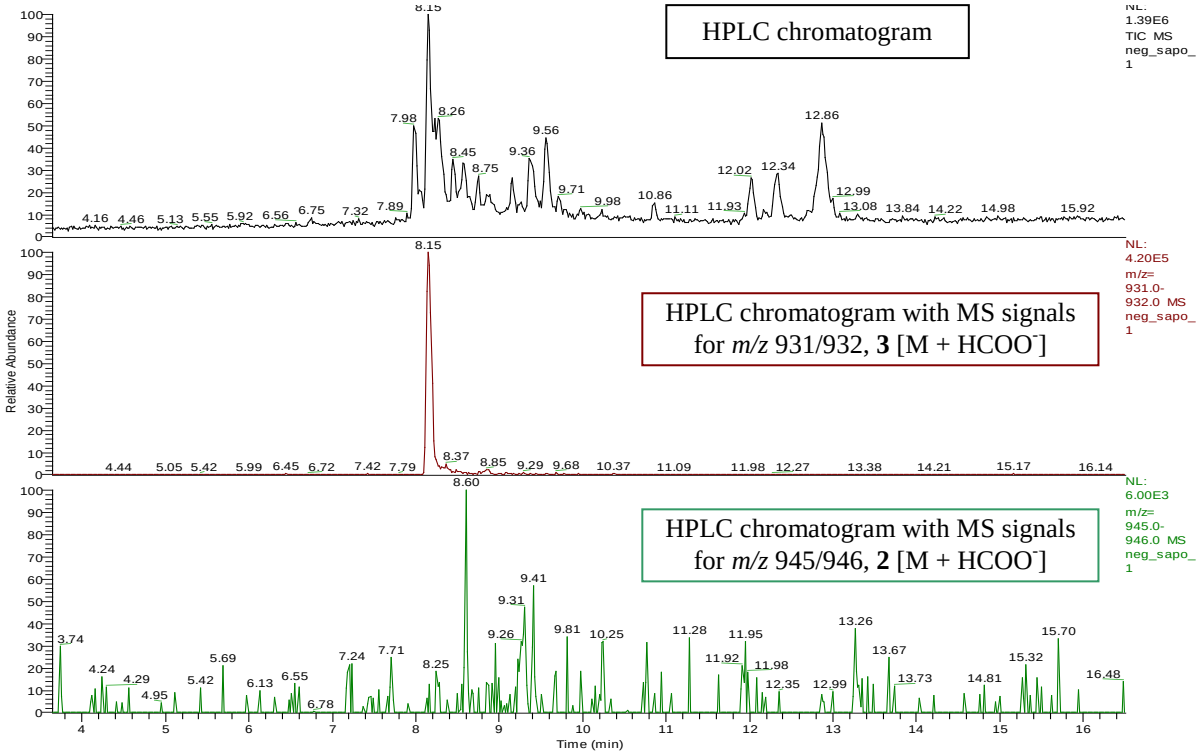

Fig. 3.50: HPLC-MS analysis of n-BuOH extract using *MS 2*, showing the HPLC chromatogram with observed ions of adducts of compounds **2** and **3**.

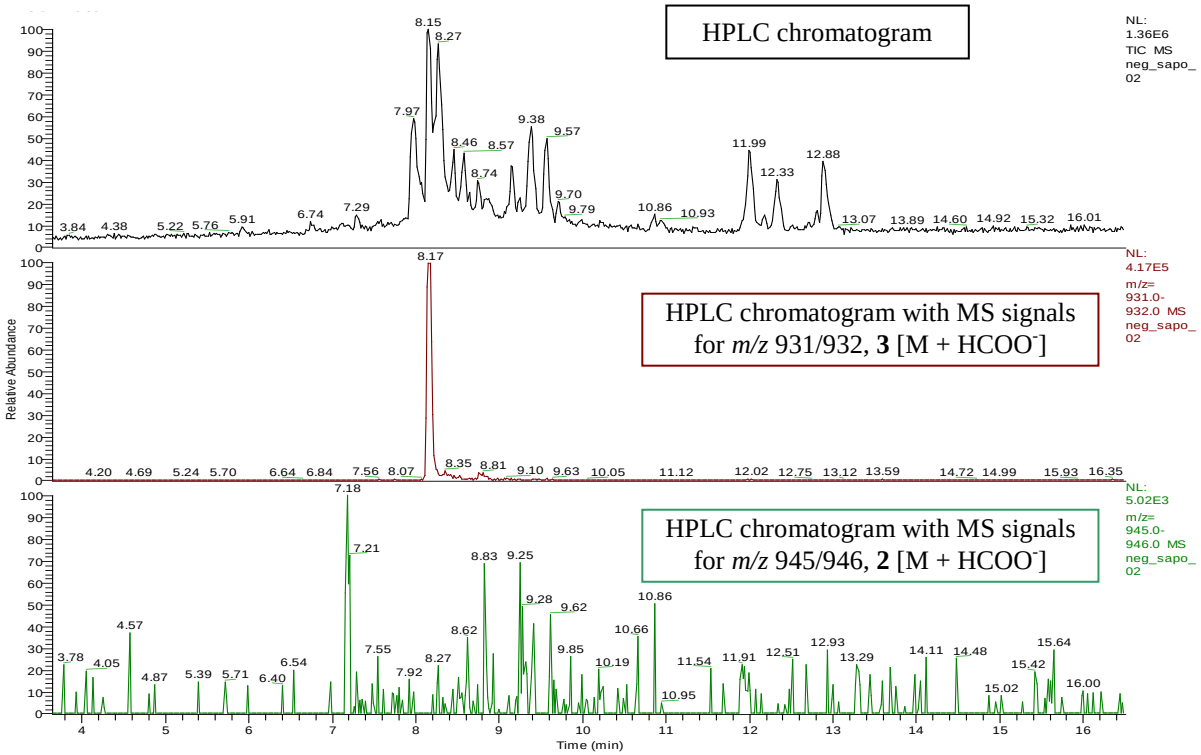

Fig. 3.51: HPLC-MS analysis of H_2O extract using *MS 2*, showing the HPLC chromatogram with observed ions of adducts of compounds **2** and **3**.

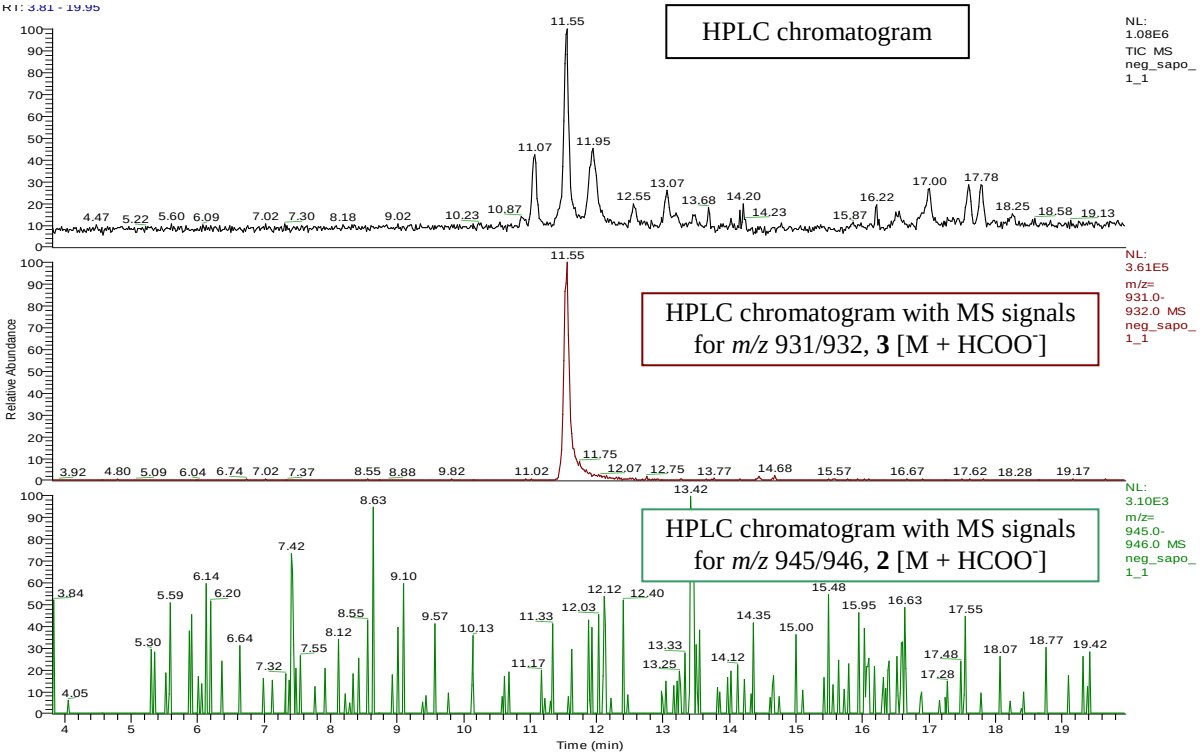

Fig. 3.52: HPLC-MS analysis of n-BuOH extract using *MS 3*, showing the HPLC chromatogram with observed ions of adducts of compounds **2** and **3**.

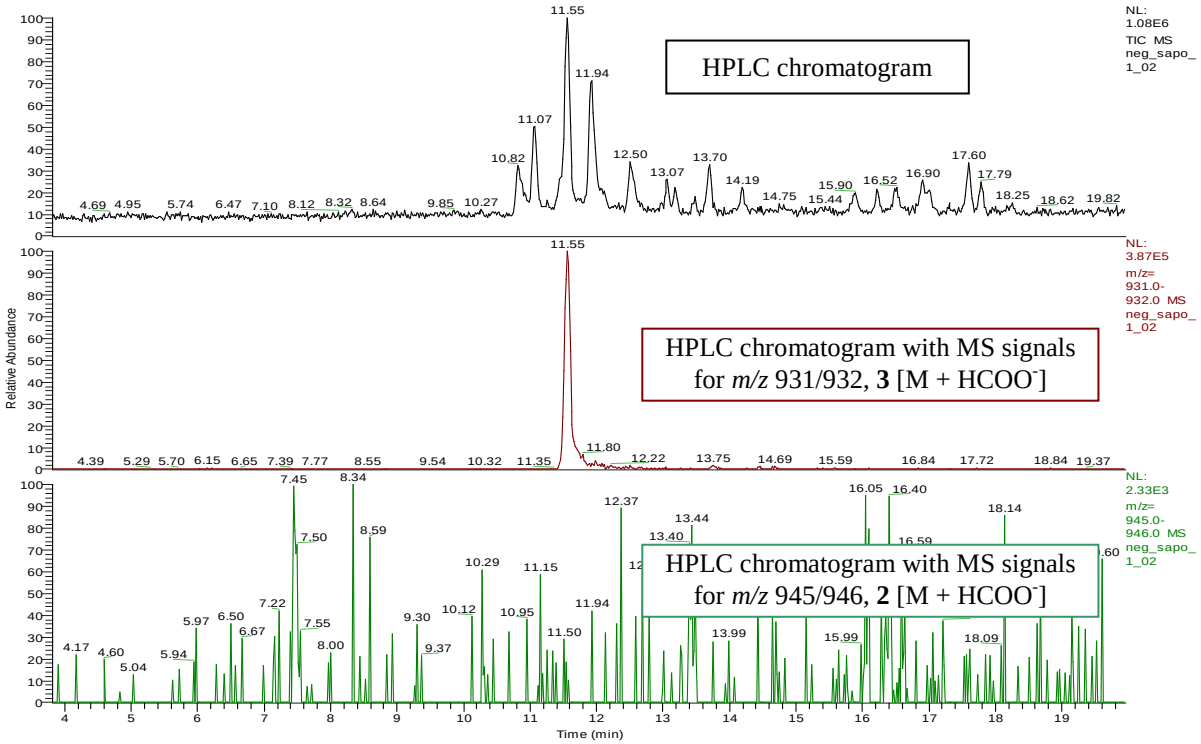

Fig. 3.53: HPLC-MS analysis of H_2O extract using *MS 3*, showing the HPLC chromatogram with observed ions of adducts of compounds **2** and **3**.

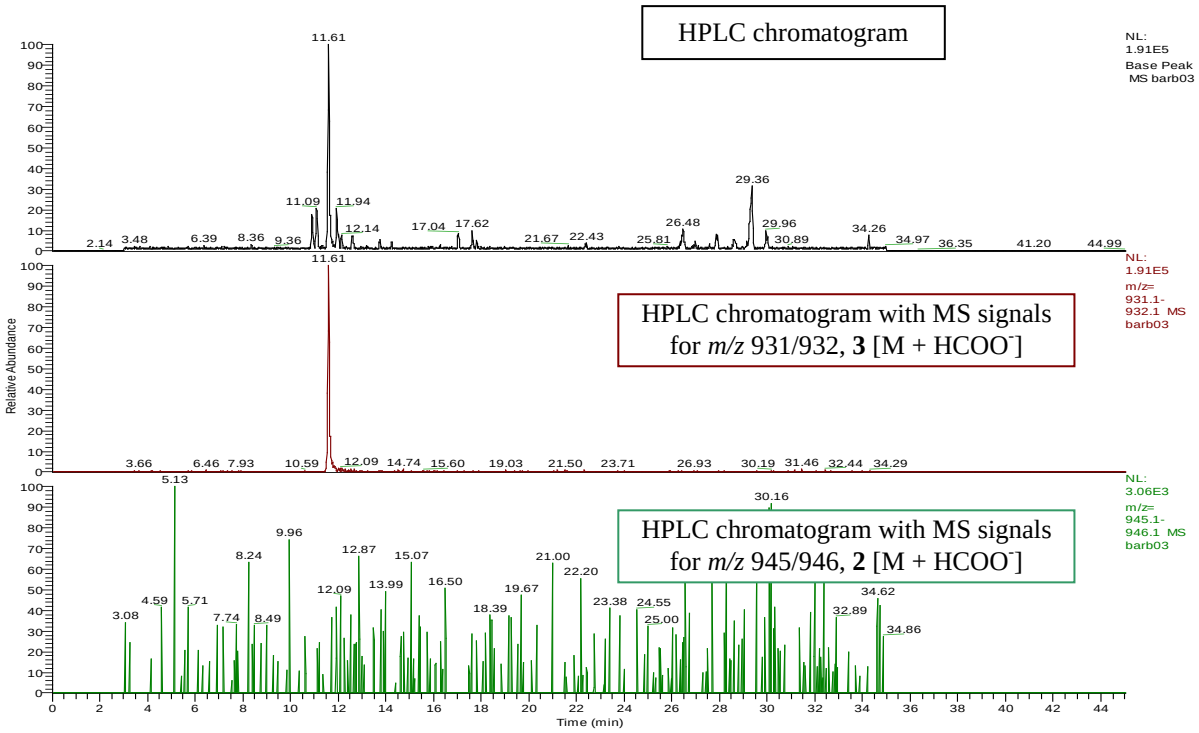

Fig. 3.54: HPLC-MS analysis of MeOH extract using *MS 3*, showing the HPLC chromatogram with observed ions of adducts of compounds **2** and **3**.

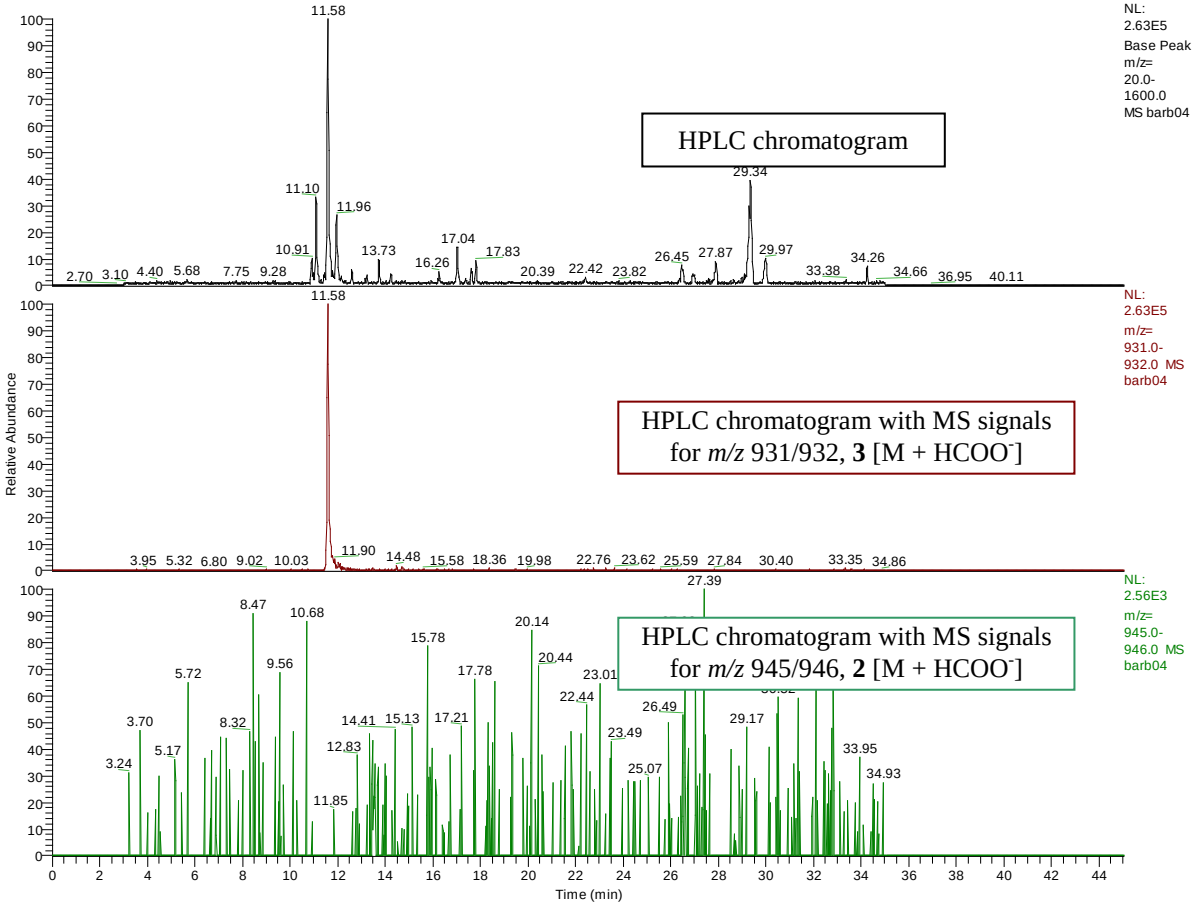

Fig. 3.55: HPLC-MS analysis of PPF fraction using *MS 3*, showing the HPLC chromatogram with observed ions of adducts of compounds **2** and **3**.

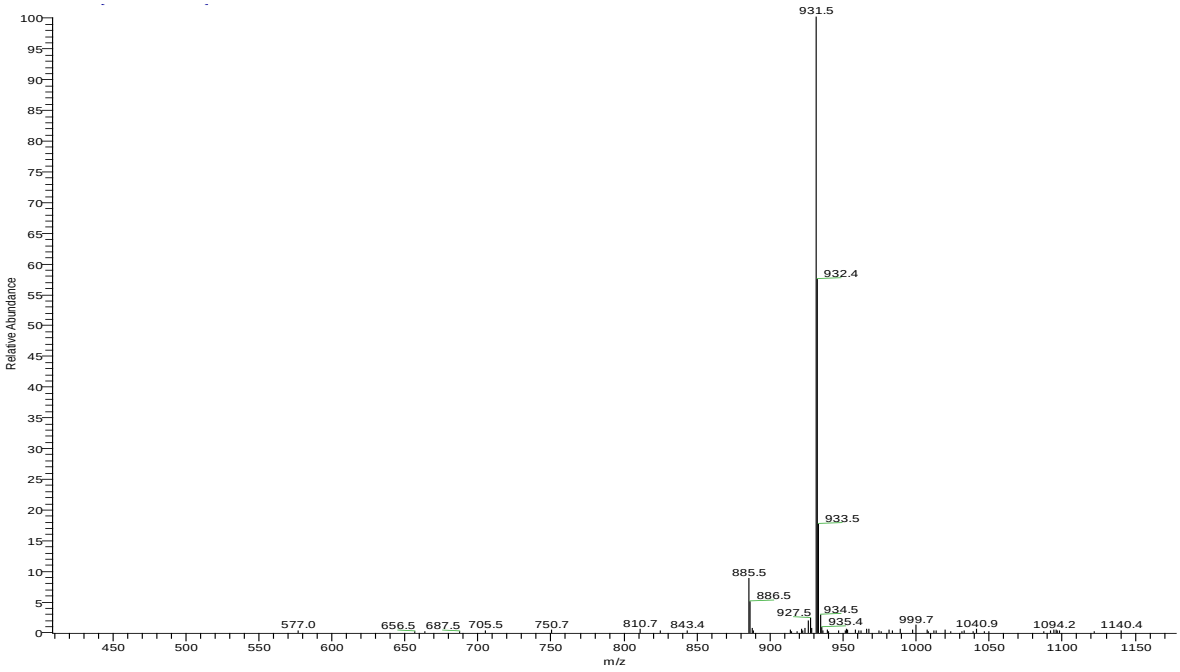

Fig. 3.56: ESI-MS signals for compound **2** ([M-H]$^-$ and [M + HCOO$^-$]) after HPLC-MS analysis using *MS 2* and *MS 3*, showing the presence of compound **2** in n-BuOH and H_2O extract.

3.4.2 Transformation of C-22 hydroxy- to C-22 methoxylated compound

The idea of this experiment was to observe, whether the compound **3** will transform from C-22 hydroxy- to C-22 methoxy-compound, when incubated in MeOD. If conversion occurred, several changes in the chemical shifts should be observed. By integration of the 'new' signals a kinetic of the transformation should be determined.

After measurment of ^{1}H experiments for several weeks, indeed some changes have been observed (**Fig. 3.57**, p. 120), but transformation at room temperature was found to be very slow. After incubation of compound **3** in MeOD for 6 months, solvent has been removed and the sample was again dissolved in pyridine d-5. 1 and 2D NMR spectra were measured to get spectra comparable to those of compound **3**. Additionally, sample was submitted to ESI-MS analysis. Furthernore, sample was dissolved in water for three days, then dried and again submitted to NMR analysis.

NMR data of the mixture was compared to those of the decomposed compound **2** performed as **2** was isolated (**Table 3.14**, p. 119). The results of NMR analysis, especially compared to

NMR data of compound **2** decomposed in water, were confusing. As it can be seen from **Table 3.14,** all the signals, including non-overlapping double signals, are completely identical to those of decomposed compound **2**. The only difference is a missing methyl group signal in carbon spectrum of our test sample.

Accordingly, ESI-MS could not confirm the presence of both **2** and **3**, meaning the transformation from compound **3** to **2** did not occur. Solely peaks with *m/z* 885 and 887 $[M-H]^-$ were found, the former belonging to $[M-H]^-$ of **3**. Second signal probably indicates the presence of a compound with an exchange of two protons with deuterium atoms in MeOD. Literature reports on the methylation of the C-22 hydroxyl group of furostanol saponins after incubation in MeOD (Lee *et al.* 2009) could not be confirmed. Observations on the kinetics measured in proton spectrum did not unveil any clear results, which could lead to final conclusions about the transformation. Like displayed in **Fig. 3.57**, p. 120, two major peak changes have been observed during the six months incubation in MeOD. Unfortunately, due to the high peak overlapping, no signal assignment was possible. After dissolving the sample in water for three days, observed mixture transformed back to compound **3**, according to the NMR spectra taken in pyridine after drying the sample.

147.3	147.3
146.9	146.9
139.6	139.7
139.6	139.6
124.8	124.8
124.8	124.8
112.5	112.4
111.1	111.1
110.7	110.7
110.4	110.4
104.0	104.0
103.9	103.9
101.8	101.8
100.5	100.4
83.6	83.6
83.6	83.6
81.5	81.5
81.3	81.3
78.7	78.7
78.6	78.6
78.6	78.6
78.6	78.6
76.0	76.0
75.2	75.2
75.2	75.2
75.2	75.2
74.3	74.3
72.7	72.7
72.6	72.6
72.1	72.1
72.1	72.1
71.7	71.7
71.7	71.7
70.2	70.2
69.5	69.5
68.3	68.3
67.4	67.4
64.2	64.2
63.9	63.9
62.9	62.9
62.8	62.8
56.8	56.8
56.7	56.7
50.5	50.5
50.4	50.4
47.4	
43.9	43.9
43.0	43.0
43.0	43.0
40.7	40.7
40.6	40.6
40.6	40.6
40.4	40.4
40.3	40.3
38.0	38.0
37.4	37.4
33.2	33.2
33.1	33.1
32.7	32.7
32.4	32.4
32.1	32.1
32.0	32.0
31.6	31.7
28.4	28.4
28.1	28.1
24.1	24.1
24.1	24.1
19.1	19.1
19.1	19.1
16.9	16.9
16.7	16.7
16.4	16.4
16.2	16.2
15.1	15.1

Table 3.14: **A**: ^{13}C (δ in ppm) signals of compound **2** partially decomposed to **3** after freeze drying
B: ^{13}C (δ in ppm) signals of compound **3** after 6 months incubation in MeOD

Experiment (150 MHz, 296 K) showed for both samples identical signals, except for the MeO- group present in mixture A (marked red).

Signal for MeO- group in mixture A indicating the presence of compound **2**, which could not be found in mixture B.

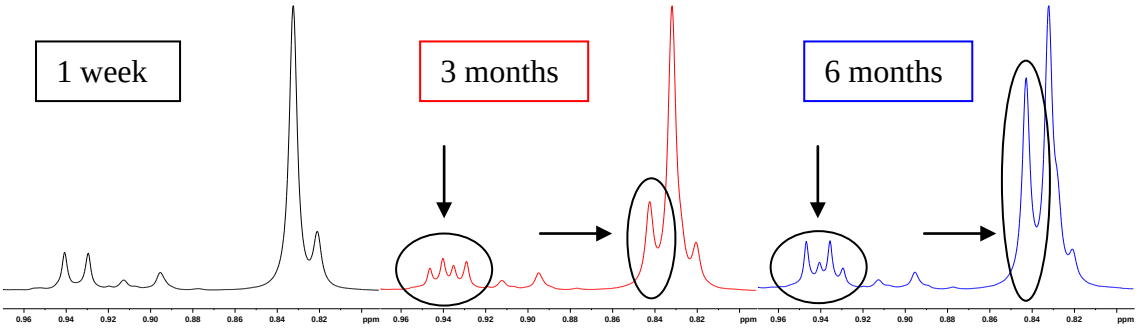

Fig. 3.57: Changes of NMR proton peaks at 0.94 and 0.84 ppm for compound **3**, incubated in MeOD for 6 months at room temperature and measured on Bruker Avance III 600 Kryo in MeOD at room temperature.

Since the transformation from **3** to **2** was excluded via LC-MS experiment, changes observed in **Fig. 3.57** must have occured due to the interference of the deuterated methanol, causing exchange of protons with deuterium. Still, it is hard to believe that shifts of ^{13}C signals of this mixture were completely identical to those from the mixture of compounds **2** and **3**, except for the methyl group (**Table 3.14**, p. 119).

3.5 Cell culture assays

As described before (Introduction, p. 7), extracts from *R. aculeatus* have shown promising results in the treatment of CVI and some other chronic vascular diseases. It has also been suggested (Introduction, p. 8) that inflammation plays a key role in development of these diseases. Endothelial hyperpermeability and expression of endothelial cell adhesion molecules are two very important features of inflammatory response. Therefore, ICAM-1 expression inhibition and macromolecular permeability assay, using human microvascular endothelial cells, were performed in order to determine the activity of fractions and compounds from Butcher's Broom. The studies have been broadened by additional experiments, such as viability assays and tests, where the influence of testing samples on endothelial cells has been observed. Results from these investigations could certainly contribute to the better knowledge of treatment of vascular diseases using products from *R. aculeatus*.

3.5.1 ICAM-1 expression inhibition assay

The results from ICAM-1 assays showed that methanolic extract and fractions from the extract influence the expression of adhesion molecules. Furthermore, several single compounds isolated from Butcher's Broom showed activity in this assay.

Extracts and fractions have all been tested relatively to the yields from fractionation, where MeOH extract was set to 100%. Parthenolide was used as a positive control. As it is toxic at 10 µM (cell cell death observed under microscope), a 5 µM solution was used in later assays with isolated compounds.

Interestingly, all extracts showed better inhibition of ICAM-1 expression at lower concentrations (**Fig. 3.58**, p. 122). Plausible explanation is that higher concentrations probably promote inflammation and thereby increase the expression of ICAM-1 molecules. Fractions PPF and PRF, both produced from n-BuOH fraction, showed inhibition at relatively low concentrations, especially PRF by inhibiting the expression down to 73% at concentrations of 0.2 and 0.02 µg/mL, respectively (**Fig. 3.59**, p. 122).

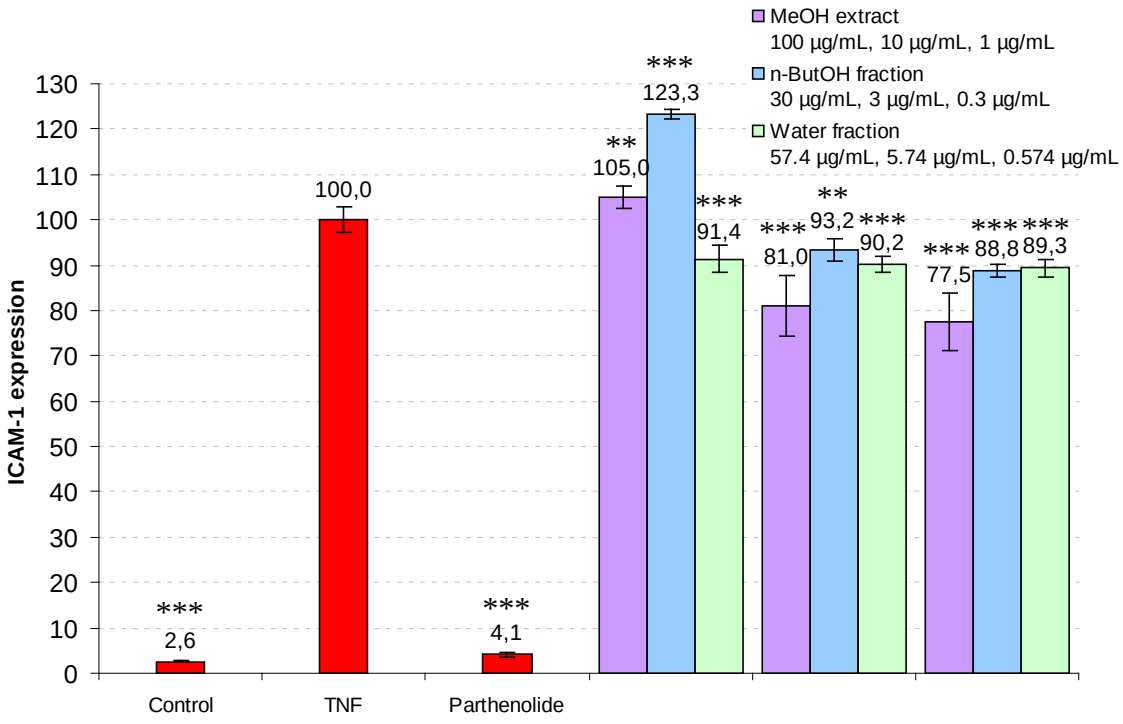

Fig. 3.58: Inhibition of ICAM-1 expression (%) after 24 h with MeOH extract, n-BuOH and H_2O fraction on the HMEC-1 cells; parthenolide (10 µM) was used as positive control; n = 3; mean ± SD; *** $p < 0.001$, ** $p < 0.01$.

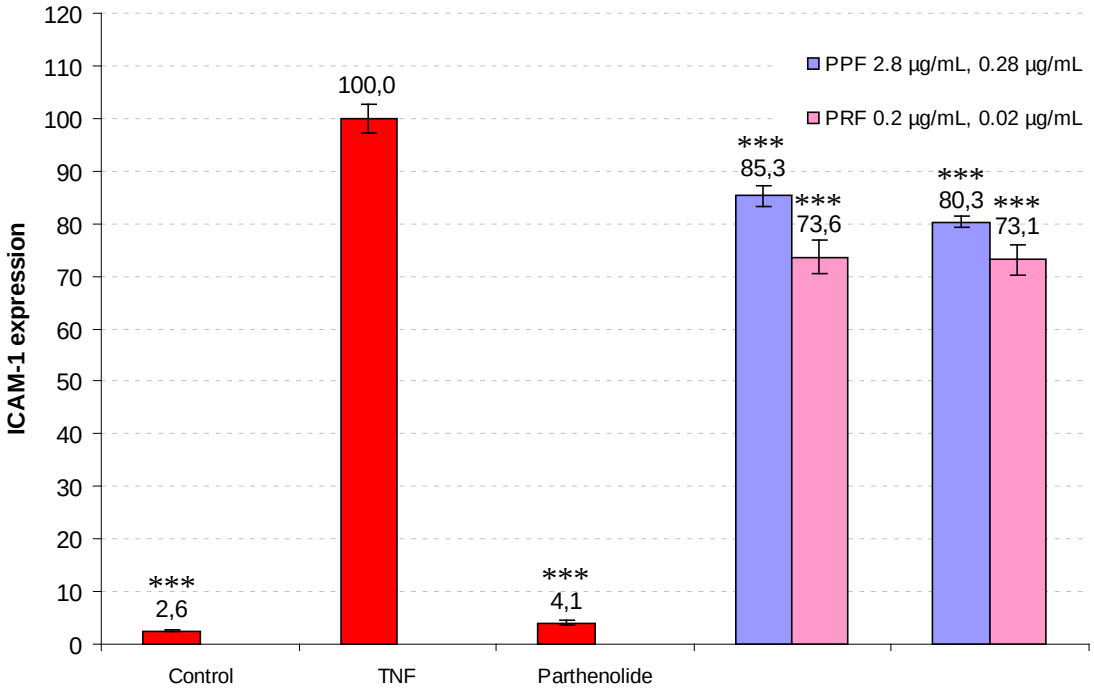

Fig. 3.59: Inhibition of ICAM-1 expression (%) after 24 h with PPF and PRF fractions on the HMEC-1 cells; parthenolide (10 µM) was used as positive control; n = 3; mean ± SD; *** $p < 0.001$.

Compounds **1**, **3**, **5**, **6**, **7**, **8**, **9** and **10** (50 µM, 10 µM, 1 µM), together with neoruscogenin, were also tested in ICAM-1 assay. Several compounds showed slight inhibition of ICAM-1 expression with ruscin (**8**) being the most effective. At concentration 50 µM, ruscin inhibited the expression down to remarkable 55% (**Fig. 3.65**, p. 126). Compounds **1** and **9** at 50 µM increased the expression significantly (**Fig. 3.60**, p. 123 and **Fig. 3.66**, p. 126). The same was observed with compound **6** at 10 µM. At 50 µM, **6** caused cell death of the HMECs (**Fig. 3.80**, p. 136), therefore inhibition of ICAM-1 expression could not be measured. Compound **3** showed no activity.

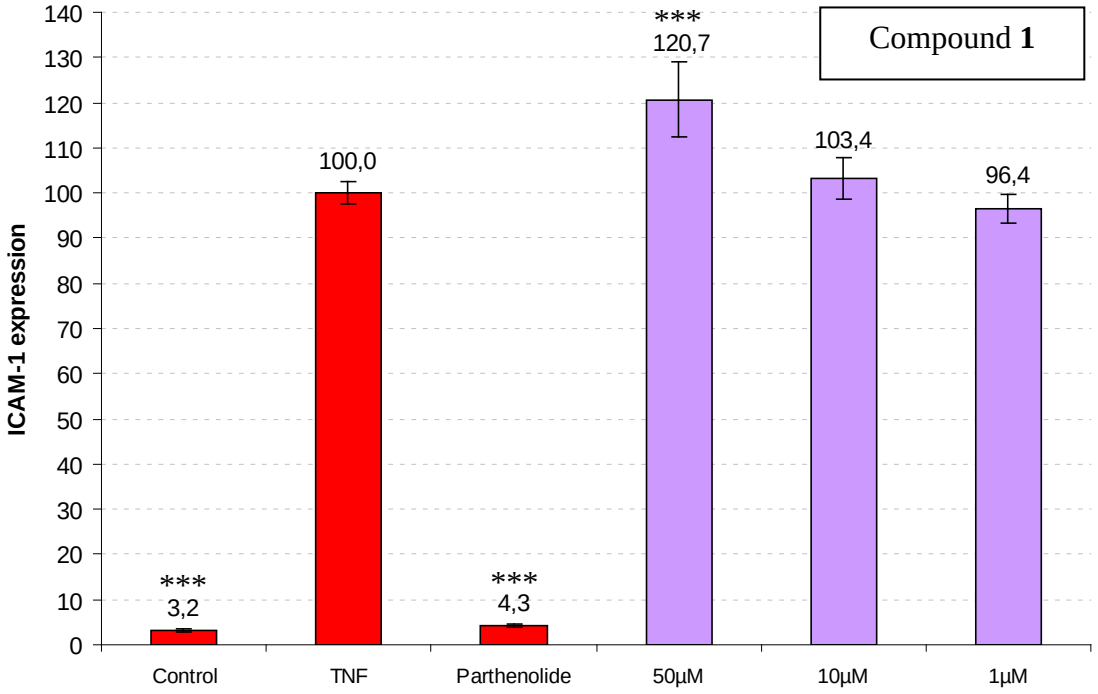

Fig. 3.60: Inhibition of ICAM-1 expression (%) after 24 h with compound **1** on the HMEC-1 cells; parthenolide (10 µM) was used as positive control; n = 3; mean ± SD; *** $p < 0.001$.

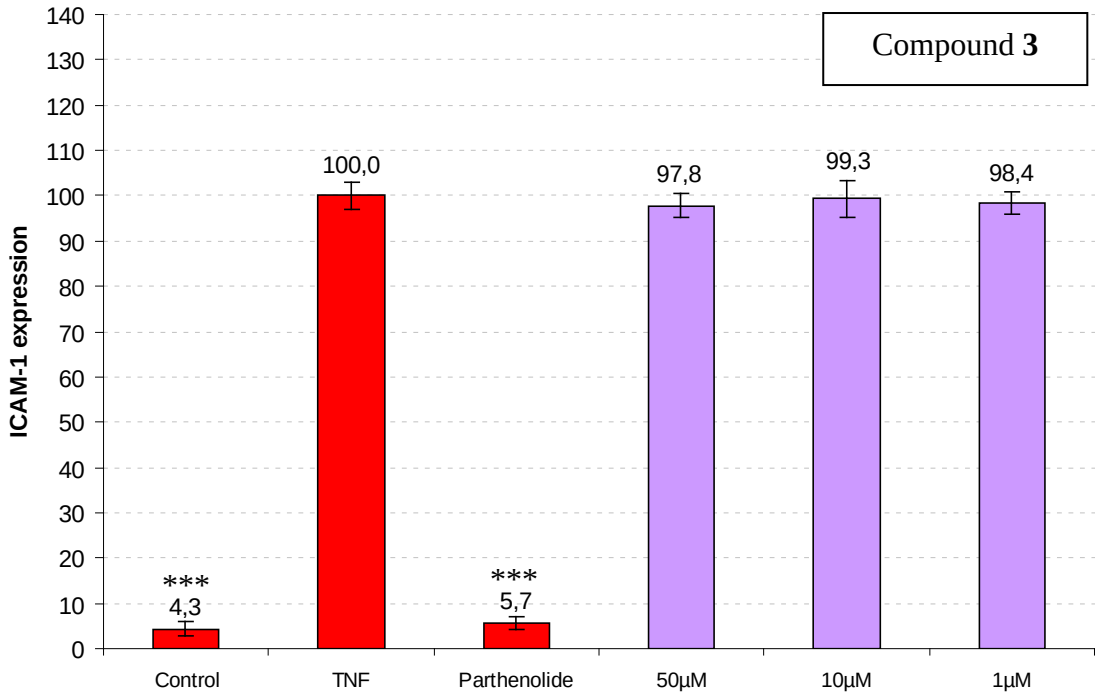

Fig. 3.61: Inhibition of ICAM-1 expression (%) after 24 h with compound **3** on the HMEC-1 cells; parthenolide (10 µM) was used as positive control; n = 3; mean ± SD; *** $p < 0.001$.

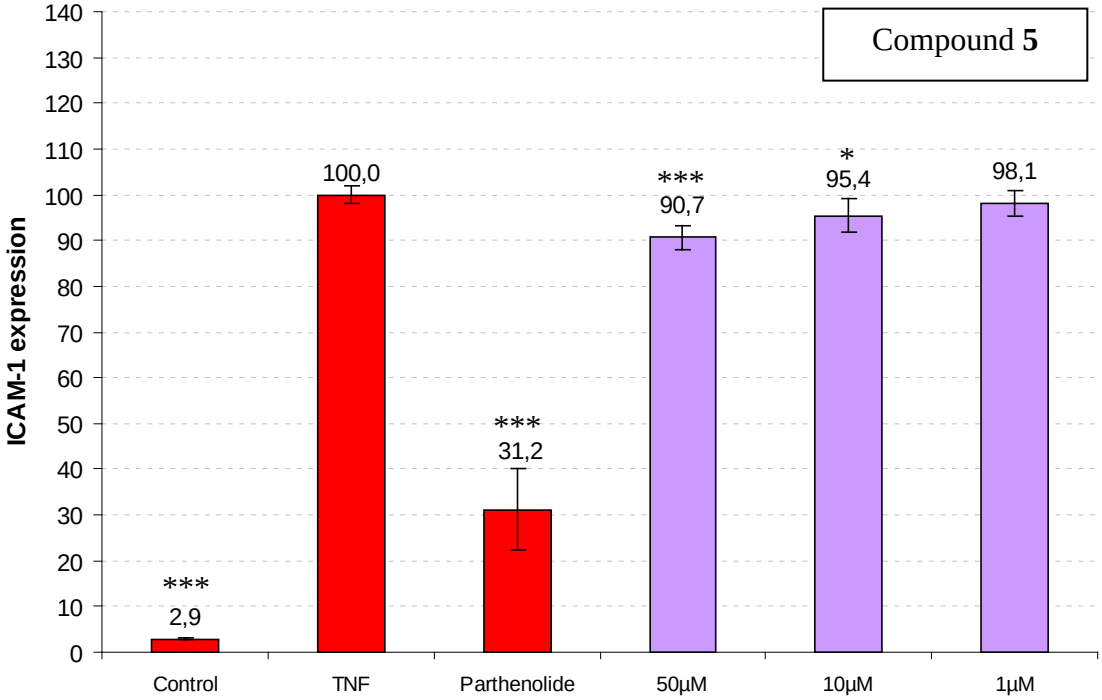

Fig. 3.62: Inhibition of ICAM-1 expression (%) after 24 h with compound **5** on the HMEC-1 cells; parthenolide (5 µM) was used as positive control; n = 3; mean ± SD; *** $p < 0.001$, * $p < 0.05$.

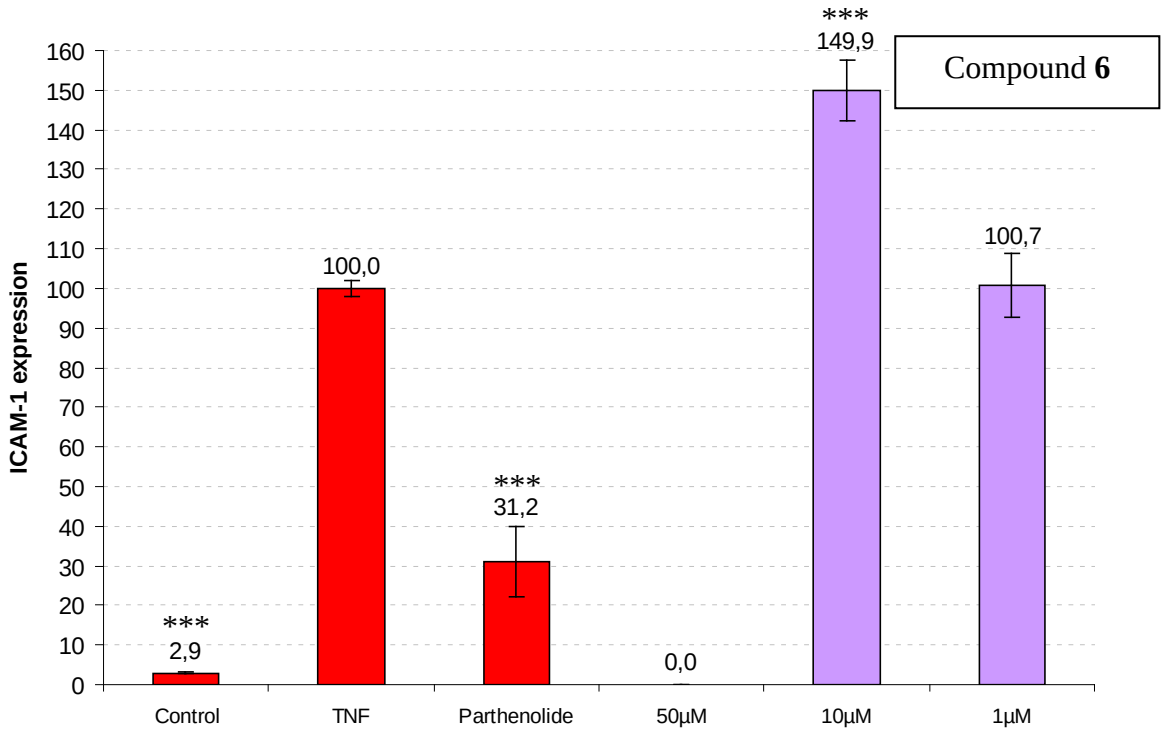

Fig. 3.63: Inhibition of ICAM-1 expression (%) after 24 h with compound **6** on the HMEC-1 cells; parthenolide (5 µM) was used as positive control; n = 3; mean ± SD; *** $p < 0.001$.

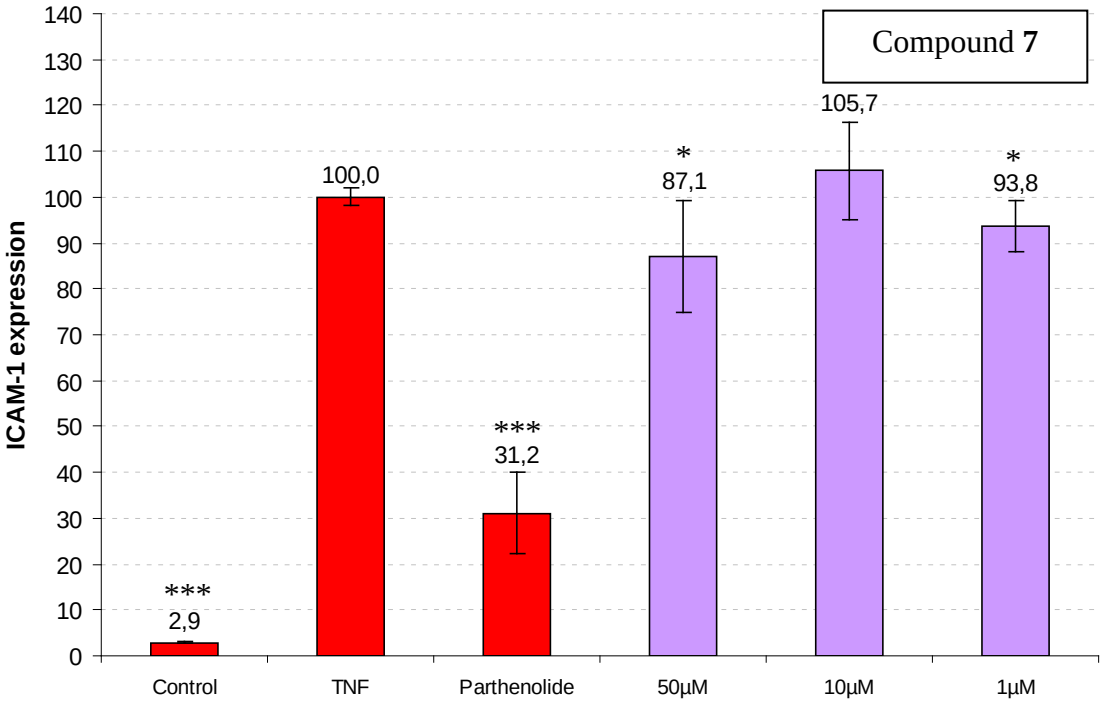

Fig. 3.64: Inhibition of ICAM-1 expression (%) after 24 h with compound **7** on the HMEC-1 cells; parthenolide (5 µM) was used as positive control; n = 3; mean ± SD; *** $p < 0.001$, * $p < 0.05$.

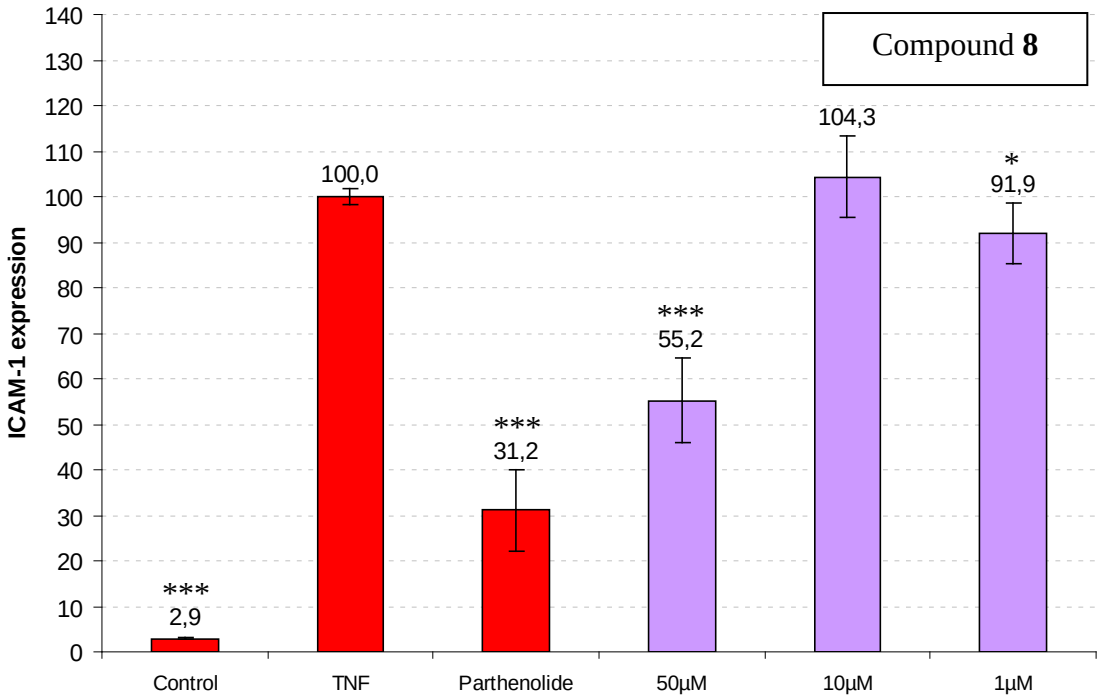

Fig. 3.65: Inhibition of ICAM-1 expression (%) after 24 h with compound **8** on the HMEC-1 cells; parthenolide (5 µM) was used as positive control; n = 3; mean ± SD; *** $p < 0.001$, * $p < 0.05$.

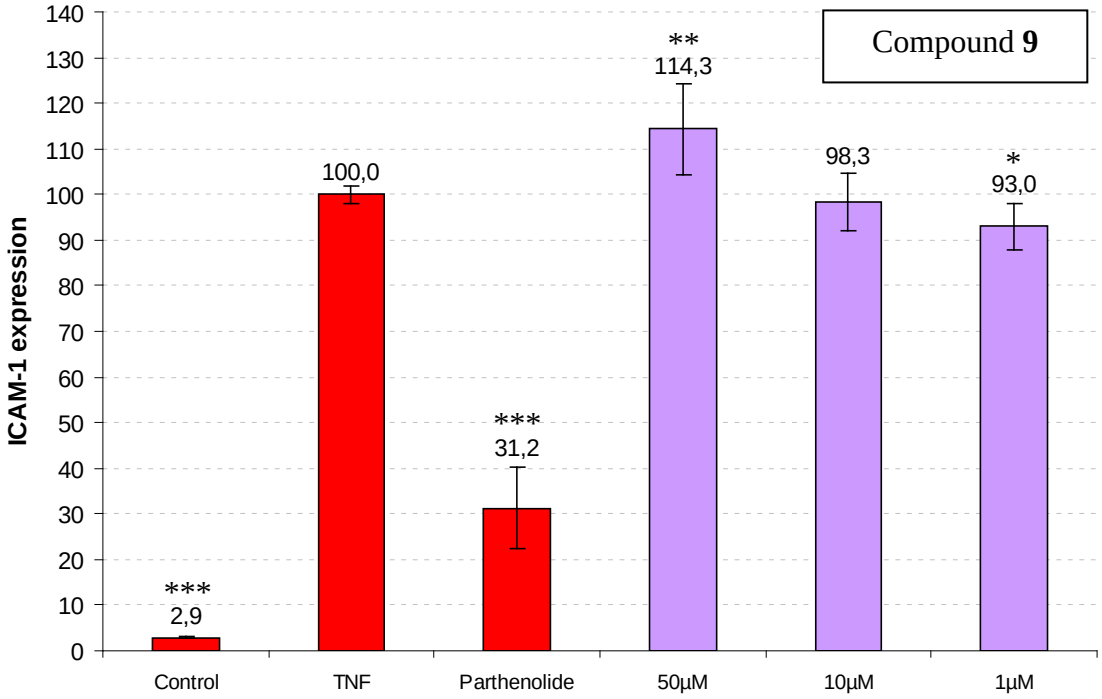

Fig. 3.66: Inhibition of ICAM-1 expression (%) after 24 h with compound **9** on the HMEC-1 cells; parthenolide (5 µM) was used as positive control; n = 3; mean ± SD; *** $p < 0.001$, ** $p < 0.01$, * $p < 0.05$.

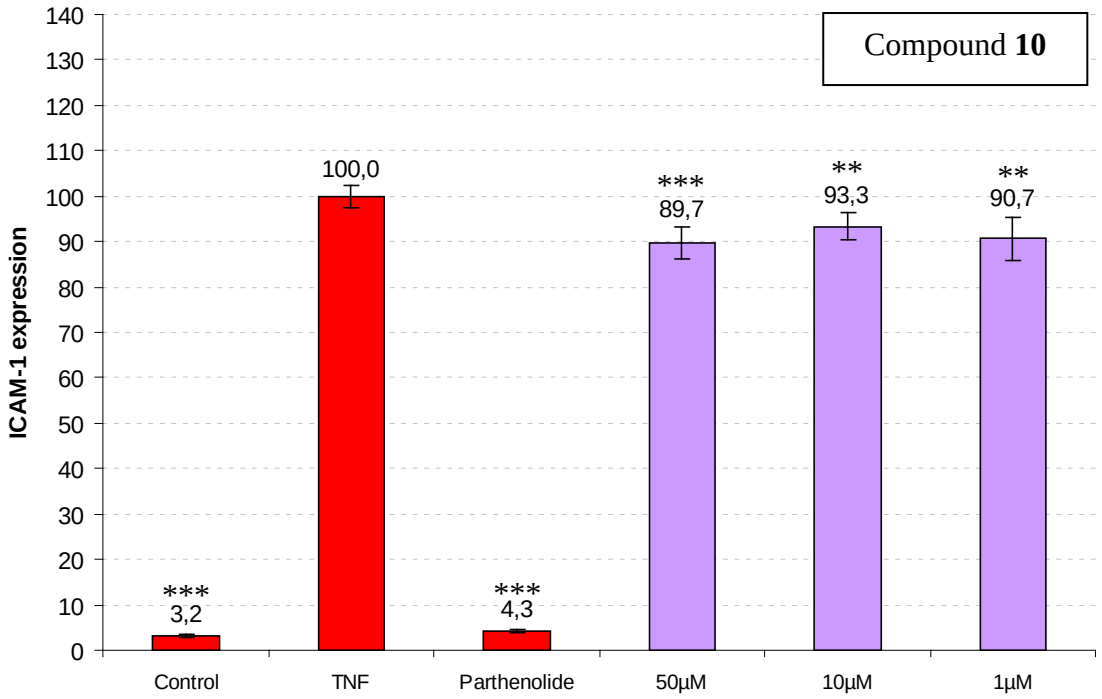

Fig. 3.67: Inhibition of ICAM-1 expression (%) after 24 h with compound **10** on the HMEC-1 cells; parthenolide (10 µM) was used as positive control; n = 3; mean ± SD; *** $p < 0.001$, ** $p < 0.01$.

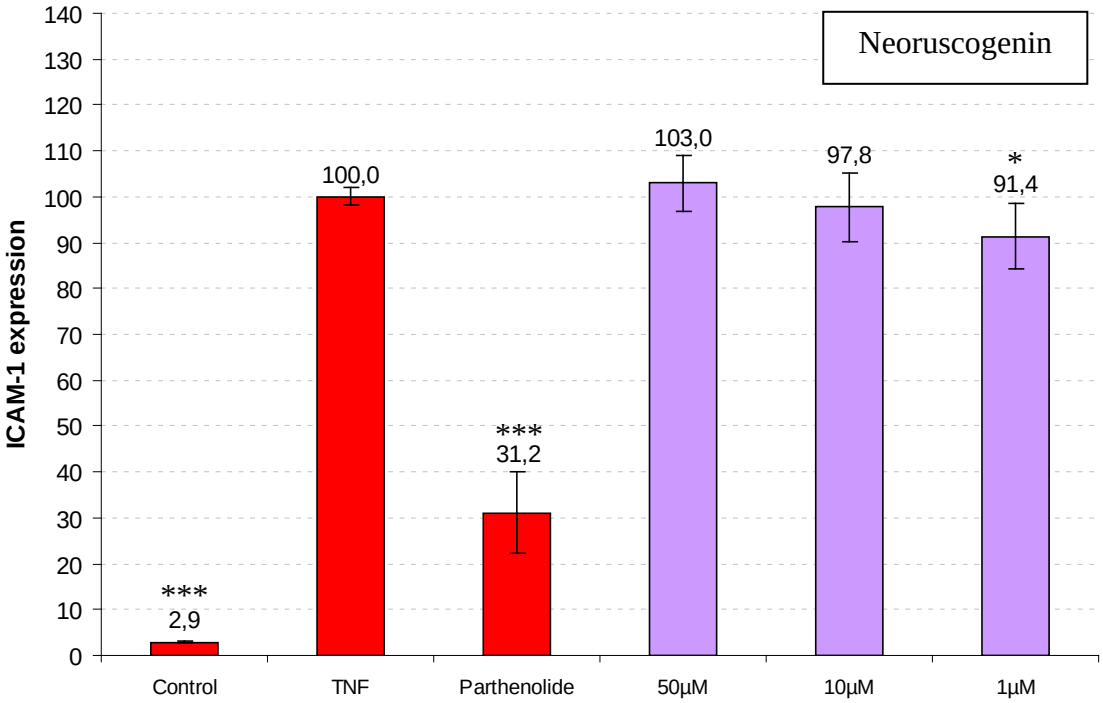

Fig. 3.68: Inhibition of ICAM-1 expression (%) after 24 h with neoruscogenin on the HMEC-1 cells; parthenolide (5 µM) was used as positive control; n = 3; mean ± SD; *** $p < 0.001$, * $p < 0.05$.

3.5.2 Macromolecular permeability assay

The hyperpermeability assays were performed by E. Willer and Dr. R. Fürst of the Institute of Pharmaceutical Biology, Ludwigs-Maximilians-University München, Germany.

Hyperpermeability of endothelial cells was induced by stimulating a confluent grown monolayer with thrombin. Thrombin causes disruption of endothelial barrier and thereby an increase in permeability. FITC-labelled dextran was used for the measurement of induced permeability. Values of the cells, treated only with dextran, were set as control value (100% diffusion). Influence of compounds on cells treated with thrombin was compared to the 100% value. Completely untreated cells were used as a negative control.

Compounds tested in this assay were **1**, **5**, **6**, **8**, **9**, **10**, **11**, **12** and neoruscogenin at 100 µM, 10 µM, 1 µM and 0.1 µM (incubated for 60 min). In general, none of the compounds showed strong reduction of thrombin induced hyperpermeability. Nevertheless some of the samples significantly diminished effects of thrombin. At a certain concentration, most of the tested saponins caused a remarkable increase in permeability, which was observed as even higher than permeability of the monolayer treated with thrombin. This phenomenon can probably be explained by the property of the saponins to promote a detergent effect at high concentrations. This leads to cell membrane disorganization and thereby higher permeability. This hypothesis was confirmed by lacking effects of aglycone neoruscogenin and sulfated aglycone ruscogenin (**5**). Interestingly, saponin **9** did not show increase in permeability in none of the testing concentrations. Even more, **9** significantly reduced thrombin induced permeability at 1 µM, 10 µM and 100 µM. Most effective compounds were ruscin (**Fig. 3.73**, p. 131), compound **5** (**Fig. 3.71**, p. 130) and deglucoruscin (**Fig. 3.70**, p. 129) at 10 µM. At higher concentrations (100 µM), compounds **1** and **8** both dramatically induced permeability of the dextran. Compound **10** (esculin) at 10 µM also significantly decreased the thrombin induced hyperpermeability (**Fig. 3.75**, p. 132).

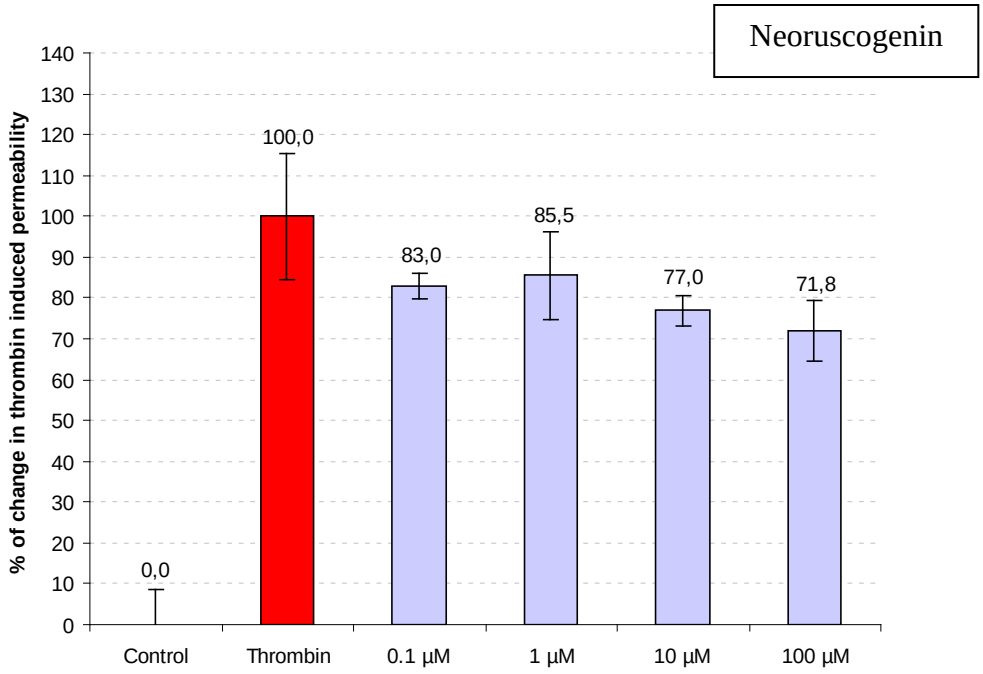

Fig. 3.69: Permeability assay for neoruscogenin after 60 min; expressed as percent of the thrombin value (100%); n = 3; mean ± SE.

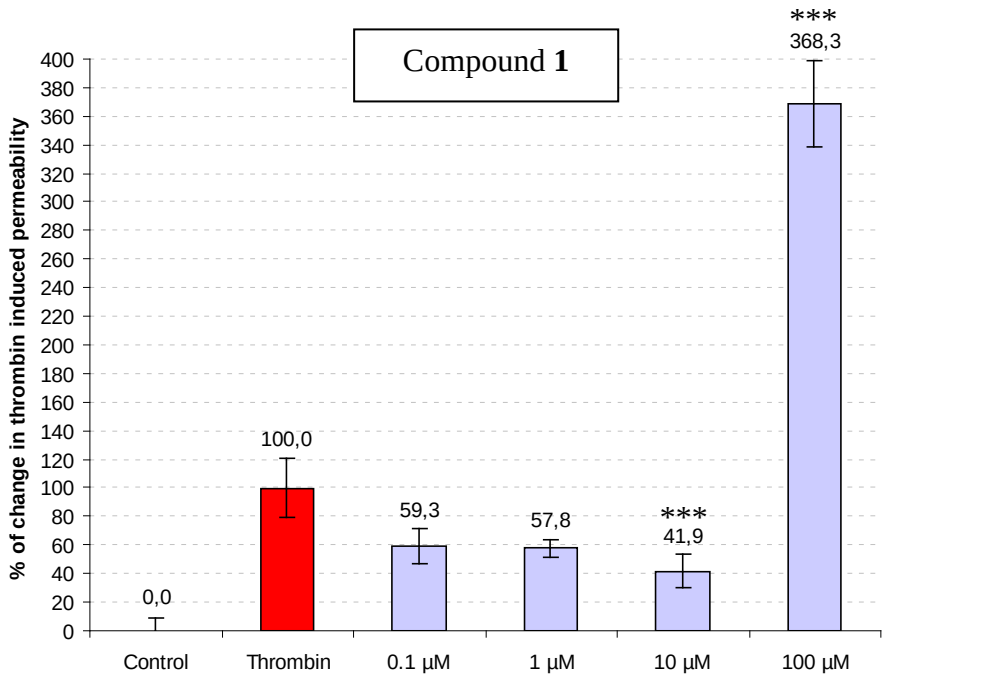

Fig. 3.70: Permeability assay for compound **1** after 60 min; expressed as percent of the thrombin value (100%); n = 3; mean ± SE; *** $p < 0.001$.

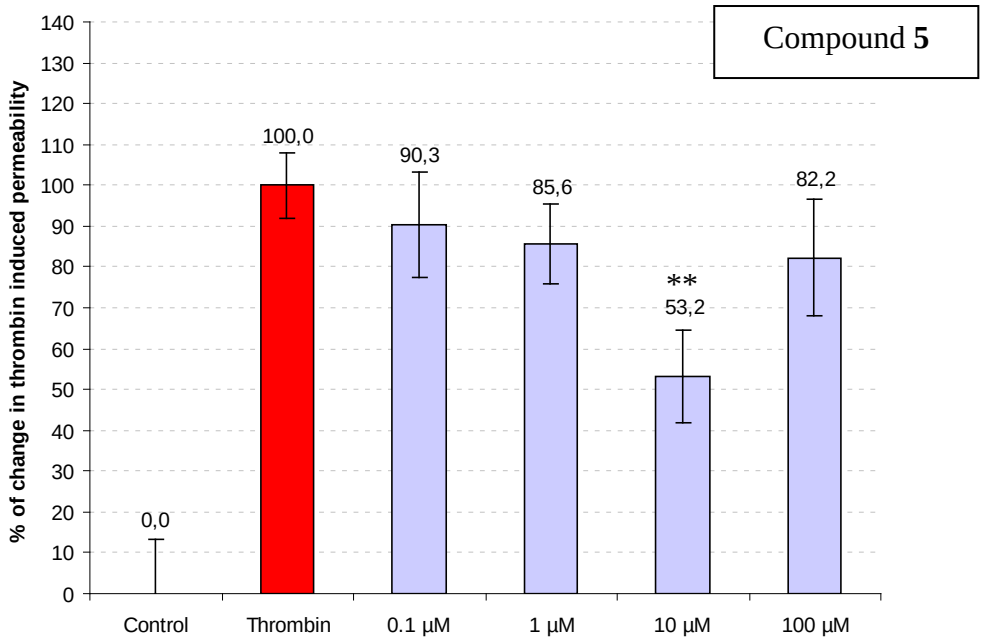

Fig. 3.71: Permeability assay for compound **5** after 60 min; expressed as percent of the thrombin value (100%); n = 3; mean ± SE; ** $p < 0.01$.

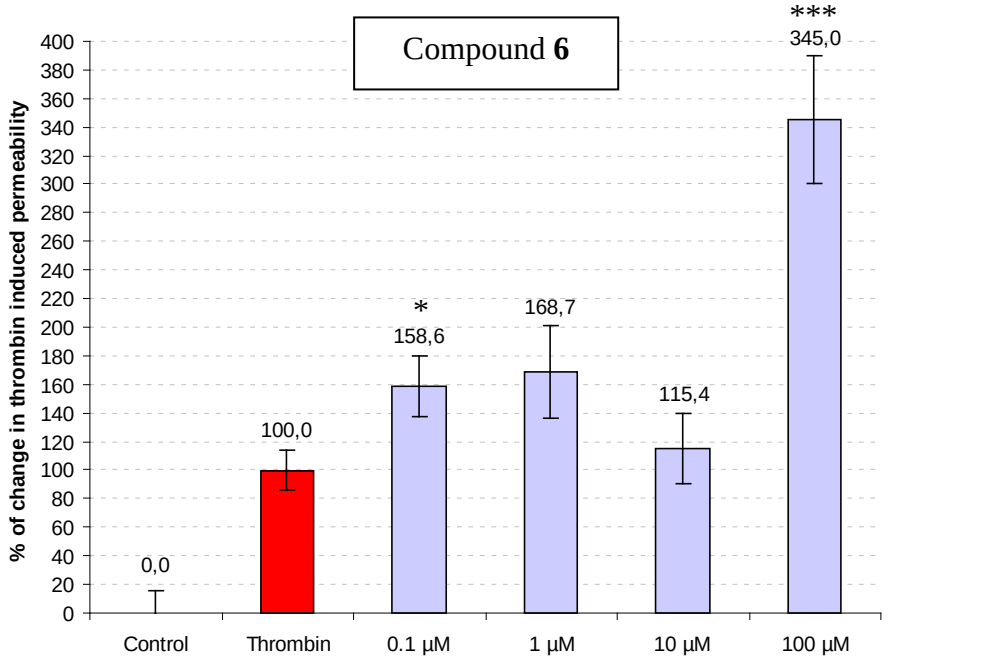

Fig. 3.72: Permeability assay for compound **6** after 60 min; expressed as percent of the thrombin value (100%); n = 3; mean ± SE; *** $p < 0.001$, * $p < 0.05$.

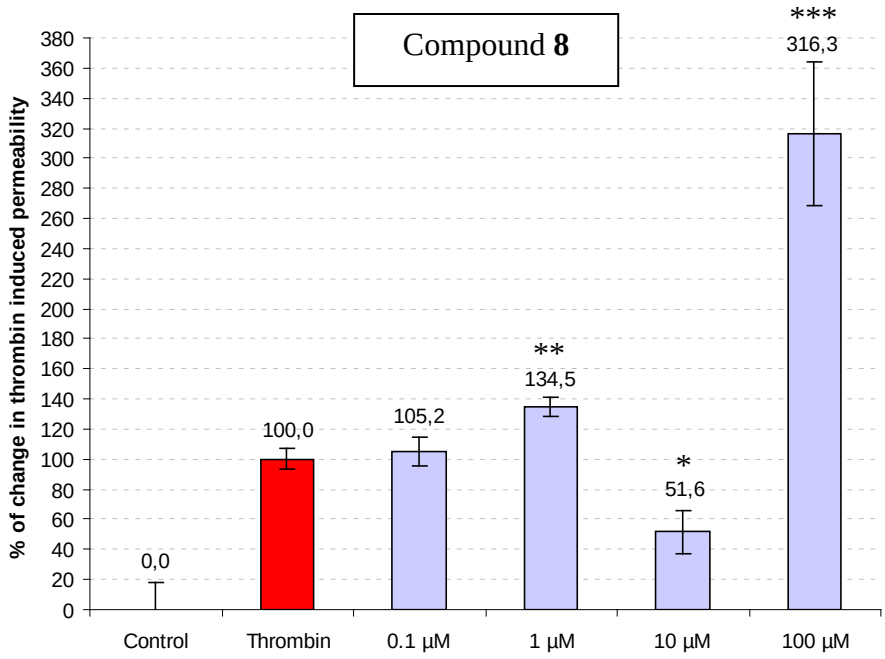

Fig. 3.73: Permeability assay for compound **8** after 60 min; expressed as percent of the thrombin value (100%); n = 3; mean ± SE; *** $p < 0.001$, ** $p < 0.01$, * $p < 0.05$.

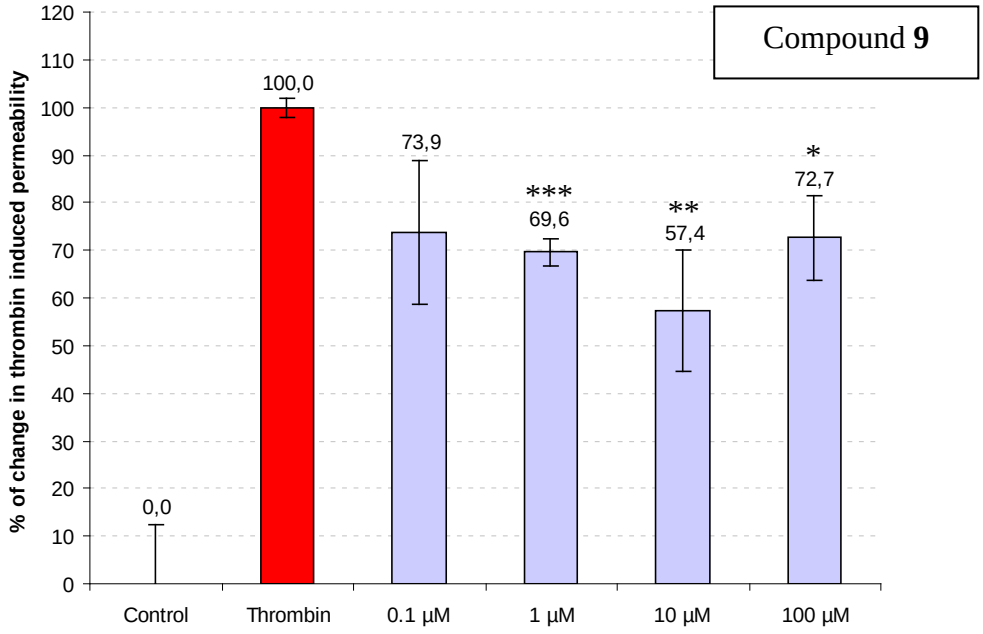

Fig. 3.74: Permeability assay for compound **9** after 60 min; expressed as percent of the thrombin value (100%); n = 3; mean ± SE; *** $p < 0.001$, ** $p < 0.01$, * $p < 0.05$.

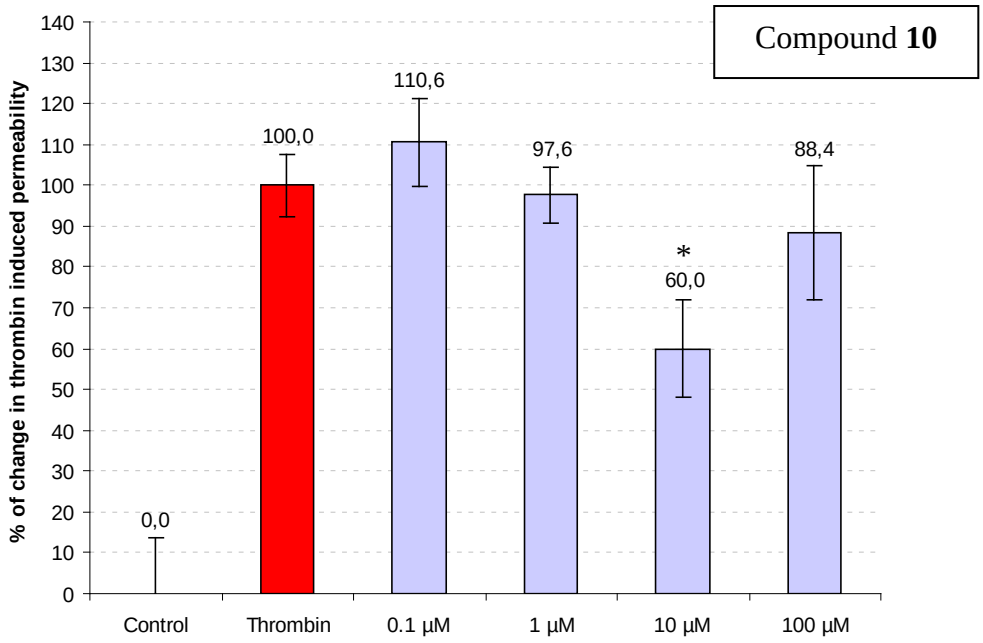

Fig. 3.75: Permeability assay for compound **10** after 60 min; expressed as percent of the thrombin value (100%); n = 3; mean ± SE; * $p < 0.05$.

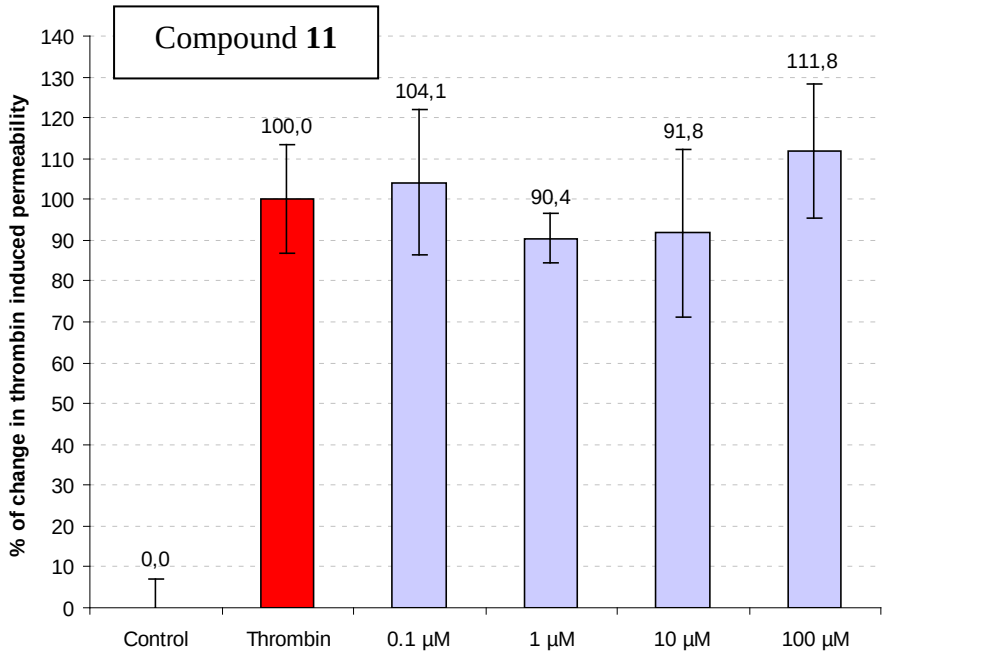

Fig. 3.76: Permeability assay for compound **11** after 60 min; expressed as percent of the thrombin value (100%); n = 3; mean ± SE.

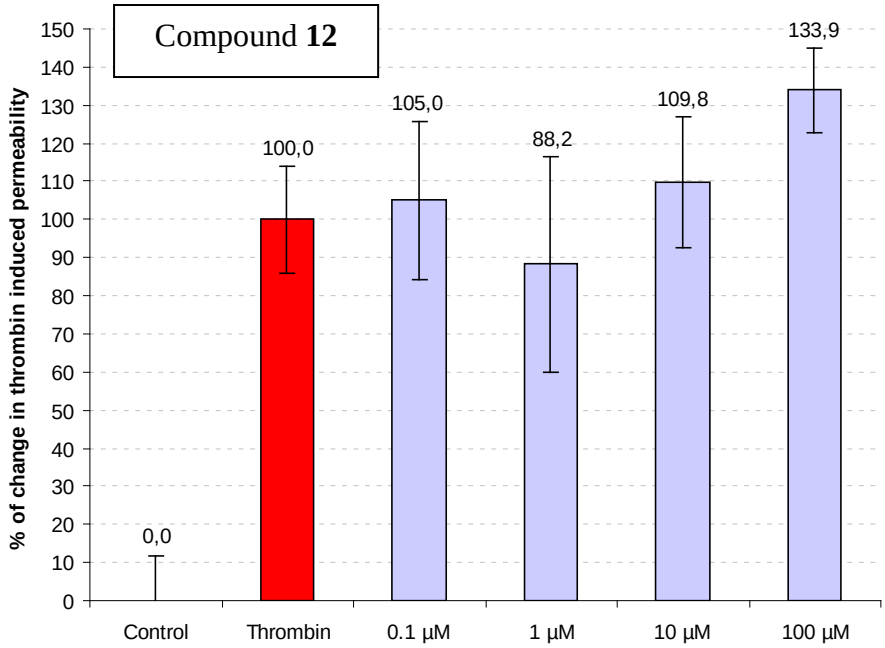

Fig. 3.77: Permeability assay for compound **12** after 60 min; expressed as percent of the thrombin value (100%); n = 3; mean ± SE.

3.5.3 Viability assay

Confluent HMECs, incubated with methanolic extract and compounds from *R. aculeatus*, were treated with MTT solution in order to determine the influence of the samples on viability of endothelial cells according to Mosmann 1983. 3-(4,5-Dimethylthiazol-2-yl)-2,5-diphenyltetrazolium bromide, shortly MTT, is a yellow coloured tetrazole, which is reduced by the mitochondrial reductase of living cells to purple coloured formazan (**Fig. 3.78**, p. 134). Control cells were also treated with MTT in order to obtain reference data, which was compared with the data from the samples. After dissolving the purple formazan, absorbance was measured on SpectraFluor plus plate reader at 560 nm. Higher absorbance correlates with higher viability, higher cell number or increased reductase activity since more MTT has been reduced to formazan.

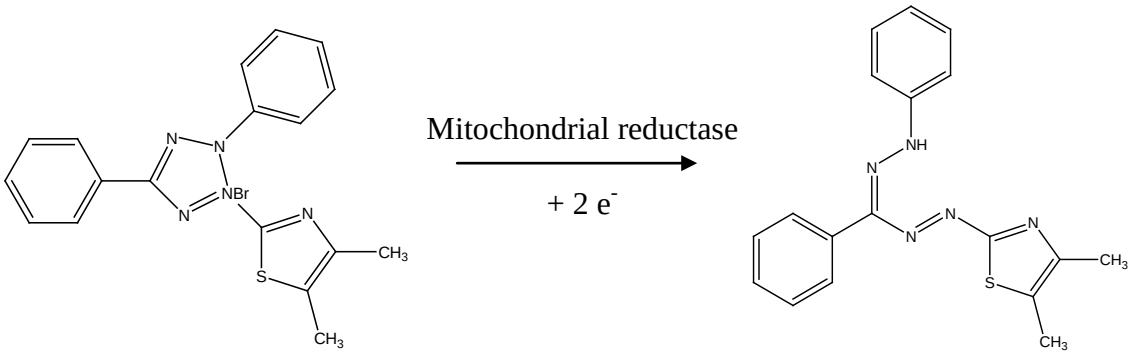

Fig. 3.78: Mitochondrial trasformation of yellow tetrazole (MTT) to purple coloured formazan.

MTT viability assay is often used for measurement of cytotoxicity. But it is important to keep in mind that viability assays only show the changes in metabolic activity of the cells. It is possible that the number of viable cells remains the same as in control, while significant changes in metabolic activity are observed.

MeOH extract was tested in concentrations of 1000 µg/mL, 100 µg/mL, 10 µg/mL and 1 µg/mL. None of the samples showed decrease of viability (**Fig. 3.79**, p. 135). The extract caused slight but significant ($p < 0.01$) increase of formazan production at 100 µg/mL.

Compounds **1**, **3**, **5**, **6**, **7**, **8**, **9**, **10** and neoruscogenine (50 and 10 µM) were investigated in MTT viability assay. Parthenolide (50 or 10 µM) was also tested. Although the structure similarity of steroid saponins might suggest comparable influence on viability, different results have been observed (**Fig. 3.80**, p. 136). Compound **6** (50 µM) was found to be toxic. Viability of the cells was decreased to 12.9% and cell death of majority of the cell was observed under microscope.

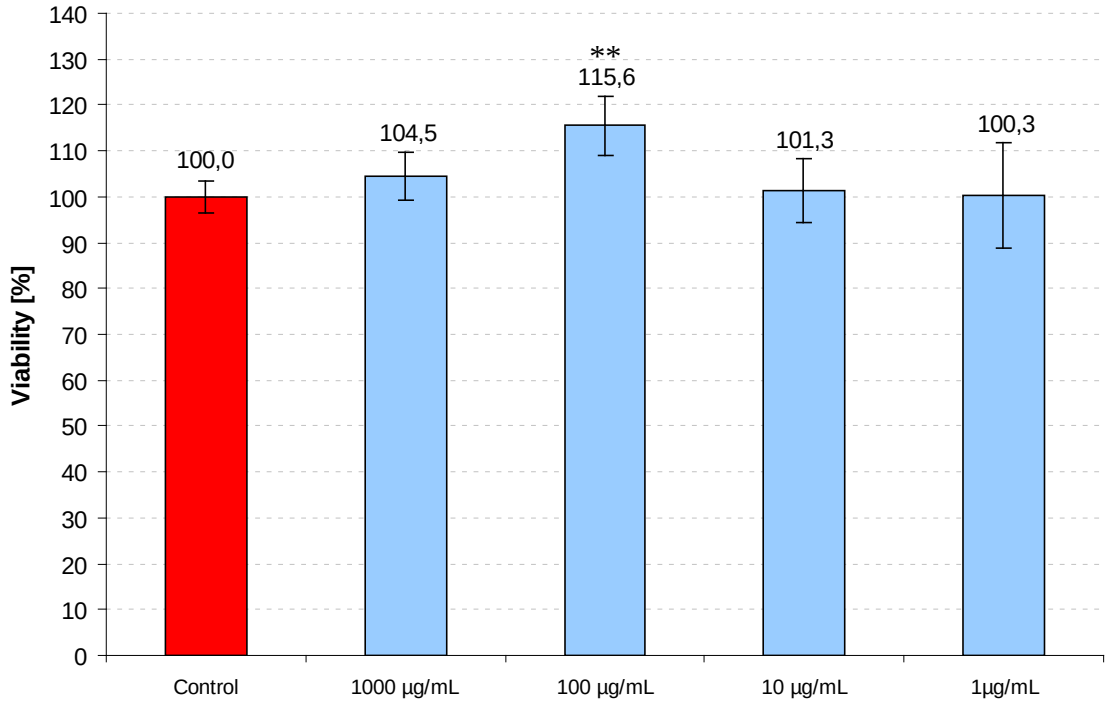

Fig. 3.79: MTT viability assay after 24 h with MeOH extract on the HMEC-1 cells; n = 3; mean ± SD; ** $p < 0.01$.

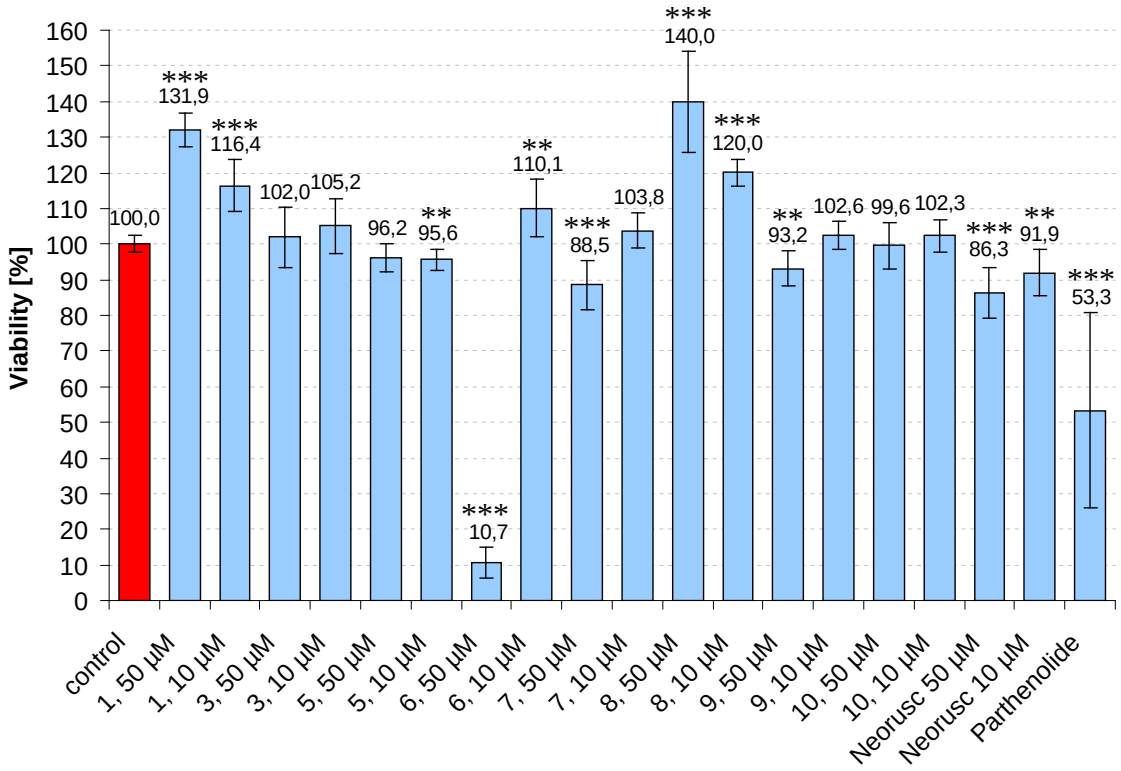

Fig. 3.80: MTT viability assay after 24 h with compounds **1**, **3**, **5**, **6**, **7**, **8**, **9**, **10**, neoruscogenine (50 and 10 µM) and parthenolide (10 µM) on the HMEC-1 cells; n = 3; mean ± SD; *** $p < 0.001$, ** $p < 0.01$.

3.5.3.1 IC_{50} value of compound **6**

IC_{50} value of compound **6** was determined using MTT viability assay. Half maximal inhibitory concentration is used to quantify efficacy of compounds in inhibitory assays. Since **6** showed cytotoxicity against HMECs at 50 µM, calculation of IC_{50} value was relevant.

Assays gave IC_{50} value for compound **6** at 33.0 ± 2.0 µM (**Fig. 3.81**; n = 3; mean ± SD).

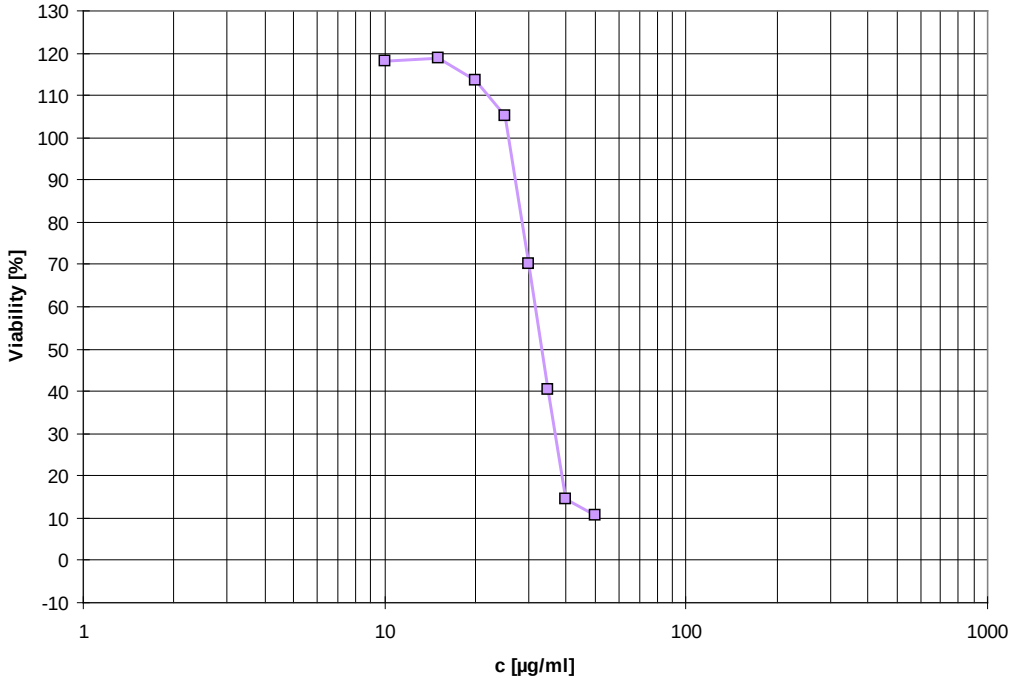

Fig. 3.81: IC_{50} value calculation curve for compound **6** using a logarithmic scale (x axis); n = 3

3.5.4 Influence of compounds 1 and 8 on the HMEC-1 cell number

3.5.4.1 Cell staining using CV

Saponins deglucoruscin and ruscin (**1** and **8**) were tested on the confluent HMECs to get data on their influence on the cell number (**Fig. 3.82**, p. 138). Crystal violet (CV) is a violet dye that stains DNA of the cells nucleus. After removing excess of CV, cells have been treated with sodium citrate solution in order to dissolve CV accumulated in cells. Control cells were pre-incubated only with growth medium and used for comparison. Lower absorption values of the cells treated with compounds would mean that less cell nuclei were stained and therefore a reduced number of cells were present.

Results showed that both compounds have influence on the cell number (**Fig. 3.82**, p. 138). Compound **1** (deglucoruscin) showed minor and unsignificant effect on the cells. On the other hand, absorbance values for compound **8** (ruscin) significantly differed from the control.

Consequently, **8** reduced the number of cells in the wells and can thereby be described as toxic at 50 µM.

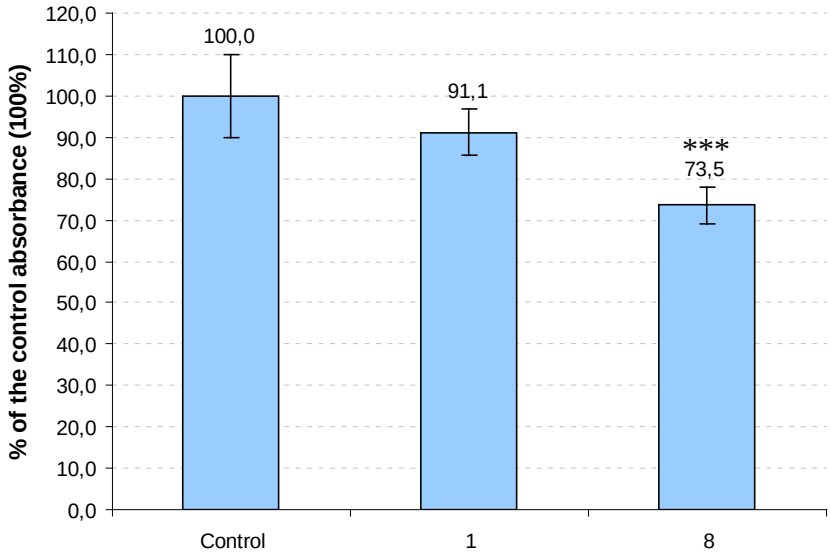

Fig. 3.82: CV cytotoxicity assay after 24 h with compounds **1** and **8** (50 µM) on the HMEC-1 cells; expressed as percent of the control value (100%); n = 3; mean ± SD; *** $p < 0.001$.

3.5.4.2 Cell counting assay using Trypan blue (24-well)

Cell counting experiment was performed in order to confirm the results from the assay using CV staining. Trypan blue is a dye that does not enter viable cells and only passes the membranes of dead or damaged cells. In this assay, we obtained absolute cell count of the HMECs present in each well, where the number of the control cells (incubated with medium) was compared to the count of the cells pre-incubated with compounds **1** and **8**.

Fig. 3.83, p. 139 clearly shows that compound **8** significantly reduced the number of HMECs present in wells in comparison with the untreated control cells. Therefore, it has been concluded that **8** is toxic at 50 µM.

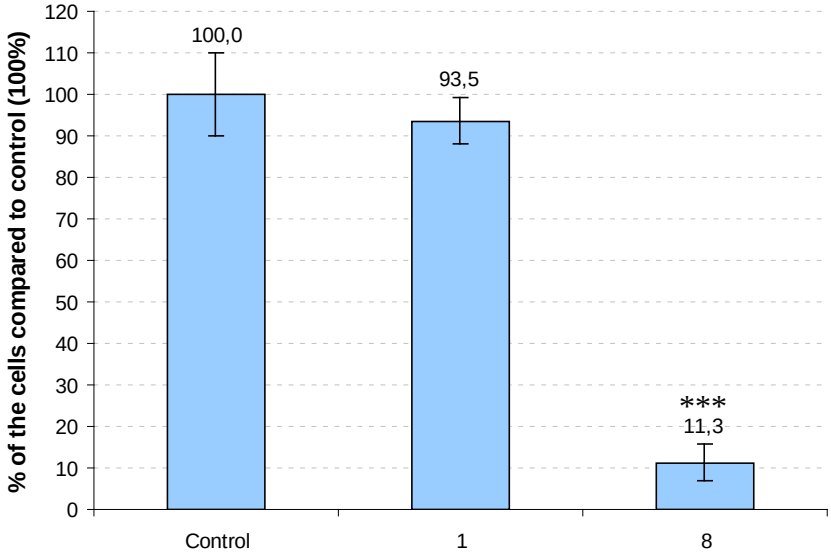

Fig. 3.83: Trypan blue cell counting cytotoxicity assay after 24 h with compounds **1** and **8** (50 µM) on the HMEC-1 cells in 24-well plates; expressed as percent of the control value (100%); n = 3; mean ± SD; *** $p < 0.001$.

3.5.4.3 Cell counting assay using Trypan blue (6-well)

Same procedure as in 24-well plates was performed in 6-well plates. It was observed that HMECs can be easier removed and counted from the 6-well than from the 24-well plates. Therefore, it was expected that better results with lower standard deviations would be measured in the assay with 6-well plates. **Fig. 3.84**, p. 140, shows that results of the assay using 6-well plates correlate with the results from the first assay using 24-well plates. Results for the control cells and compound **1** were almost identical to the values and standard deviations from the first trypan blue assay. Compound **8** gave different percent of the cells after 24 h in comparison to the control. As in the first assay and the CV staining, **8** has significantly reduced the number of cells in comparison to the control value and can therefore be confirmed as toxic. Since the 6-well assays were easier to handle and the fact that more cells could have been removed from 6-well than from 24-well plates, the 6-well assay is considered to be more appropriate for cell counting cytotoxicity assays.

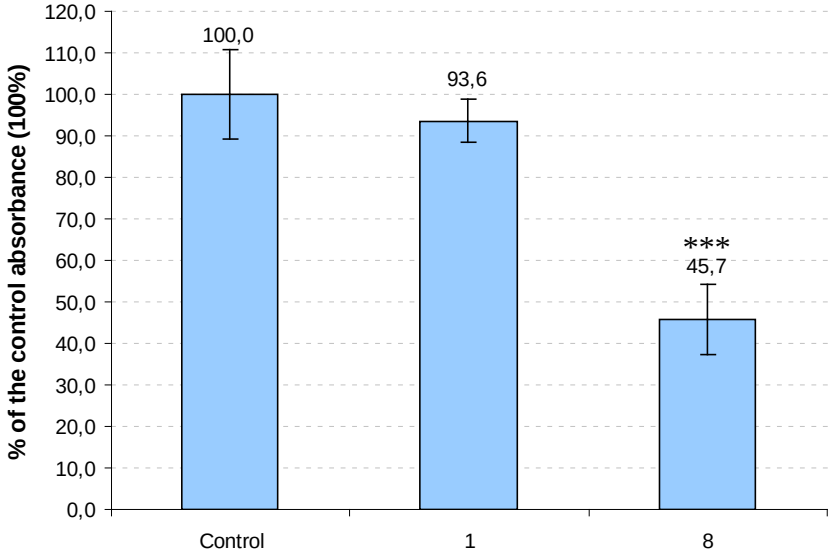

Fig. 3.84: Trypan blue cell counting cytotoxicity assay after 24 h with compounds **1** and **8** (50 µM) on the HMEC-1 cells in 6-well plates; expressed as percent of the control value (100%); n = 3; mean ± SD; *** $p < 0.001$.

3.6 Summary and final discussion including the biological assays

Extracts from *R. aculeatus* nowadays are mainly used to treat chronic venous diseases, such as chronic venous insufficiency (CVI) and hemorrhoids. Bergan 2007 and Bergan *et al.* 2008 postulated that inflammation might play the key role in the development of these diseases. Several *in vitro, in vivo* and clinical studies have been performed in order to determine the treatment prospects and options of products from Butcher's Broom (Escop). Results of these studies using extracts from the underground parts of Butcher's Broom have shown remarkable improvements of venous disorders. Therefore, treatment with *R. aculeatus* has to be considered as a good option in the therapy of chronic venous diseases.

Major constituents of Rusci rhizoma are steroid saponins and several have already been isolated (Mimaki *et al.*1998 a/b/c, 1999, 2003, 2008). Due to the high amount of saponins in the rhizomes of Butcher's Broom, it has been believed that they are responsible for the positive effects on the symptoms of chronic venous diseases. Rauwald & Grünwald 1991 have also proven that saponins of Rusci rhizoma can be found in human blood after oral administration. These results support the theory that they contribute to the efficacy of the extracts. On the other hand, no thorough analysis of other type of compounds, such as phenols, has been performed so far. Although amount of these substances in underground parts of *R. aculeatus* is low, the influence of them should be taken into consideration.

The main goal of this thesis was to isolate compounds from Rusci rhizoma and test them in several cell culture assays, which are related to possible targets present in the venous system *in vitro*. Since expression of adhesion molecules and vascular hyperpermeability are considered as two very important features of inflammatory response and the fact that inflammation is one of the main reasons for development of chronic venous diseases, ICAM-1 expression inhibition and macromolecular permeability assays have been chosen for our research.

In order to separate steroid saponins from other smaller compounds, a method using Sephadex LH 20® has been developed (Sephadex fractionation II, p. 33). After repeating the procedure for several times, two major fractions have been produced, a 'fraction rich on saponins', also described as 'fraction poor on phenolics' (PPF) and a fraction 'rich on phenolics' (PRF). TLC overview on the main constituents was confirmed by the quantification of both fractions (p. 108). Quantification of saponins showed an interesting phenomenon. In **Fig. 3.46**, p. 109, it

can be observed that main MeOH fraction contained similar amount of ruscogenin and neoruscogenin-type saponins (1.40% for ruscogenin and 1.53% for neoruscogenin). All fractions produced from MeOH extract contained much more ruscogenin than neoruscogenin-type saponins, suggesting that some chemical transformations occurred. Interestingly, in this research work we were able to isolate more of neoruscogenin-type steroid saponins.

Another interesting observation has been made during the isolation process and has been described before by Kite *et al.* 2007. Compound **2** was identified as a C-22 methoxylated deglucoruscoside and was partially transformed into **3** after addition of water. In this case, this is a very unusual reaction, where an acetal (ketal) is converted back to hemiacetal under aqueos conditions without addition of an acid, which is normally required. Also surprising is the reaction kinetic as over night approx. half of compound **2** decomposed into compound **3**. Since this transformation occurs very fast and under neutral conditions, it is questionable whether the C-22 methoxylated compounds really exist as natural product of *R. aculeatus*. It is hard to believe that a plant would produce and accumulate compounds which are instable in water. It would be energetically non-favourable. More reasonable explanation would is that C-22 methoxylated compounds are only artefacts and side products of the extraction and isolation procedure. Methanol has been used in chromatography as one of the main solvents. This indicates the possibility of methoxylation of the hydroxyl group at the C-22.

Some tests on the extracts and compounds from Butcher's Broom were performed in order to investigate this phenomenon. To get inert extracts (p. 112), the use of water and methanol was excluded from the extraction procedure. DCM and EtOAc were used to defat the plant material and n-BuOH to get the main extract. Extraction with water was performed to obtain a parallel sample, in order to observe the influence of water on the extract. The results of LC-MS analysis (p. 112) showed that none of the analysed samples contained compound **2**. Consequently the methoxylated product was not present in the starting material. Compound **3** (C-22 hydroxylated) was found in all investigated samples. The same result was obtained for fraction PPF, meaning that methanol did not have an influence on the compounds in the initial fractionation. On the other hand, compound **2** was isolated during this research and has also been reported before (Mimaki *et al.* 1998 b). This suggests that at some point of the isolation, compound **3** partially transformed into **2**. Every further fraction during the fractionation process contained fewer compounds, which increased the chance of methoxylation. The whole matrix of compounds is far less susceptible to the influence of MeOH than the smaller fractions that contain only few substances. All the fractions were also evaporated using a rotary evaporator at higher temperatures, which could catalyze the reaction. Considering all

these facts and the LC-MS data, it is highly believable that **2** and other potential C-22 methoxylated compounds are only side products of the isolation and do not occur genuine in nature.

These findings have also implications for the saponin quantification as some of the compounds in the extract from Butcher's Broom are less stable than others and can thereby contribute to the different results of fractionation and isolation.

Observations of the transformation kinetic from compound **3** to **2** in MeOD at room temperature did not show clear results (p. 117). In order to improve this experiment, non-deuterated MeOH with occasional increase in temperature should be used for incubation of compound **3** to simulate conditions similar to those during the isolation process.

Results of all biological assays performed during this research work showed that extracts, fractions and compounds from *R. aculeatus* can have an influence on the human microvascular endothelial cells *in vitro*.

ICAM-1 inhibition assay simulated part of inflammation process in veins. Expression of ICAM-1 molecules at the top of the vascular cells is one of the key features of the inflammatory response. In the case of inflammation, molecules such as TNF-α are released in order to stimulate the expression of endothelial adhesions cells like ICAM-1, which are important for the transmigration of the leucocytes into the tissue (Sprague & Khalil 2009, Lawson & Wolf 2009). In the case of chronic inflammation, endothelial activation leads to a chronically higher expression of the adhesion molecules, which furthermore resulted into inflammation. Inhibiting the expression of such molecules, chronic inflammation could be likely reduced.

After 24 h of incubation, all main extracts (MeOH extract, n-BuOH and H_2O fraction) showed inhibition of the TNF-α induced ICAM-1 expression at low concentrations. Interestingly, high concentrations resulted into an increase of ICAM-1 expression (**Fig. 3.58**, p. 122). Similar results were obtained by testing the PRF and PPF fraction (**Fig. 3.59**, p. 122). With inhibition down to approx. 73% of the maximal expression caused by TNF-α for PRF and 80% for PPF, these fractions were considered as very promising for further analysis.

Single compounds also showed certain effect, but not as high as expected from the results of the major fractions. Most of the compounds showed only minor and mostly statistically not significant inhibition of expression. Most effective compound was ruscin (compound **8**), which inhibited the expression of ICAMs significantly down to 55% at 50 µM. This is a

remarkable result but must unfortunately be observed with cautious, because of the results from the viability and cell counting assays (**Fig. 3.80,** p. 136; **Fig. 3.82**, p. 138**; Fig. 3.83**, p. 139 and **Fig. 3.84**, p. 140). MTT viability assay of compound **8** showed hyperactivity of the cells at 50 µM. Viability value was increased to 140% of the control cells value. Ruscin was also tested in the cytotoxicity assays (**Fig. 3.82**, p. 138**; Fig. 3.83**, p. 139 and **Fig. 3.84**, p. 140) and gave surprising results. Both assays (KV staining, trypan blue cell counting in 6- and 24-well plates) showed that **8** was toxic at 50 µM, since the cell count significantly dropped in comparison to the control cells. It has again been proven that MTT viability assay do not match exactly the cytotoxicity assays. Results from both assays can significantly deviate from each other.

A further important finding was the higher activity of the isolated compounds, tested in ICAM-1 assay, in comparison to the aglycone neoruscogenin. This suggests that steroid saponins from Butcher's Broom are probably more responsible for the effect in venous system in comparison to their aglycones. Huang *et al.* 2008 tested ruscogenin on its activity in a similar assay and it was found to be active. It is possible that ruscogenin is more potent than neoruscogenin. Furthermore, the assay set-up was also different. An important difference was the incubation time, as Huang *et al.* used an incubation time of only 4 h in comparison to 24 h in this assay. To compare the activity of the aglycones, both compounds should be tested in the same assay.

MTT viability assay showed that compound **6** is toxic at 50 µM, since all the cells dissolved from the plate. Same was observed during the measurements of the fluorescence by the FACS analysis, where no cells were detectable after performing the ICAM-1 inhibition assay. Interestingly, compounds **1** and **9** showing no cytotoxicity, do not differ much from **6**. For this reason, it has been concluded that the side chain on the C-4' of the arabinose in compound **6** must be responsible for the toxic effect (MTT IC_{50} = 33.0 ± 2.0 µM). Compounds **1**, **6**, **8** and **9** would therefore be eligible for thorough analysis of the mechanism of action. However, a possible explanation is that small structural changes contribute to the different intensity of the detergent effect. To investigate these aspects, measurements of critical micelle concentration or hemolysis can be considered as appropriate assays.

One of the most important aspects of endothelium activation and inflammatory response is macromolecular hyperpermeability. Increase in permeability of the vascular cells in veins leads to higher permeability for proteins and fluids. In case of CVI, this manifests as edema and leads to further activation of endothelium.

Influence on permeability of human microvascular endothelial cells was analyzed by measuring the influence of compounds from *R. aculeatus* on the thrombin-induced permeability of FITC-labelled dextran through the confluent grown monolayer of HMECs. The results of this assay were more remarkable than those in the ICAM-1 assay. Most of the compounds showed tendency to decrease the induced permeability, but effects were often not significant. Most active compounds were compounds **1**, **5** and **8**, reducing the permeability of the dextran at 10 µM down to 42%, 53% and 52%, respectively, after 1 h of incubation. At 100 µM all saponins, except for **9**, dramatically increased the permeability. Higher concentrations of saponins most probably dissolved or damaged the cells and thereby caused the increase in permeability through the monolayer. Significant decrease in permeability of the FITC-labelled dextran showed also compound **10** at 10 µM (60%) and was thereby the only phenolic compound active in this assay.

Compound **6** showed tendency to induce the permeability at all tested concentrations (**Fig. 3.74**, p. 131). MTT viability assay revealed that **6** caused cell death at 50 µM and was thereby the only compound that showed such dramatic changes in the MTT assay.

Unfortunately, not every isolated compound was tested in biological assays. Yields around 1 mg per sample or less did not allow testing in cell culture assays. Phenols are surely one of the most interesting research topics of this thesis, but due to the low amounts no thorough tests for activity in selected assays were performed. Much higher amount of the starting material should be used for fractionation and isolation of the phenolic compounds to obtain significant amounts.

Compounds **1** and **8** showed interesting results in ICAM-1 and MTT assay. In combination with the data from the permeability assay no clear conclusions about the activity could have been drawn. Ruscin (**8**) showed high ICAM-1 expression inhibition at 50 µM (**Fig. 3.65**, p. 126), but caused high activity of the mitochondrial enzymes in MTT assay like deglucoruscin (**1**) (**Fig. 3.80**, p. 136). Therefore, cytotoxicity assays based on cell counting were developed to determine the influence on the cells and actual cytotoxic effect of the compounds (p. 137). In all three assays, it has been proven that **8** is toxic at 50 µM. Possible explanation is the attempt to down-regulate mechanisms, which are not vital for the existence (expression of ICAM-1 molecules) and up-regulate processes that are used as the last resort to survive, in this case mitochondrial activity. This was not the case for compound **1**. Since **1** at 50 µM showed similar behavior as **8** at 10 µM in ICAM assay, it is possible that toxic concentration of compound **1** has not been reached yet. Since the permeability assay showed that **1** greatly

increases the permeability through the HMEC monolayer at 100 µM, it would be reasonable to test **1** at concentrations between 50 µM and 100 µM in both ICAM and MTT assay, in order to get a clear answer about the activity. It is also possible that the other isolated saponins show similar effects, but only at different concentrations, which have not been included in testing. Furthermore, it has to be considered that in permeability assay, cells were stimulated for only 1 h in comparison to ICAM-1 and MTT assay, where 24 h incubation times were used.

From ICAM-1 and permeability assay, it can be concluded that steroid saponins cause partly a dose-dependent response, resulting at least to an U-shaped activity curve. At several concentrations, tested saponins diminished *in vitro* stimulated inflammation (higher ICAM-1 expression via TNF-α and higher permeability via thrombin) but can on the other hand act pro-inflammatory and also cause cell death at higher concentrations. In order to describe the activity and to get the full dose-dependent curve of single compounds, same assays should be performed using diverse concentrations of the compounds. Therefore, higher amounts of the selected compounds should be isolated and a higher quantity of starting material should be used for fractionation and isolation.

Cell counting assays have shown that the assay using 6-well plates was better to handle with. The cells in the 6-well plates were easily resuspended using trypsin/EDTA solution and cell scraper. On the other hand, in 24 well plates the cells growing on the edge of the wells could not be completely removed, which most certainly influenced the final results. The results in both assays showed the same tendency but gave different results for compound **8** at 50 µM. There are two factors, which might be the reason for that. It has to be considered that the cell count obtained in 24-well assay was too low, due to the cells from the edge that could not be counted. For the values of compound **1**, which were not significantly different to the values of the control cells, this did not cause a great change. For compound **8**, where the cell count was dramatically reduced down to 45 % in 6-well assay, leaving out the cells from the edge would mean a bigger change in the cell count and therefore even lower values in the 24-well assay.

Second parameter that might influence the results of the cell counting assay is the absolute quantity of the compounds to area of the well ratio. In 24-well plates 0.5 mL to 2 cm^2 ratio was used, which means higher absolute amount of compound per cm^2 than in 6-well plates (2 mL to 9.6 cm^2 ratio). This could also contribute to the higher cytotoxic effect measured in the 24-well assay. Since 6-well assay was better to handle with and all the HMECs were removed

from the plate, the cell counting assay using 6-well plates should be considered as more appropriate.

During this study it has been proven *in vitro* that extracts, fractions and compounds from the underground part of *R. aculeatus* could have an influence on the human venous system. *In vitro* assays, such as ICAM-1 expression inhibition and permeability assay, showed that isolates from Butcher's Broom have an effect on the inflammatory response of the human microvascular endothelial cells, which is suggested to play the key role in the development and progression of chronic venous diseases (Bergan 2007 and Bergan *et al.* 2008). None of the compounds could be observed as very potent, but if single constituents and their minor activity are considered as only the part of a matrix of substances, the appropriate dose and composition of compounds could have a larger impact on the inflammatory response and would thereby lead to improvement of chronic venous diseases, such as CVI or hemorrhoids.
In this thesis, it has also been shown that saponins are more active than the aglycone neoruscogenin, which makes studies on *R. aculeatus* more fascinating and indicating that steroid saponins should be included in other experiments, where normally only raw extracts have been tested (Escop).
New compounds have also been found (see compounds **4**, **6**, **7**, **11** and **14** and discussion about isolation on p. 105). Among these compounds **11** and **14** showed novel skeleton. It also seems to be important to broaden the knowledge about the contribution of phenolic compounds from *R. aculeatus* to the overall efficacy of Butcher´s Broom.

4 References

Aird W C. (2008)
Endothelium in health and disease.
Pharmacol Rep. **60**: 139-43

Beltramino R, Penenory A, Buceta A M. (2000)
An open-label, randomized multicenter study comparing the efficacy and safety of Cyclo 3 Fort versus hydroxyethyl rutoside in chronic venous lymphatic insufficiency.
Angiology. **51**: 535-44

Benedek B, Kopp B, Melzig M F. (2007)
Achillea millefolium L.s.l. - Is the anti-inflammatory activity mediated by protease inhibition?
J. Ethnopharmacol. **113**: 312-7

Bergan J J. (2007)
Molecular mechanisms in chronic venous insufficiency.
Ann. Vasc. Surg. **21**: 260-6

Bergan J J, Pascarella L, Schmid-Schönbein G W. (2008)
Pathogenesis of primary chronic venous disease: Insights from animal models of venous hypertension.
J. Vasc. Surg. **47**: 183-92

Boisseau M R. (2002)
Pharmacological targets of drugs employed in chronic venous and lymphatic insufficiency.
Int. Angiol. **21**: 33-39

Bouskela E. (1991)
Microcirculatory responses to *Ruscus* extract in the hamster cheek pouch. Return circulation and norepinephrine: an update.
(P. Vanhoutte, Ed.), John Libbey Eurotext. 207-18

Bouskela E, Cyrino F Z, Marcelon G. (1993)
Inhibitory effect of the *Ruscus* extract and of the flavonoid hesperidine methylchalcone on increased microvascular permeability induced by various agents in the hamster cheek pouch.
J. Cardiovasc. Pharm. **22**: 225-30

Bouskela E, Cyrino F Z G A. (1994)
Possible mechanisms for the effects of *Ruscus* extract on microvascular permeability and diameter.
Clinical Hemorheology **14**: S23-S36

Boyle P, Diehm C, Robertson C. (2003)
Meta-analysis of clinical trials of Cyclo 3 Fort in the treatment of chronic venous insufficiency.
Int. Angiol. **22**: 250-62

Dirsch V M, Keiss H P, Vollmar A M. (2004)
Garlic metabolites failed to inhibit the activation of the transcription factor NF-kappaB and subsequent expression of the adhesion molecule E-selectin in human endothelial cells.
Eur. J. Nutr. **43**: 55-9

Eberhardt R T, Raffetto J D. (2005)
Chronic Venous Insufficiency.
Circulation **111**: 2398-2409

El Sohly M, Knapp J E, Slatkin K F, Schiff P L Jr, Doorenbos N J, Quimby M W. (1975)
Constituents of *Ruscus aculeatus.*
Lloydia **38**: 106-8

Escop Monographs
Second edition. Rusci rhizoma, Butcher's Broom. 417-44

European Pharmacopoeia 5.3 German edition

Facino R, Carini M, Stefani R, Aldini G, Saibene L. (1995)
Anti-elastase and ant-hyaluronidase activities of saponins and sapogenins from *Hedera helix, Aesculus hippocastanum* and *Ruscus aculeatus*: Factors contrubuting to their efficacy in the treatment of venous unsufficiency.
Arch. Pharm. (Weinheim) **328**: 721-4

Frohne D.
Heilpflanzen-Lexikon.
Wissenschaftliche Verlagsgesellschaft mbH Stuttgart, 7. Auflage, 2002. 483-4

Glasl H. (1983)
Zur Photometrie in der Drogenstandardisierung
DAZ, **123**:1979-87

Hansson G K. (2009)
Inflammatory mechanisms in atherosclerosis.
J. Thromb. Haemost. **7 Suppl 1**: 328-31

Harker C T, Marcelon G, Vanhoutte P M. (1988)
Temperature, oestrogens and contractions of venous smooth muscle of the rabbit.
Phlebology **3**, 77-82.

Hänsel R, Sticher O.
Pharmakognosie, Phytopharmazie.
Springer Verlag, 8 Auflage , 2007. 986-9

Hönig I, Felix W. (1989)
Effect on the permeability of the isolated eat vein of the pig; a comparison between flavonoids and saponins.
Phlebologie (A. Davy, and R. Stemmer, Eds.), John Libbet Eurotext Ltd. 680-2

Huang Y L, Kou J P, Ma L, Song J X, Yu B Y. (2008)
Possible mechanism of the anti-inflammatory activity of ruscogenin: Role of Intracellular Adhesion Molecule-1 and Nuclear Factor- κB.
J. Pharmacol. Sci. **108**: 198-205

Jürgenliemk G. (2000)
Phenolische Inhaltstoffe aus dem Kraut von *Hypericum perforatum* L. - analytische, biopharmazeutische und pharmakologische Aspekte.
Dissertation

Kameyama A, Shibuya Y, Kusuoku H, Nishizawa Y, Nakano S, Tatsuda K. (2003)
Isolation and structural determination of spilacleosides A and B having a novel 1,3-dioxan-4-one ring.
Tetrahedron Letters **44**: 2737-9

Kite G C, Porter E A, Simmonds M S. (2007)
Chromatographic behaviour of steroidal saponins studied by high-performance liquid chromatography-mass spectrometry.
J. Chromatogr. A **1148**: 177-83

Kueng W, Silber E, Eppenberger U. (1989)
Quantification of cells cultured on 96-well plates.
Analyt. Biochem. **182**: 16-9

Lauressergues H, Vilain P. (1984)
Pharmacological activities of *Ruscus* extract on venous smooth muscle.
Inter. Angio. **3**: 70-3

Lawson C, Wolf S. (2009)
ICAM-1 signaling in endothelial cells.
Pharmacol. Rep. **61**: 22-32

Lee S T, Mitchell R B, Wang Z, Heiss C, Gardner D R, Azadi P. (2009)
Isolation, characterizaton and quantification of steroidal saponins in switchgrass (*Panicum virgatum* L.).
J. Agric. Food Chem. **57**: 2599-2604

MacKay D. (2001)
Hemorrhoids and varicose veins: a review of treatment options.
Altern. Med. Rev. **6**:126-40

Marcelon G, Verbeuren T J, Lauressergues H, Vanhoutte P M. (1983)
Effect of *Ruscus aculeatus* on isolated canine cutaneous veins.
General Pharmacology **14**: 103-6

Marcelon G, Vanhoutte P M. (1988)
Veinotonic effect of *Ruscus* under variable temperature conditions in vitro.
Phlebology **3**: 51-4

Marcus B C, Gewertz M D. (1998)
Measurement of endothelial permeability.
Ann. Vasc. Surg. **12**: 384-90

Markham K R. (1989)
Carbon-13 NMR studies on flavonoids III: Natural occuring flavonoid glycosides and their acetylated derivatives.
Tetrahedron **34**: 1389-97

Martinez-Palle E, Aronne G. (1999)
Flower development and reproductive continuity in Mediterranean *Ruscus aculeatus* L.
Protoplasma **208**: 58-64

Methlie C B, Schjøtt J. (2009)
Horse chestnut-remedy for chronic insufficiency.
Tidsskr Nor Laegeforen **129**:420-2

Miller V M, Rud K S, Gloviczki P. (2000)
Pharmacological assessment of adrenergic receptors in human varicose veins.
Int Angiol **19**: 176-83.

Mimaki Y, Kuroda M, Kameyama A, Yokosuka A, Sashida Y. (1998 a)
Steroidal saponins from the underground parts of *Ruscus aculeatus* and their cytostatic activity on HL-60 cells.
Phytochemistry **48**: 485-93

Mimaki Y, Kuroda M, Kameyama A, Yokosuka A, Sashida Y. (1998 b)
New steroidal constituents of the underground parts of *Ruscus aculeatus* and their cytostatic activity on HL-60 cells.
Chem. Pharm. Bull. **46**: 298-303

Mimaki Y, Kuroda M, Kameyama A, Yokosuka A, Sashida Y. (1998 c)
Aculeoside B, a new bidesmosidic spirostanol saponin from the underground parts of *Ruscus aculeatus*.
J. Nat. Prod. **61**: 1279-82

Mimaki Y, Kuroda M, Yokosuka A, Sashida Y. (1999)
A spirostanol saponin from underground parts of *Ruscus aculeatus*.
Phytochemistry **51**: 689-92

Mimaki Y, Aoki T, Jitsuno M, Kiliç C S, Coşkun M. (2008)
Steroidal glycosides from the rhizomes of *Ruscus hypophyllum*.
Phytochemistry **69**: 729-37

Monsieur R, Van Snick G. (2006)
Efficacy of the red vine leaf extract AS 195 in Chronic Venous Insufficiency.
Praxis (Bern 1994), **95**:187-90

Mosmann T. (1983)
Rapid colorimetric assay for cellular growth and survival: application to proliferation and cytotoxicity assays.
J. Immunol. **65**: 55–63

Noe C R, Freissmuth J. (1995)
Capillary zone electrophoresis of aldose enantiomers: Separation after derivatization with *S*-(-)-1-phenylethylamine.
J. Chromatography A **704**: 503-12

Oulad-Ali A, Guillaume D, Belle R, David B, Anton R. (1996)
Sulphated steroidal derivatives from *Ruscus aculeatus*.
Phytochemistry **42**: 895-7

Pasyk K A, Jakobczak B A. (2004)
Vascular endothelium: recent advances.
Eur. J. Dermatol. **14**: 209-13

Ph. Eur. - see **European Pharmacopoeia**

Pries A R, Secomb T W, Gaehtgens P. (2000)
The endothelial surface layer.
Pflugers Arch. **440**: 653-66

Rauwald H J, Grünwald J. (1991)
Ruscus aculeatus extract: Unambiguous proof of the absorption of spirostanol glycosides in human plasma after oral administration.
Planta Medica **57**: A75-A76

Rubanyi G, Marcelon G, Vanhoutte P M. (1984)
Effect of temperature on the responsiveness of cutaneous veins to the extract of *Ruscus aculeatus*. General pharmacology **15**: 431-4

Schönfelder I, Schönfelder P.
Das neue Handbuch der Heilpflanzen.
Kosmos Verlag, 2004. 390

Sitte P, Ziegler H, Ehrendorfer F, Bresinski A.
Strasburger - Lehrbuch der Botanik für Hochschulen.
35. Auflage. Spektrum-Akademischer Verlag, 2002

Sprague A H, Khalil R A. (2009)
Inflammatory cytokines in vascular dysfunction and vascular disease.
Biochem. Pharmacol. **78**: 539-52

Vanscheidt W, Jost V, Wolna P. (2002)
Efficacy and safety of a Butcher's broom preparation *(Ruscus aculeatus* L. extract) compared to placebo in patients suffering from chronic venous insufficiency.
Arzneimittelforschung **52**: 243-50

Weis S M. (2008)
Vascular permeability in cardiovascular disease and cancer.
Curr. Opin. Hematol. **15**: 243-9

Wichtl M.
Teedrogen und Phytopharmaka.
Wissenschaftliche Verlagsgesellschaft mbH Stuttgart, 4. Auflage, 2002.

Statement of Authorship

I, the undersigned, hereby declare that I am the sole author of this thesis, which describes only my own work, unless otherwise aknowledged. This document does not contain scientific data from other dissertations or publications, previously presented at this or any other university.

Matej Barbič Regensburg, 02 March 2011

Curriculum vitae

Matej Barbič
Pharmacist
Laaberstraße 6
93059 Regensburg

Date of Birth	07/05/1981
Place of Birth	Ljubljana, Slovenia
Nationality	Slovenian
Gender	Male
Marital Status	Married

WORK EXPERIENCE

Research Associate Since 12/2006
Department of Pharmaceutical Biology
University of Regensburg, Germany

- Supervision of diploma projects
- Training and supervision of pharmacy students and technicians
- Examination of pharmacy students
- Reports and presentations about field research progress

PhD Student - funded by DAAD Since 12/2006
(Deutscher Akademischer Austausch Dienst)
Department of Pharmaceutical Biology
University of Regensburg, Germany
"**Isolation and identification of the constituents from *Ruscus aculeatus* L. and their *in vitro* activity**"

- Bio-assay guided isolation of compounds from *Ruscus aculeatus*
- Cell cultivation and biological assays
- Characterization and structure elucidation of compounds
- Determination of structure-effect correlations

PC Administrator and Workgroup Manager Since 04/2007
Department of Pharmaceutical Biology
University of Regensburg, Germany

- Software and Hardware support
- Training of department members to use special software
- Network and homepage management

EDUCATION

Faculty of Pharmacy 09/2000 – 06/2006
University of Ljubljana, Slovenia
Degree: Diploma
Title: **Mag. Pharm.**
Grammar school - SŠ Josip Jurčič Ivančna 09/1996 – 06/2000
Gorica, Slovenia

INTERNATIONAL WORK / EDUCATION

Diploma (practical part) 11/2005 – 04/2006
Department of Pharmaceutical Biology
University of Regensburg, Germany
- Isolation and identification of new compounds from *Astargalus illyricus*

Research project under supervision of Prof. Ihsan Calis 06/2005 – 08/2005
Department of Pharmaceutical Biology
University of Regensburg, Germany
- Fractionation of plant extracts and isolation of new compounds
- Structure elucidation

Exchange student
Funded by Socrates/Erasmus 10/2004 – 06/2005
University of Regensburg, Germany
- Pharmacy study
- Research in field of medicinal chemistry

ADDITIONAL INFORMATION

Skills
- Excellent verbal and written communication skills
- Team leadership as well as integrating as a team member

Languages
- Slovenian native speaker
- English fluent, both spoken and written
- German fluent, both spoken and written
- Serbo-Croatian very good, spoken
- Bulgarian basic, spoken

Computer skills
- Microsoft Windows very good
- Microsoft Office very good
- Bruker Top Spin very good
- ChemDraw very good
- Graphics software very good
- Web design software basic

Memberships
- Slovenian Pharmaceutical Society (since 2003)
- DAAD – Scholar and member of Deutscher Akademischer Austausch Dienst (since 2007)

Hobbies and other
- Sports (volleyball, skiing, basketball, tennis)
- Music (guitar), cooking
- Representative of the Slovenian students of Pharmacy in Regensburg, Germany (tutoring and coordination)

PUBLICATIONS AND POSTERS

Barbič M, Macabeo A P G, Kreft S, Heilmann J. (2010) Cycloastragenol glycosides from *Astragalus illyricus*. Biochemical Systematics and Ecology **38**: 460-2

Vogel S, Barbič M, Jürgenliemk G, Heilmann J. (2010) Synthesis, cytotoxicity, anti-oxidative and anti-inflammatory activity of chalcones and influence of A-Ring modifications on the pharmacological effect. European Journal of Medicinal Chemistry **45**: 2206-13.

Caliş I, Barbič M, Jürgenliemk G. (2008) Bioactive cycloartane-type triterpene glycosides from *Astragalus elongatus*. Zeitschrift für Naturforschung C. **63**: 813-20.

Barbič M, Heilmann J, Melzig M, Jürgenliemk G. (2008) Inhibition of ICAM-1 expression and elastase by an extract and fractions from the roots of *Ruscus aculeatus*. Planta Medica **74**: 1125

Barbič M, Willer EA, Fürst R, Jürgenliemk G. (2010) Esculin from Butcher´s broom reduces the permeability of endothelial cells *in vitro*.
Poster: 58th International GA-Conference; Berlin, Sep. 2010

Vogel S, Barbič M, Brunner G, Jürgenliemk G, Heilmann J. (2009) Anti-inflammatory activity of natural and non-natural chalcones.
Poster: International DPhG congress in Pichlarn, Austria, Nov. 2009

Barbič M, Heilmann J, Melzig M, Jürgenliemk G. (2008) Inhibition of ICAM-1 expression and elastase by an extract and fractions from the roots of *Ruscus aculeatus.*
Poster: 7th Joint Meeting of AFERP, ASP, GA, PSE & SIF; Athens, Greece, Aug. 2008